Ultracold Atoms and Bose-Einstein Condensates

Peter Schlagheck
Université de Liège

Chapter 1

Quantum statistical physics

1.1 Ergodicity of a classical gas

We consider a dilute gas of some $N \sim 10^5 \dots 10^{10}$ classical particles that are confined in some finite region in space. A typical example of the classical Hamiltonian that governs this system is written as

$$H \equiv H(\mathbf{r}_1, \mathbf{p}_1, \dots, \mathbf{r}_N, \mathbf{p}_N) = \sum_{i=1}^{N} \left(\frac{p_i^2}{2m} + V(\mathbf{r}_i) \right) + \frac{1}{2} \sum_{i \neq j = 1}^{N} U(\mathbf{r}_i - \mathbf{r}_j) \,. \quad (1.1)$$

Here $\mathbf{r}_i = (x_i, y_i, z_i) \in \mathbb{R}^3$ represents the position and $\mathbf{p}_i = (p_{xi}, p_{yi}, p_{zi}) \in \mathbb{R}^3$ the momentum of the particle $i = 1, \dots, N$, m is the mass of the particles, $V(\mathbf{r})$ is the external confinement potential that the particles experience at position $\mathbf{r}$, and $U(\mathbf{r}_i - \mathbf{r}_j) \equiv U(|\mathbf{r}_i - \mathbf{r}_j|)$ represents a two-body interaction potential between two particles at positions $\mathbf{r}_i$ and $\mathbf{r}_j$ which effectively depends only on the distance $|\mathbf{r}_i - \mathbf{r}_j|$ between the particles. The equations of motion that result from this classical Hamiltonian are given by

$$\frac{d\mathbf{r}_i}{dt}(t) = \frac{\partial H}{\partial \mathbf{p}_i} \left[\mathbf{r}_1(t), \mathbf{p}_1(t), \dots, \mathbf{r}_N(t), \mathbf{p}_N(t) \right] , \quad (1.2)$$

$$\frac{d\mathbf{p}_i}{dt}(t) = -\frac{\partial H}{\partial \mathbf{r}_i} \left[\mathbf{r}_1(t), \mathbf{p}_1(t), \dots, \mathbf{r}_N(t), \mathbf{p}_N(t) \right] \quad (1.3)$$

for all $i = 1, \dots, N$. For given initial conditions they generate a trajectory $[\mathbf{r}_1(t), \mathbf{p}_1(t), \dots, \mathbf{r}_N(t), \mathbf{p}_N(t)]$ that evolves within a $6N$ dimensional phase space spanned by the position and momentum coordinates of the individual particles.

The symplectic structure of the equations of motion (1.2) and (1.3) gives rise to *Liouville's theorem* which essentially states that phase space volumes are preserved during the time evolution. That is, if we consider a subset $\Sigma \subset \mathbb{R}^{6N}$ of the phase space with finite volume $\mathcal{V} = \mathrm{vol}(\Sigma) > 0$ and let this subset evolve under the equations of motion (1.2) and (1.3) over a finite time $t >$

0 (namely by evolving each individual initial point within Σ over that time), then the resulting subset $\Sigma' \subset \mathbb{R}^{6N}$ is generally different from Σ but has still the same volume $\mathcal{V} = \mathrm{vol}(\Sigma) = \mathrm{vol}(\Sigma')$. This theorem is essentially a consequence of the fact that the variable transformation from the initial phase space variables $\mathbf{r}_1(0), \mathbf{p}_1(0), \ldots, \mathbf{r}_N(0), \mathbf{p}_N(0)$ to the final phase space variables $\mathbf{r}_1(t), \mathbf{p}_1(t), \ldots, \mathbf{r}_N(t), \mathbf{p}_N(t)$ is canonical and hence the Jacobian associated with this variable transformation, which effectively enters into the calculation of the evolved volume, is unity.

Owing to Liouville's theorem as well as to the high dimensionality of the phase space and the presence of *chaos* that generically arises within interacting many-body systems — which implies that small deviations in the initial conditions will (especially after two-body collisions) exponentially increase with the evolution time — we can safely postulate *ergodicity* for our classical gas. Colloquially speaking, this means that over a sufficiently long evolution time $t \to \infty$ each region in phase space is visited with the *same frequency* as any other region in phase space, provided the access to this region is not inhibited by general conservation laws such as the conservation of total energy (in the case of Hamiltonians that do not explicitly depend on time, as is the case in Eq. (1.1)), of total momentum (in the absence of an external confinement potential, $V \equiv 0$), or of total angular momentum (in the presence of spherically symmetric confinement potentials, $V(\mathbf{r}) \equiv V(|\mathbf{r}|)$). More precisely, if we consider an observable $f \equiv f(\mathbf{r}_1, \mathbf{p}_1, \ldots, \mathbf{r}_N, \mathbf{p}_N)$ that depends on the individual positions and momenta of the particles, the *time average* of that observable along a given trajectory is, in the limit of long evolution times $t \to \infty$, identical to the *phase space average* of the observable within the accessible part of the phase space, *i.e.*, within the submanifold of the phase space that is characterized by the same values of the system's constants of motion as the trajectory under consideration. This ergodicity property implicitly assumes that there are no additional dynamical barriers to the evolution of the trajectory in the phase space besides the constants of motion of the system, which can safely be taken for granted in the case of dilute and weakly interacting gases.

In practice, as confinement potentials can hardly be generated with perfect spherical or cylindrical symmetry, only the total energy is generally assumed to remain constant in the course of time evolution. Assuming that this total energy equals E for the trajectory under consideration, the ergodicity postulate is then formulated as

$$\begin{aligned} \overline{f} &\equiv \lim_{T\to\infty} \frac{1}{T} \int_0^T f[\mathbf{r}_1(t), \mathbf{p}_1(t), \ldots, \mathbf{r}_N(t), \mathbf{p}_N(t)] dt \qquad (1.4) \\ &= \int d^3r_1 \int d^3p_1 \cdots \int d^3r_N \int d^3p_N \rho(\mathbf{r}_1, \mathbf{p}_1, \ldots, \mathbf{r}_N, \mathbf{p}_N) f(\mathbf{r}_1, \mathbf{p}_1, \ldots, \mathbf{r}_N, \mathbf{p}_N) \end{aligned}$$

for any observable f defined in the phase space of the many-body system, where

we introduce by

$$\rho(\mathbf{r}_1, \mathbf{p}_1, \ldots, \mathbf{r}_N, \mathbf{p}_N) = \frac{1}{\Omega}\delta\left[E - H(\mathbf{r}_1, \mathbf{p}_1, \ldots, \mathbf{r}_N, \mathbf{p}_N)\right] \tag{1.5}$$

the microscopic probability density to encounter the system at the phase space point $(\mathbf{r}_1, \mathbf{p}_1, \ldots, \mathbf{r}_N, \mathbf{p}_N)$ at some finite time $t > 0$, with

$$\Omega = \int d^3r_1 \int d^3p_1 \cdots \int d^3r_N \int d^3p_N \delta\left[E - H(\mathbf{r}_1, \mathbf{p}_1, \ldots, \mathbf{r}_N, \mathbf{p}_N)\right] \tag{1.6}$$

the phase space volume of the hypersurface at constant energy E. In other words, the statistical average $\overline{f}$ of the observable f is essentially determined by the *absence of any information* about the microscopic state of the system apart from the total energy E. Eqs. (1.5) and (1.6) define the *microcanonical ensemble* of the classical gas under consideration.

It is instructive to calculate the phase space volume $\Omega \equiv \Omega(E, N)$ for the special case of a non-interacting gas, *i.e.* with $U \equiv 0$, which is confined within a container of (spatial) volume V. Neglecting the effect of gravity, the particles of the gas are essentially freely moving within the container, which implies that the Hamiltonian (1.1) is reduced to its kinetic term. This then yields

$$\Omega(E, N) = \frac{V^N (2\pi m E)^{\frac{3}{2}N}}{\Gamma\left(\frac{3}{2}N\right) E}\,, \tag{1.7}$$

i.e. for a large number N of particles the phase space volume scales as $\Omega \sim E^{\frac{3}{2}N}$ with the energy E of the system.

Problems

1.1 Show the validity of Eq. (1.7).

1.2 Quantum ergodicity

We now consider a quantum gas of N particles. The latter is described by a wavefunction $\Psi_t \equiv \Psi_t(\mathbf{r}_1, \ldots, \mathbf{r}_N) \equiv \langle \mathbf{r}_1, \ldots, \mathbf{r}_N | \Psi_t \rangle$ which depends on the positions $\mathbf{r}_1, \ldots, \mathbf{r}_N$ of the individual particles and on the time t. Its time evolution is governed by the Schrödinger equation

$$i\hbar \frac{\partial}{\partial t} \Psi_t(\mathbf{r}_1, \ldots, \mathbf{r}_N) = \hat{H} \Psi_t(\mathbf{r}_1, \ldots, \mathbf{r}_N) \tag{1.8}$$

where the quantum Hamiltonian $\hat{H} = H(\hat{\mathbf{r}}_1, \hat{\mathbf{p}}_1, \ldots, \hat{\mathbf{r}}_N, \hat{\mathbf{p}}_N)$ can be obtained by a direct quantization of the classical Hamiltonian H with $\hat{\mathbf{p}}_j \equiv -i\hbar(\partial/\partial \mathbf{r}_j)$. and

$\hat{\mathbf{r}}_j \equiv \mathbf{r}_j$. This yields

$$\hat{H} = \sum_{j=1}^{N} \left(-\frac{\hbar^2}{2m} \frac{\partial^2}{\partial r_j^2} + V(\mathbf{r}_i) \right) + \frac{1}{2} \sum_{i \neq j=1}^{N} U(\mathbf{r}_i - \mathbf{r}_j) \,. \tag{1.9}$$

as quantum analog of the classical Hamiltonian specified in Eq. (1.1).

In the case of a spatially confined gas, we can assume that the Hamiltonian $\hat{H}$ exhibits a discrete spectrum of eigenenergies E_n with $n \in \mathbb{N}_0$ where the associated orthonormal eigenfunctions Φ_n satisfy the eigenvalue equations

$$\hat{H}\Phi_n(\mathbf{r}_1, \ldots, \mathbf{r}_N) = E_n \Phi_n(\mathbf{r}_1, \ldots, \mathbf{r}_N) \tag{1.10}$$

or alternatively, using the Dirac notation,

$$\hat{H}|\Phi_n\rangle = E_n|\Phi_n\rangle \,. \tag{1.11}$$

The Schrödinger equation (1.8) is therefore solved according to

$$|\Psi_t\rangle = \sum_{n=0}^{\infty} C_n e^{-iE_n t/\hbar} |\Phi_n\rangle \tag{1.12}$$

where the coefficients

$$C_n = \langle \Phi_n | \Psi_0 \rangle \tag{1.13}$$

are obtained from the expansion of the initial state $|\Psi_0\rangle = \sum_{n=0}^{\infty} C_n |\Phi_n\rangle$ within the eigenbasis of the Hamiltonian. This then yields

$$\langle \hat{f} \rangle_t = \langle \Psi_t | \hat{f} | \Psi_t \rangle = \sum_{n,n'=0}^{\infty} C_n^* C_{n'} \langle \Phi_n | \hat{f} | \Phi_{n'} \rangle e^{i(E_n - E_{n'})t/\hbar} \tag{1.14}$$

as the expectation value of the hermitian operator $\hat{f} \equiv f(\hat{\mathbf{r}}_1, \hat{\mathbf{p}}_1, \ldots, \hat{\mathbf{r}}_N, \hat{\mathbf{p}}_N)$ that corresponds to the quantum analog of the classical observable f defined in the phase space of the many-body system. Performing a temporal average of Eq. (1.14) and assuming that total energy is the only conserved quantity of the system, which generally implies that $E_n = E_{n'}$ only if $n = n'$ due to the absence of any additional (*e.g.* spherical) symmetry of the system, we obtain

$$\overline{\langle \hat{f} \rangle} \equiv \lim_{T \to \infty} \frac{1}{T} \int_0^T \langle \hat{f} \rangle_t dt = \sum_{n=0}^{\infty} |C_n|^2 \langle \Phi_n | \hat{f} | \Phi_n \rangle \tag{1.15}$$

for the average expectation value of $\hat{f}$.

To keep the analogy with the classical microcanonical ensemble as close as possible, we may consider an initial quantum state Ψ_0 which in the many-body phase space forms a minimum-uncertainty wave packet that is centred around a

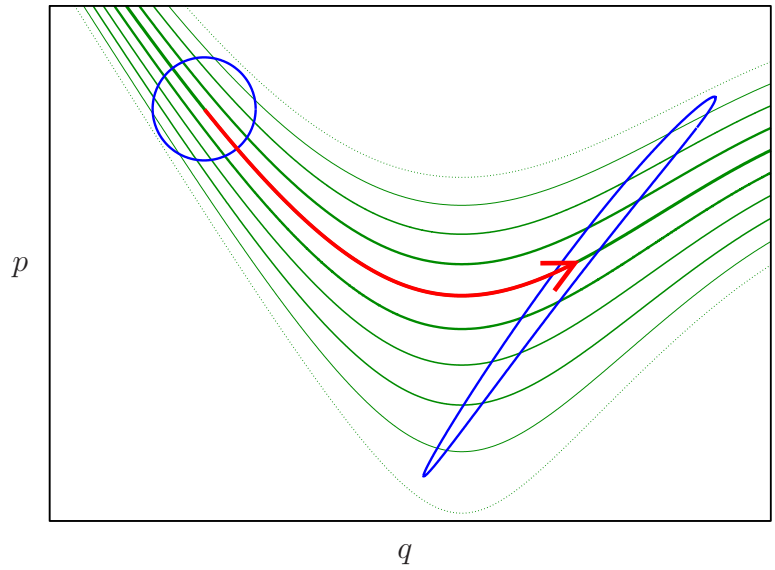

Figure 1.1: Visualization of classical and quantum time evolution in the phase space. A quantum minimum-uncertainty wave packet (illustrated by the blue circle in the upper left corner) evolves along the classical trajectory (shown by the red arrow) that emanates from the wave packet's central position and momentum coordinates. It undergoes spreading due to the fact that the classical evolution of the phase-space volume initially occupied by the wave packet becomes distorted in the course of time evolution (as indicated by the distorted blue ellipse). The green lines indicate the energy levels associated with the quantized eigenstates of the system that effectively contribute to the decomposition of the wave packet in the quantum eigenbasis of the system. According to the eigenstate thermalization hypothesis, those eigenstates are essentially equidistributed around the surfaces of constant eigenenergy in the phase space. The admixture of a given eigenstate to the wave packet (the strength of which is indicated by the thickness of the associated green line) then only depends on the phase-space overlap of the associated eigenenergy surface with the wave packet, or, expressed in an alternative manner, on the vicinity of this eigenenergy to the wave packet's central energy.

given set of initial positions $\mathbf{r}_1^{(0)}, \ldots, \mathbf{r}_N^{(0)}$ and momenta $\mathbf{p}_1^{(0)}, \ldots, \mathbf{p}_N^{(0)}$. As is seen from Eq. (1.15), the crucial ingredient for determining the average expectation values of quantum observables is then given by the set of expansion coefficients C_n of this initial state within the eigenbasis of the Hamiltonian — or, conversely, by the overlap of the eigenstates Φ_n with the specific region in phase space in which this initial state is defined. While there is no rigorous analytical argument that makes any statement about this overlap, numerical evidence obtained in specific, numerically tractable contexts seems to confirm the so-called *eigenstate thermalization hypothesis*[1] for such a system. The latter states in this context that the vast majority of the eigenstates Φ_n of this interacting and classically chaotic quantum gas are expected to be *equidistributed* around the hypersurface of constant energy E_n in the phase space, *i.e.*, the overlap of any such eigenstate with any specific phase space region should depend only on the comparison of the associated eigenenergy E_n with the energy of the phase space region, but not significantly on the particular state Φ_n itself.

In practice, the eigenstate thermalization hypothesis entitles us to substitute $|C_n|^2 \equiv p(E_n)$ in Eq. (1.15), where $p(E_n)$ would then corresponds to the admixture of eigenstates with energy E_n to the initial state Ψ_0. If this initial state is well defined around a given classical phase space point that is characterized by the total energy E, we can write $p(E_n) \propto \delta_{\delta E}(E - E_n)$ for some energetic uncertainty $\delta E > 0$ where $\delta_{\delta E}(E - E_n)$ represents a regularization of the Dirac distribution with the width δE. This then finally yields

$$\overline{\langle \hat{f} \rangle} = \mathrm{Tr}[\hat{\rho}\hat{f}] = \sum_{n=0}^{\infty} \langle \Phi_n | \hat{\rho}\hat{f} | \Phi_n \rangle \tag{1.16}$$

as statistical average of $\hat{f}$ where we define by

$$\hat{\rho} = \frac{1}{g} \sum_{n=0}^{\infty} \delta_{\delta E}(E - E_n) |\Phi_n\rangle\langle\Phi_n| = \frac{1}{g} \delta_{\delta E}(E - \hat{H}) \tag{1.17}$$

the *statistical density operator* of the microcanonical ensemble. By normalization we have

$$g = \sum_{n=0}^{\infty} \delta_{\delta E}(E - E_n) \tag{1.18}$$

which in the limit $\delta E \to 0$ turns into the density of states

$$g = \sum_{n=0}^{\infty} \delta(E - E_n) \equiv g(E, N) \tag{1.19}$$

[1] J. M. Deutsch, *Quantum statistical mechanics in a closed system*, Phys. Rev. A 43, 2046 (1991); M. Srednicki, *Chaos and quantum thermalization*, Phys. Rev. E 50, 888 (1994).

of the many-body quantum system. By semiclassical considerations one can show that

$$g(E,N) \simeq \frac{\Omega(E,N)}{(2\pi\hbar)^{3N}} \tag{1.20}$$

for large E and N (for which the density of states becomes extremely high and therefore quasi-continuous), with $\Omega(E,N)$ being the classical phase space volume at energy E given by Eq. (1.6). This expresses the *Bohr-Sommerfeld quantization rule* which states that there is exactly one quantum state per Planck cell with volume $(2\pi\hbar)^{3N}$ in the N-particle phase space.

Clearly, choosing an initial state that is localized in phase space around well-defined positions $\mathbf{r}_i$ and momenta $\mathbf{p}_i$ of the individual particles $i = 1,\ldots,N$ generally violates the *symmetry postulate* associated with indistinguishable quantum particles, which implies that the wavefunction must be fully symmetrized or antisymmetrized in its coordinates $\mathbf{r}_1,\ldots,\mathbf{r}_N$. While such a symmetrization or antisymmetrization does not alter the implications of the eigenstate thermalization hypothesis, it does affect the density of states of the system insofar as we would have

$$g(E,N) \simeq \frac{\Omega(E,N)}{N!(2\pi\hbar)^{3N}} \tag{1.21}$$

for large E and N, due to the restriction to the fully symmetrized or antisymmetrized submanifold of the classical phase space. This consideration will become important in the following.

Problems

1.2 Show the validity of Eq. (1.20) in the formal semiclassical limit $\hbar \to 0$.

1.3 Thermal equilibrium

Before dealing with the issue of quantum indistinguishability in more detail, let us first consider the case of a system that is composed of two gases of (not necessarily indistinguishable) quantum particles, which are denoted by A and B and respectively contain N_A and N_B particles. These gases are supposed to be separated from each other *e.g.* by some sort of wall, which means that no particle from the gas A (or B) can penetrate into the gas B (or A). However, they can exchange energy with each other *e.g.* through collisions of particles from either side with the wall.

Assuming that this composed system exhibits quantum ergodicity and was initially prepared in a state with total energy E, we can again describe average expectation values of observables defined within this system through the statistical density operator

$$\hat{\rho} = \frac{1}{g}\delta(E-\hat{H}) \tag{1.22}$$

where g is the density of eigenstates of this system at energy E and $\hat{H}$ denotes its quantum Hamiltonian. The latter is written as

$$\hat{H} = \hat{H}_A + \hat{H}_B + \hat{W} \tag{1.23}$$

where $\hat{H}_X = H_X(\hat{\mathbf{r}}_1^X, \hat{\mathbf{p}}_1^X, \ldots, \hat{\mathbf{r}}_{N_X}^X, \hat{\mathbf{p}}_{N_X}^X)$ with $X = A$ or B denotes the internal Hamiltonian of the gas A or B, respectively, which one would encounter in the presence of mutual isolation of these gases from each other. Neglecting the relevance of the internal (solid-state) degrees of freedom within the wall, the energetic coupling between the two subsystems A and B can be modeled by an operator of the generic form

$$\hat{W} = W\left(\hat{\mathbf{r}}_1^A, \hat{\mathbf{p}}_1^A, \ldots, \hat{\mathbf{r}}_{N_A}^A, \hat{\mathbf{p}}_{N_A}^A, \hat{\mathbf{r}}_1^B, \hat{\mathbf{p}}_1^B, \ldots, \hat{\mathbf{r}}_{N_B}^B, \hat{\mathbf{p}}_{N_B}^B\right) . \tag{1.24}$$

While it technically depends on the positions $\hat{\mathbf{r}}_j^X$ and momenta $\hat{\mathbf{p}}_j^X$ of all particles ($j = 1, \ldots, N_X$) that are contained within the gases $X = A$ and B, only a tiny fraction of them do actually contribute to this coupling energy in practice, namely those that happen to be located within a very small (typically nanometric) distance from the separating wall which mediates the transfer of energy. The expectation value $\langle\hat{W}\rangle$ of this coupling operator can therefore be considered to be negligibly small as compared to the expectation values of the internal Hamiltonians $\hat{H}_A$ and $\hat{H}_B$ of the two gases, provided the latter are prepared at a reasonably finite (*i.e.* not ultra-low) total energy and within a reasonably large (*i.e.* not ultra-small) volume. We therefore permit ourselves to neglect the contribution of the coupling energy to the total Hamiltonian, which thence will be approximated as $\hat{H} \simeq \hat{H}_A + \hat{H}_B$ in the expression (1.22) for the density operator. The latter can then be expressed as

$$\hat{\rho} \simeq \frac{1}{g}\delta(E - \hat{H}_A - \hat{H}_B) = \frac{1}{g}\int dE_A \delta(E_A - \hat{H}_A)\delta(E - E_A - \hat{H}_B) . \tag{1.25}$$

We shall now consider an observable $\hat{f} \equiv f(\hat{\mathbf{r}}_1^A, \hat{\mathbf{p}}_1^A, \ldots, \hat{\mathbf{r}}_N^A, \hat{\mathbf{p}}_N^A)$ that is restricted to the gas A, *i.e.*, it only depends on the position and momentum operators of the particles that are contained within this particular subsystem. The statistical average of its expectation value is then straightforwardly evaluated by virtue of Eqs. (1.16) and (1.25) yielding

$$\begin{aligned} \overline{\langle\hat{f}\rangle} &= \mathrm{Tr}[\hat{\rho}\hat{f}] \simeq \frac{1}{g}\int dE_A \mathrm{Tr}\left[\hat{f}\delta(E_A - \hat{H}_A)\delta(E - E_A - \hat{H}_B)\right] \\ &= \frac{1}{g}\int dE_A \mathrm{Tr}_A\left[\hat{f}\delta(E_A - \hat{H}_A)\right]\mathrm{Tr}_B\left[\delta(E - E_A - \hat{H}_B)\right] . \end{aligned} \tag{1.26}$$

Here Tr_X denotes the *partial trace* associated with the subsystem $X = A$ or B, which can be defined in terms the orthonormal eigenfunctions Φ_n^X of $\hat{H}_X$ (or in

terms of any other orthonormal set of basis functions spanning the Hilbert space of the subsystem X) as

$$\mathrm{Tr}_X[\hat{O}] = \sum_n \langle \Phi_n^X | \hat{O} | \Phi_n^X \rangle \tag{1.27}$$

for any operator $\hat{O}$ acting within that subsystem. Equation (1.26) exploits the identity

$$\mathrm{Tr}[\hat{F}_A \hat{G}_B] = \mathrm{Tr}_A[\hat{F}_A]\mathrm{Tr}_B[\hat{G}_B] \tag{1.28}$$

for any product of operators $\hat{F}_A$ and $\hat{G}_B$ that are restricted to the Hilbert spaces of the subsystems A and B, respectively, which can be explicitly shown by evaluating the trace of $\hat{F}_A \hat{G}_B$ within the product basis formed by combining the eigenfunctions Φ_n^A and $\Phi_{n'}^B$ for every possible pair (n, n'). Utilizing now the expression

$$g_X(E_X) = \mathrm{Tr}_X \left[\delta(E_X - \hat{H}_X) \right] \tag{1.29}$$

for the density of eigenstates within the (isolated) subsystem $X = A$ or B, we finally obtain

$$\overline{\langle \hat{f} \rangle} = \mathrm{Tr}_A[\hat{\rho}_A \hat{f}] \tag{1.30}$$

from Eq. (1.26) with the effective density operator

$$\hat{\rho}_A = \frac{1}{g} \int dE_A \delta(E_A - \hat{H}_A) g_B(E - E_A) = \frac{1}{g} g_B(E - \hat{H}_A) \tag{1.31}$$

of the subsystem A.

As a particularly relevant special case, we shall now consider the observable $\hat{f} = \delta(E_A - \hat{H}_A)$ whose expectation value yields the probability density to encounter the partial energy E_A within the subsystem A. The statistical average of this probability density is evaluated from Eqs. (1.30) and (1.31) as

$$\begin{aligned} P_A(E_A) &= \overline{\langle \delta(E_A - \hat{H}_A) \rangle} = \frac{1}{g} \sum_n g_B(E - E_n^A) \delta(E_A - E_n^A) \\ &= \frac{1}{g} g_B(E - E_A) g_A(E_A) \,, \end{aligned} \tag{1.32}$$

where we evaluate the partial trace of the subsystem A within the eigenbasis of the corresponding Hamiltonian $\hat{H}_A$ whose eigenenergies are denoted by E_n^A. Insight into the general behaviour of this function can be obtained from the typical scaling law

$$g_X(E_X) \propto E_X^{\frac{3}{2}N_X} \tag{1.33}$$

of the density of states for very weakly interacting (isolated) three-dimensional gases containing N_X particles, which results from the expression (1.7) of the classical phase space volume at the energy E_X in combination with the identification

(1.20) (or (1.21)). This yields

$$P_A(E_A) \propto E_A^{\frac{3}{2}N_A}(E-E_A)^{\frac{3}{2}N_B}\,. \tag{1.34}$$

It is now straightforward to convince oneself that P_A represents an extremely strongly peaked function in the thermodynamic limit of large numbers of particles $N_A, N_B \gtrsim 10^5 \ldots 10^{10}$ within the two subsystems, which exhibits a very sharp maximum at some well-defined energy $\overline{E}_A$ within the interval $0 < \overline{E}_A < E$. Using the notation

$$g'_X(\mathcal{E}) \equiv \left.\frac{dg_X}{dE_X}\right|_{E_X=\mathcal{E}}\,, \tag{1.35}$$

this particular maximum can be determined from the property

$$0 = \frac{dP_A}{dE_A}(\overline{E}_A) = \frac{g_B(E-\overline{E}_A)g'_A(\overline{E}_A) - g_A(\overline{E}_A)g'_B(E-\overline{E}_A)}{g} \tag{1.36}$$

from which we obtain the relation

$$\frac{g'_A(\overline{E}_A)}{g_A(\overline{E}_A)} = \frac{g'_B(E-\overline{E}_A)}{g_B(E-\overline{E}_A)} \tag{1.37}$$

or, equivalently,

$$\left.\frac{d}{E_A}\ln g_A\right|_{E_A=\overline{E}_A} = \left.\frac{d}{E_B}\ln g_B\right|_{E_B=E-\overline{E}_A}\,. \tag{1.38}$$

It is now appropriate to introduce the concepts of entropy and temperature. The *entropy* of the subsystem $X = A$ or B can be defined as

$$S_X(E_X) = k_B \ln\left[\delta E g_X(E_X)\right] \tag{1.39}$$

as a function its energy E_X, where $g_X(E_X)$ denotes again its density of states at E_X and $k_B \simeq 1.38 \times 10^{-23}\,\mathrm{J/K}$ is the Boltzmann constant. δE represents a typical scale for the uncertainty of the total energy which is associated with the preparation of the initial state of the system as was discussed in Section 1.2. $\exp[S_X(E_X)/k_B]$ yields then a characteristic scale for the number of many-body eigenstates that are effectively involved in the time evolution of the (isolated) system X, provided the latter was initially prepared in a wave packet state that is sharply defined about the energy E_X with the uncertainty δE. The *temperature* of the subsystem X is then obtained as

$$T_X(E_X) = \frac{1}{k_B\beta_X(E_X)} \tag{1.40}$$

where we define

$$\beta_X(E_X) = \frac{1}{k_B}\frac{\partial S_X}{\partial E_X}(E_X)\,. \tag{1.41}$$

The condition (1.38) can then be rewritten as

$$T_A(\overline{E}_A) = T_B(E - \overline{E}_A)\,, \tag{1.42}$$

which simply implies that the two parts of the system are *thermalized*, *i.e.*, they exhibit the same temperature.

In the special case of an ideal, *i.e.* non-interacting, gas within the subsystem $X = A$ or B, we can obtain its density of states at the energy E_X by combining the expression (1.7) of the classical phase space volume at E_X with the identification (1.20). This yields

$$g_X(E_X) = C(N_X) E_X^{\frac{3}{2}N_X - 1} \tag{1.43}$$

for some positive prefactor $C(N_X) > 0$ which is not important in the following. The associated entropy is then given by

$$S_X(E_X) = k_B \ln\left[\delta E\, C(N_X) E_X^{\frac{3}{2}N_X - 1}\right] \simeq \frac{3}{2} N_X k_B \ln E_X + k_B \ln[\delta E\, C(N_X)] \tag{1.44}$$

using $N_X \gg 1$, and we therefore obtain

$$T_X(E_X) = \frac{2E_X}{3N_X k_B} \tag{1.45}$$

for the temperature within this gas. The thermalization condition $T_A(E_A) = T_B(E_B)$ can then be rewritten as $E_A/N_A = E_B/N_B$, which essentially states that each particle of the system has, on average, the same energy. This yields

$$\overline{E}_A = \frac{N_A}{N_A + N_B} E \tag{1.46}$$

as explicit expression for the most probable partial energy to be encountered within the subsystem A.

Let us now suppose that the subsystem B is much larger than the subsystem A, insofar as we have $N_B \gg N_A$ and hence, by virtue of Eq. (1.46), $\overline{E}_A \ll E$. It is tempting to simplify the expression for the effective density operator (1.31) for the subsystem A in that case, namely by performing a Taylor series expansion of $g_B(E_B = E - \hat{H}_A)$ about $E_B = E$. We should note, however, that $g_B(E_B)$ generally increases as a power law $\propto E_B^\nu$ with an extremely large exponent $\nu = 3N_B/2 \gg 1$. Hence, a Taylor series about $E_B = E$ would yield a good approximation of $g_B(E_B)$ only within an extremely small energy window around E, namely for $|E_B - E| < \Delta E$ with $\Delta E \sim E/N_B$, which would be too small to be of any usefulness in practice. As we can see from the expressions (1.39) and (1.44), the *entropy* of the subsystem B, on the other hand, is a rather well-behaved (namely logarithmic) function of E_B, for which a Taylor series expansion would yield a reasonable approximation within a finite energy interval. We therefore rewrite Eq. (1.31) as

$$\hat{\rho}_A = \frac{1}{g} g_B(E - \hat{H}_A) = \frac{1}{g} \exp\left[\ln g_B(E - \hat{H}_A)\right] \tag{1.47}$$

and expand

$$\ln g_B(E - \hat{H}_A) \simeq \ln g_B(E) - \beta_B(E)\hat{H}_A \tag{1.48}$$

in first order in $\hat{H}_A$ in the exponent, using $\beta_B(E_B) = \partial \ln g_B(E_B)/\partial E_B$ according to Eq. (1.41). This yields

$$\hat{\rho}_A = \frac{g_B(E)}{g} \exp\left[-\beta_B(E)\hat{H}_A\right] . \tag{1.49}$$

These considerations finally give rise to the *canonical ensemble* which applies to a quantum gas that is not isolated but energetically coupled to a large reservoir of heat. Identifying the latter with the subsystem B and the quantum gas with the subsystem A, we can infer from the above reasoning that average expectation values of observables defined within such a gas are described by the density operator

$$\hat{\rho} = \frac{1}{Z} e^{-\beta \hat{H}} \tag{1.50}$$

where $\hat{H}$ denotes the Hamiltonian of the quantum gas and $T = 1/(k_B\beta)$ is the temperature of the reservoir. From the normalization condition $\mathrm{Tr}[\hat{\rho}] = 1$ that any density operator has to satisfy, we determine the prefactor as

$$Z = \mathrm{Tr}\left[e^{-\beta \hat{H}}\right] , \tag{1.51}$$

which is also called *partition function* of the canonical ensemble.

In contrast to the microcanonical ensemble discussed in Section 1.2, the energy of the quantum gas under consideration is no longer constant but may fluctuate due to the coupling of the system with the reservoir. It is instructive to compare the root-mean-square (rms) width ΔH of these fluctuations with the average energy $\overline{\langle \hat{H} \rangle}$ contained within the gas. We assume for this purpose again that we are dealing with a rather weakly interacting gas, such that we can approximately express the scaling of the density of states with its energy E as

$$g(E) = \sum_n \delta(E - E_n) = C(N) E^{\frac{3}{2}N - 1} , \tag{1.52}$$

where E_n with $n \in \mathbb{N}_0$ are the eigenenergies of the quantum gas and $C(N) > 0$ is a positive prefactor that depends on the number N of particles within the gas. This yields

$$\left(\frac{\Delta H}{\overline{\langle \hat{H} \rangle}}\right)^2 = \frac{\overline{\langle \hat{H}^2 \rangle} - \overline{\langle \hat{H} \rangle}^2}{\overline{\langle \hat{H} \rangle}^2} = \frac{2}{3N} \ll 1 \tag{1.53}$$

As a consequence, fluctuations of the energy within the gas become relatively unimportant in the thermodynamic limit $N \to \infty$ as compared to its mean energy. Hence, given the fact that $N \gtrsim 10^5 \ldots 10^{10}$, the canonical ensemble yields, for all practical purposes, identical predictions as the microcanonical ensemble for the mean value of observables $\hat{f} \equiv f(\hat{H})$ that can be expressed as functions of the Hamiltonian.

Problems

1.3 Show the validity of Eq. (1.53).

1.4 Bosons and fermions

While a generic gas such as ordinary air may be constituted by atoms and/or molecules that belong to several species, we shall, in the following, focus on the special case of a monoatomic gas containing atoms of only one species, *e.g.* ^{87}Rb, which is most relevant for the realization of Bose-Einstein condensates. We are then dealing with a system of *indistinguishable* quantum particles that have identical properties, which implies that the many-body Hamiltonian governing the time evolution of this system is invariant under permutations of particles. The *symmetry postulate* of quantum mechanics then states that it is as a matter of principle strictly impossible to distinguish any particle in this many-body system with respect to the others. This is formally expressed by the fact that the wavefunction describing a physically admissible state of the system has to be either fully symmetric or fully antisymmetric with respect to the permutation of particles, in which case the latter would respectively be named *bosons* or *fermions*.

It is known from the theory of elementary particles that the quarks and leptons are fermions. Their wavefunctions are given by Dirac spinors which feature a half-integer spin, namely spin 1/2. Exchange particles such as the photon as well as the W and Z bosons, on the other hand, can be interpreted as the quanta that arise from the quantization of a classical field theory (*e.g.*, electromagnetic theory in the case of photons) and are consequently bosons. They are described by a four-potential $(A^\nu) \equiv (A^0, \mathbf{A})$ which generally exhibits three independent components[2] due to the Lorenz gauge $\frac{\partial}{\partial t} A^0(\mathbf{r}, t) + \nabla \cdot \mathbf{A}(\mathbf{r}, t) = 0$. This implies that they have an integer spin, namely spin 1.

In order to determine the bosonic or fermionic nature of a composite particle, such as an atom or molecule, we need to count the number of elementary fermionic particles by which it is constituted. If this number is odd, we are dealing with a fermion, while in the opposite case of an even number of fermionic constituents the particle under consideration would behave as a boson. The proton, for instance, is a fermion as it is constituted by three quarks. It contains an uncountable number of gluons and virtual quark-antiquark pairs as well, but those do not alter the fact that its total number of fermionic constituents is odd. Exactly the same holds true for the neutron. The hydrogen atom, on the other hand, is a boson as it is formed by a proton and an electron and therefore contains an even number of fermionic constituents. Indeed, a physically admissible wavefunction describing

[2]This is different for massless exchange particles such as the photon, whose associated four-potential features only two independent components. They nevertheless have spin 1 as well.

two hydrogen atoms, which has to be fully antisymmetric in the coordinates of all the involved elementary fermionic particles (*i.e.*, the quarks and electrons in this case), will undergo an even number of sign changes when the sets of fermionic coordinates constituting the two atoms are interchanged one by one, which in effect implies that it keeps its sign under the exchange of the two atoms.

As a fully equivalent alternative to the counting of elementary fermionic constituents, we can also infer the bosonic or fermionic nature of a particle species from its total spin, using basic rules for the addition of angular momentum operators. A half-integer total spin necessarily arises from an odd number of fermionic constituents and therefore corresponds to a fermionic particle, while in the case of an integer total spin we are dealing with a boson. This is the essence of the spin-statistics theorem.

Let us now consider a quantum gas consisting of N indistinguishable particles that are of bosonic or fermionic nature. For the sake of simplicity, we assume that they all feature the same internal spin state, which implies that we can effectively neglect their spin degree of freedom in the following. If $(\phi_k)_{k\in\mathbb{N}_0}$ with $\phi_k : \mathbb{R}^3 \to \mathbb{C}$ represents an orthonormal basis of the single-particle Hilbert space of the system, we can construct properly normalized basis states of the many-body system under consideration through

$$\Phi_{k_1\cdots k_N}(\mathbf{r}_1,\ldots,\mathbf{r}_N) = \frac{1}{\sqrt{N!\prod_{k=0}^{\infty} n_k!}} \sum_{\pi\in\Pi_N} (\pm 1)^{\pi} \phi_{k_{\pi(1)}}(\mathbf{r}_1)\cdots\phi_{k_{\pi(N)}}(\mathbf{r}_N) \quad (1.54)$$

in the case of bosons (upper sign) and fermions (lower sign). Here, Π_N represents the set of all permutations $\pi : \{1,\ldots,N\} \to \{1,\ldots,N\}$ of the first N positive natural numbers. Their *sign* can be defined through

$$(-1)^{\pi} \equiv \prod_{n=2}^{N} \prod_{n'=1}^{n-1} \frac{\pi(n)-\pi(n')}{n-n'} \,. \quad (1.55)$$

It equals 1 for a permutation π that can be decomposed into an even number of elementary transpositions, while it is -1 if this number is odd. n_k denotes the number of times that k is listed in the set of quantum numbers $\{k_1,\ldots,k_N\}$. To avoid multiple listing of identical states in the many-body basis, we impose the restriction $k_1 \geq k_2 \geq \ldots \geq k_N$ in the case of bosons as well as $k_1 > k_2 > \ldots > k_N$ in the case of fermions. The latter choice is motivated from the *Pauli exclusion principle* for fermions stating that $\Phi^{-}_{k_1\cdots k_N}(\mathbf{r}_1,\ldots,\mathbf{r}_N) = 0$ for all $\mathbf{r}_1,\ldots,\mathbf{r}_N$ if $k_i = k_j$ for a pair of indices $1 \leq i < j \leq N$, as we can infer from Eq. (1.54). This yields binary occupancies $n_k \in \{0,1\}$ in the case of fermions, while we would have $n_k \in \mathbb{N}_0$ for bosons.

It is convenient to express the above many-body basis states as $|\Phi_{k_1,\ldots,k_N}\rangle \equiv |n_0,n_1,\ldots\rangle$ in terms of the occupancies n_k that are associated with the chosen single-particle basis $(\phi_k)_{k\in\mathbb{N}_0}$. The collection of such *Fock states* $|n_0,n_1,\ldots\rangle$ for all

possible values of n_k that respect the bosonic or fermionic nature of the particle species under consideration (but are not restricted to a given total number of particles) span the *Fock space* of the many-body system under consideration. Within this Fock space we introduce *creation* and *annihilation* operators $\hat{a}_k^\dagger$, $\hat{a}_k$, which respectively create or remove a particle on the one-body state ϕ_k. In the case of bosons they are defined as

$$\hat{a}_k|n_0, n_1, \ldots, n_k, \ldots\rangle = \sqrt{n_k}|n_0, n_1, \ldots, n_k - 1, \ldots\rangle\,, \tag{1.56}$$
$$\hat{a}_k^\dagger|n_0, n_1, \ldots, n_k, \ldots\rangle = \sqrt{n_k + 1}|n_0, n_1, \ldots, n_k + 1, \ldots\rangle\,, \tag{1.57}$$

which implies the commutation relations

$$[\hat{a}_k, \hat{a}_{k'}^\dagger] \equiv \hat{a}_k\hat{a}_{k'}^\dagger - \hat{a}_{k'}^\dagger\hat{a}_k = \delta_{kk'} \tag{1.58}$$

as well as $[\hat{a}_k, \hat{a}_{k'}] = 0 = [\hat{a}_k^\dagger, \hat{a}_{k'}^\dagger]$ for all $k, k' \in \mathbb{N}_0$. For fermions we define them according to

$$\hat{a}_k|n_0, \ldots, n_k, \ldots\rangle = (-1)^{n_0+\ldots+n_{k-1}} n_k|n_0, \ldots, n_k - 1, \ldots\rangle\,, \tag{1.59}$$
$$\hat{a}_k^\dagger|n_0, \ldots, n_k, \ldots\rangle = (-1)^{n_0+\ldots+n_{k-1}}(1 - n_k)|n_0, \ldots, n_k + 1, \ldots\rangle\,, \tag{1.60}$$

in order to account for the sign convention that is adopted in the definition (1.54) of the fermionic basis states. They therefore satisfy the anticommutation relations

$$\{\hat{a}_k, \hat{a}_{k'}^\dagger\} \equiv \hat{a}_k\hat{a}_{k'}^\dagger + \hat{a}_{k'}^\dagger\hat{a}_k = \delta_{kk'} \tag{1.61}$$

as well as $\{\hat{a}_k, \hat{a}_{k'}\} = 0 = \{\hat{a}_k^\dagger, \hat{a}_{k'}^\dagger\}$ for all k, k'.

While the above creation and annihilation operators are intimately connected with a given (discrete) single-particle basis, we can generalize the underlying concept to the (continuous) position space through the introduction of the *field operators*

$$\hat{\psi}^\dagger(\mathbf{r}) = \sum_{k=0}^{\infty} \phi_k^*(\mathbf{r})\hat{a}_k^\dagger \quad \text{and} \quad \hat{\psi}(\mathbf{r}) = \sum_{k=0}^{\infty} \phi_k(\mathbf{r})\hat{a}_k\,, \tag{1.62}$$

which respectively create and annihilate a particle at the position $\mathbf{r} \in \mathbb{R}^3$. As can be straightforwardly inferred from the above definition in combination with the orthogonality and completeness of the single-particle basis $(\phi_k)_{k\in\mathbb{N}_0}$, these field operators satisfy for all $\mathbf{r}, \mathbf{r}' \in \mathbb{R}^3$ the commutation relations

$$[\hat{\psi}(\mathbf{r}), \hat{\psi}^\dagger(\mathbf{r}')] = \delta(\mathbf{r} - \mathbf{r}') \tag{1.63}$$

and $[\hat{\psi}(\mathbf{r}), \hat{\psi}(\mathbf{r}')] = 0 = [\hat{\psi}^\dagger(\mathbf{r}), \hat{\psi}^\dagger(\mathbf{r}')]$ for bosons as well as the anticommutation relations

$$\{\hat{\psi}(\mathbf{r}), \hat{\psi}^\dagger(\mathbf{r}')\} = \delta(\mathbf{r} - \mathbf{r}') \tag{1.64}$$

and $\{\hat{\psi}(\mathbf{r}), \hat{\psi}(\mathbf{r}')\} = 0 = \{\hat{\psi}^\dagger(\mathbf{r}), \hat{\psi}^\dagger(\mathbf{r}')\}$ for fermions. They allow one to represent the many-body equivalent of single-particle observables in a rather straightforward and compact manner. Consider, for instance, a one-body observable $A \equiv A(\mathbf{r}, \mathbf{p})$ (such as the energy of a particle within some confinement potential) which is most generally defined in terms of the position and momentum operators of the particle. Its quantum many-body equivalent (which would then yield the total single-particle energy of a quantum gas in the above example) is then expressed as

$$\hat{A} = \sum_{j=1}^{N} A(\hat{\mathbf{r}}_j, \hat{\mathbf{p}}_j) = \int d^3r \, \hat{\psi}^\dagger(\mathbf{r}) \, A\left(\mathbf{r}, \frac{\hbar}{i}\frac{\partial}{\partial \mathbf{r}}\right) \, \hat{\psi}(\mathbf{r}) \tag{1.65}$$

in terms of the field operators, as can be shown by applying this operator onto the many-particle basis states (1.54) using the decomposition (1.62) in combination with Eqs. (1.56) and (1.57) for bosons as well as with Eqs. (1.59) and (1.60) for fermions. Similarly, the many-body equivalent of a two-body observable $B \equiv B(\mathbf{r}, \mathbf{r}') = B(\mathbf{r}', \mathbf{r})$ that is expressed in terms of the positions $\mathbf{r}$ and $\mathbf{r}'$ of the two particles (such as the interaction energy between two particles) is, for both bosons and fermions, obtained as

$$\hat{B} = \frac{1}{2} \sum_{i \neq j = 1}^{N} B(\mathbf{r}_i, \mathbf{r}_j) = \frac{1}{2} \int d^3r \int d^3r' \hat{\psi}^\dagger(\mathbf{r}) \hat{\psi}^\dagger(\mathbf{r}') B(\mathbf{r}, \mathbf{r}') \hat{\psi}(\mathbf{r}') \hat{\psi}(\mathbf{r}) \tag{1.66}$$

in terms of the field operators. We can consequently rewrite the expression (1.9) for a typical many-body Hamiltonian featuring a generic two-body interaction as

$$\begin{aligned} \hat{H} \;\; = \;\; & \int d^3r \hat{\psi}^\dagger(\mathbf{r}) \left(-\frac{\hbar^2}{2m}\frac{\partial^2}{\partial \mathbf{r}^2} + V(\mathbf{r}) \right) \hat{\psi}(\mathbf{r}) \\ & + \frac{1}{2} \int d^3r \int d^3r' U(\mathbf{r} - \mathbf{r}') \hat{\psi}^\dagger(\mathbf{r}) \hat{\psi}^\dagger(\mathbf{r}') \hat{\psi}(\mathbf{r}') \hat{\psi}(\mathbf{r}) \, . \end{aligned} \tag{1.67}$$

As was already indicated at the end of Section 1.2, the above symmetry considerations have dramatic consequences on the definition of the quantum microcanonical ensemble. Indeed, if we apply the line of reasoning that we developed within Section 1.2 to a system of N indistinguishable particles of, say, bosonic (or fermionic) nature, the minimum-uncertainty wave packet that we considered in that section to be centred about the initial positions $\mathbf{r}_1^{(0)}, \ldots, \mathbf{r}_N^{(0)}$ and momenta $\mathbf{p}_1^{(0)}, \ldots, \mathbf{p}_N^{(0)}$ in the classical phase space ought to be fully symmetrized (or antisymmetrized) with respect to permutations of particles, in close analogy with the expression (1.54). Consequently, the time evolution of this wave packet takes place within the fully symmetric (or antisymmetric) subspace of the Hilbert space, which implies that the many-body eigenstates Φ_n in terms of which the wave packet is represented according to Eq. (1.12) belong to that subspace, too.

The phase space that is explored by this wave packed in the course of time evolution is then effectively restricted to a desymmetrized simplex of the total phase space volume (1.6) of the hypersurface at constant energy. This in turn reduces the density of quantum states by the factor $N!$, as expressed within Eq. (1.21).

It is insightful to stress that the occurrence of this latter prefactor $1/N!$ is not a genuinely quantum feature *per se*. Indeed, the reduction of the phase space volume to a desymmetrized simplex would effectively arise also in the classical microcanonical ensemble expressed by Eq. (1.5), simply because in a system of indistinguishable particles we are practically unable to discriminate a specific microscopic measurement outcome $(\mathbf{r}_1, \mathbf{p}_1, \ldots, \mathbf{r}_N, \mathbf{p}_N)$ given by the positions and momenta of the particles from any of its permutations $(\mathbf{r}_{\pi(1)}, \mathbf{p}_{\pi(1)}, \ldots, \mathbf{r}_{\pi(N)}, \mathbf{p}_{\pi(N)})$. This implies that as a matter of practice we would have to replace the considered observable through

$$\begin{aligned} f(\mathbf{r}_1, \mathbf{p}_1, \ldots, \mathbf{r}_N, \mathbf{p}_N) \;&\mapsto\; \sum_{\pi \in \Pi_N} f\left(\mathbf{r}_{\pi(1)}, \mathbf{p}_{\pi(1)}, \ldots, \mathbf{r}_{\pi(N)}, \mathbf{p}_{\pi(N)}\right) \\ &=\; N! f(\mathbf{r}_1, \mathbf{p}_1, \ldots, \mathbf{r}_N, \mathbf{p}_N) \end{aligned} \tag{1.68}$$

in the expression (1.4) for its statistical average (taking into account that f ought to be invariant under permutations of particles to represent a valid observable in a system of indistinguishable particles) — or, alternatively, that we would have to divide Ω by $N!$ in the expression (1.5) for the microscopic probability density that constitutes the classical microcanonical ensemble, in perfect analogy with the corresponding quantum system.

Despite this apparent similarity, classical and quantum systems of indistinguishable particles do not exhibit identical statistical properties. This is spectacularly evidenced in the regime of *quantum degeneracy*, where the number of particles contained in the system becomes comparable to or even larger than the number of accessible single-particle states at a given total energy (or at a given temperature of the reservoir, in the framework of the canonical ensemble). Consider, for instance, a system of two particles that can occupy two single-particle states A or B with equal probability. If these particles are distinguishable, the system can be in four different two-particle states, namely AA, AB, BA, and BB (where the first letter denotes the state occupied by the first particle and the second letter refers to the second particle), which implies that the probability for each one of those states to be encountered equals $1/4$. From a classical point of view, these considerations would also hold for indistinguishable particles, with the only amendment that one would not be able to discriminate the two-particle states AB and BA in practice. The state AA, however, would still be encountered with the probability $1/4$.

Owing to the symmetry postulate, the situation is quite different in a system of two *quantum* indistinguishable particles. If these particles are bosons, we would encounter with equal probability the states AA, BB, and AB, where the latter

corresponds to the symmetric superposition of the two-body states AB and BA and should actually read $AB+BA$ (up to a normalization factor). Consequently, the probability to detect the system in the state AA equals $1/3$ instead of $1/4$. If we were dealing with fermions instead, this probability would vanish due to the Pauli principle, and the system could be encountered in one single state only, namely $AB \equiv AB-BA$ corresponding to the antisymmetric superposition of the two-body states AB and BA.

The above enhancement effect in the bosonic case is dramatically amplified if we increase the number of particles and states. In a system of three indistinguishable particles that can occupy three one-body states A, B, or C with equal probability, classical statistical considerations would predict the probability $1/27$ to detect it in the state AAA, as there are $3^3 = 27$ different possibilities to distribute three particles among three states. This number is significantly reduced if we are dealing with bosonic quantum particles, in which case the system can be found with equal likelihood in the states AAA, BBB, CCC, $AAB \equiv AAB + ABA + BAA$ (and similarly for the others), AAC, BBA, BBC, CCA, CCB, as well as $ABC \equiv ABC+BCA+CAB+BAC+ACB+CBA$. The probability to detect the system in the state AAA hence equals $1/10$ and is therefore dramatically increased as compared to the prediction $1/27$ that is based on classical intuition. This *Bose enhancement* lies at the heart of Bose-Einstein condensation. Again, the fermionic counterpart of this system features only one possible three-particle state, namely $ABC \equiv ABC+BCA+CAB-BAC-ACB-CBA$.

Chapter 2

Bose-Einstein condensation

2.1 The grand canonical ensemble

In principle, the canonical ensemble discussed in Section 1.3 appears perfectly appropriate to describe the cooling process of a gas of neutral atoms. Indeed, as shall be detailed in Chapter 3, those atoms are, for that purpose, confined in trapping configurations that are created by magnetic fields or laser fields in high vacuum. Cooling of the gas is then achieved via its interaction with a suitably tuned electromagnetic radiation which effectively plays the role of an external heat bath with which the atoms can exchange energy.

From the point of view of analytical calculations, however, the canonical ensemble is not well suited for the evaluation of statistical expectation values in the context of indistiguishable quantum particles. As a matter of fact, those expectation values are most conveniently calculated in the Fock space that is defined with respect to a suitably chosen single-particle basis, and the restriction to a fixed total number of particles that is inherent in the canonical ensemble gives then rise to rather involved combinatorial expressions which are hard to deal with. We shall therefore consider a slightly modified trapping and cooling scenario with respect to the experimental reality, namely where the atomic gas is in permanent contact with a fictitious reservoir of particles, and then rely on the general expectation that predictions obtained within this particular framework ought to be equivalent, at least in the thermodynamic limit, to those resulting from the canonical ensemble. Note that this distinction between a "system" containing the gas to be cooled and the surrounding thermal "environment" with which the gas exchanges energy and particles can be totally artificial, to the extent that no true barrier may exist between the two.

In analogy with Section 1.3, the system and the environment, which will respectively be named A and B in the following, are considered to constitute two subsystems of a global system of indistinguishable quantum particles that is thermally isolated. Formally, we define these subsystems through two mu-

tually orthogonal and complementary projectors in the one-body Hilbert space that cover disjoint regions in configuration space. Those projectors can be represented in terms of sets of mutually orthogonal and properly normed one-body basis functions $(\phi_0^A, \phi_1^A, \ldots)$ and $(\phi_0^B, \phi_1^B, \ldots)$ associated with the subsystems A and B, respectively, such that the union of these two sets constitutes an orthonormal basis of the entire one-particle Hilbert space. The construction of fully symmetrized or antisymmetrized many-particle basis functions upon this one-body basis gives then rise to the Fock states $|n_0^A, n_1^A, \ldots, n_0^B, n_1^B, \ldots\rangle$ that are parametrized in terms of the occupancies n_k^X of the one-body states ϕ_k^X (for $X = A$ or B), which are non-negative integer numbers in the case of bosons and binary numbers in the case of fermions.

Denoting the associated creation and annihilation operators as $\hat{a}_0^\dagger, \hat{a}_0, \hat{a}_1^\dagger, \hat{a}_1, \ldots$ as well as $\hat{b}_0^\dagger, \hat{b}_0, \hat{b}_1^\dagger, \hat{b}_1, \ldots$ for the thereby defined subsystems A and B, respectively, we can, in analogy with the expression (1.23), propose a rather generic form of the many-body Hamiltonian governing this system, namely

$$\begin{aligned} \hat{H} &= \hat{H}_A(\hat{a}_0^\dagger, \hat{a}_0, \hat{a}_1^\dagger, \hat{a}_1, \ldots) + \hat{H}_B(\hat{b}_0^\dagger, \hat{b}_0, \hat{b}_1^\dagger, \hat{b}_1, \ldots) \\ &\quad + \hat{W}(\hat{a}_0^\dagger, \hat{a}_0, \hat{a}_1^\dagger, \hat{a}_1, \ldots, \hat{b}_0^\dagger, \hat{b}_0, \hat{b}_1^\dagger, \hat{b}_1, \ldots) \end{aligned} \tag{2.1}$$

where the operators $\hat{H}_A$ and $\hat{H}_B$ denote the partial energies in the subsystems A and B, respectively, and therefore depend only on the creation and annihilation operators defined for those subsystems. The operator $\hat{W}$ describes the exchange of particles between the two subsystems and can, for instance, be modeled as

$$\hat{W} = \sum_{k,l} t_{kl} \left(\hat{a}_k^\dagger \hat{b}_l + \hat{b}_l^\dagger \hat{a}_k \right) \tag{2.2}$$

in terms of one-body matrix elements t_{kl} that characterize the rate of passage of a particle from the states ϕ_k^A to the states ϕ_l^B or vice versa. Provided the two subsystems A and B are rather sharply defined in configuration space, we can safely assume that the contribution of this coupling operator $\hat{W}$ to the mean value of the total energy is negligible as compared to the respective contributions of $\hat{H}_A$ and $\hat{H}_B$, owing to the fact that only particles that happen to be very close to this (possibly purely virtual) barrier between the subsystems will effectively contribute to a non-vanishing mean value of $\hat{W}$.

As in Section 1.3, this latter consideration substantially facilitates the calculation of the statistical expectation values of operators that are exclusively defined within one of the two subsystems. The starting point for such a calculation is, as usual, the assumption of quantum ergodicity and the presence of a microcanonical ensemble within the entire system. In Fock space, the corresponding density operator is written as

$$\hat{\rho} = \frac{1}{g} \delta(E - \hat{H}) \delta_{N,\hat{N}} \tag{2.3}$$

with $g = \mathrm{Tr}[\delta(E-\hat{H})\delta_{N,\hat{N}}]$. The Kronecker delta in the particle number operator $\hat{N}$ is required in order to restrict traces in Fock space, which are evaluated as

$$\mathrm{Tr}[\hat{A}] = \sum_{n_0^A, n_1^A, \ldots} \sum_{n_0^B, n_1^B, \ldots} \langle n_0^A, n_1^A, \ldots, n_0^B, n_1^B, \ldots | \hat{A} | n_0^A, n_1^A, \ldots, n_0^B, n_1^B, \ldots \rangle \quad (2.4)$$

for generic many-body operators $\hat{A}$, to those Fock states that feature exactly N particles. Decomposing $\hat{N} = \hat{N}_A + \hat{N}_B$ with

$$\hat{N}_X = \sum_{k=0}^{\infty} \hat{x}_k^\dagger \hat{x}_k \quad (2.5)$$

for $X = A$ or B (and correspondingly $x = a$ or b) and approximating the Hamiltonian (2.1) as $\hat{H} \simeq \hat{H}_A + \hat{H}_B$ within the argument of Dirac's delta function in Eq. (2.3) allow us to rewrite this expression as

$$\hat{\rho} \simeq \frac{1}{g} \sum_{N_A=0}^{N} \int dE_A \delta(E_A - \hat{H}_A) \delta_{N_A,\hat{N}_A} \delta(E - E_A - \hat{H}_B) \delta_{N,N_A+\hat{N}_B} \,. \quad (2.6)$$

Let us now consider an observable represented by a many-body operator $\hat{f}$ that is exclusively defined within the subsystem A, *i.e.*, we can formally express it as $\hat{f} \equiv \hat{f}(\hat{a}_0^\dagger, \hat{a}_0, \hat{a}_1^\dagger, \hat{a}_1, \ldots)$. Exploiting the identity (1.28), we can decompose

$$\begin{aligned} &\mathrm{Tr}\left[\hat{f}\delta(E_A - \hat{H}_A)\delta_{N_A,\hat{N}_A}\delta(E - E_A - \hat{H}_B)\delta_{N,N_A+\hat{N}_B}\right] \\ &= \mathrm{Tr}_A\left[\hat{f}\delta(E_A - \hat{H}_A)\delta_{N_A,\hat{N}_A}\right] g_B(E - E_A, N - N_A) \end{aligned} \quad (2.7)$$

with

$$g_X(E_X) = \mathrm{Tr}_X\left[\delta(E_X - \hat{H}_X)\delta_{N_X,\hat{N}_X}\right] \quad (2.8)$$

the density of states within the subsystem $X = A$ or B, where

$$\mathrm{Tr}_X \hat{A} = \sum_{n_0^X, n_1^X, \ldots} \langle n_0^X, n_1^X, \ldots | \hat{A} | n_0^X, n_1^X, \ldots \rangle \quad (2.9)$$

denotes the partial trace of an operator $\hat{A}$ defined within the subsystem X. The statistical average of the expectation value of this operator $\hat{f}$ is then evaluated as

$$\overline{\langle \hat{f} \rangle} = \mathrm{Tr}[\hat{\rho}\hat{f}] = \mathrm{Tr}_A[\hat{\rho}_A \hat{f}] \quad (2.10)$$

using Eqs. (2.6)–(2.9), where we define the effective density operator

$$\hat{\rho}_A = \frac{1}{g} g_B(E - \hat{H}_A, N - \hat{N}_A) \quad (2.11)$$

for the subsystem A.

We now make use of the fact that the subsystem B is supposed to represent a particle reservoir for the "system" A that describes the trapped gas of atoms. It can therefore be considered to be much larger in volume than the latter, to the extent that we have $\langle\hat{N}_A\rangle \ll \langle\hat{N}_B\rangle \simeq N$ and $\langle\hat{H}_A\rangle \ll \langle\hat{H}_B\rangle \simeq E$ for the corresponding expectation values of the particle numbers and the energies. This reasoning allows us to simplify the expression (2.11) through a Taylor series expansion to be carried out in $\hat{H}_A$ and $\hat{N}_A$. Evidently, as the density of states $g_B(E_B, N_B)$ features a rather singular power-law scaling $\propto E_B^{3N_B/2}$ for large reservoir energies and populations, this Taylor series must not be carried out for g_B itself but for its logarithm corresponding to the reservoir's entropy, which yields in first order

$$\begin{aligned}\ln g_B(E-\hat{H}_A, N-\hat{N}_A) &\simeq \ln g_B(E,N) - \frac{\partial \ln g_B}{\partial E}(E,N)\hat{H}_A \\ &\quad - \frac{\partial \ln g_B}{\partial N}(E,N)\hat{N}_A\,. \end{aligned} \tag{2.12}$$

Using the definition (1.41)

$$\beta_B(E,N) = \frac{\partial \ln g_B}{\partial E}(E,N) = \frac{1}{k_B T_B}\,, \tag{2.13}$$

where T_B is the temperature of the reservoir, and defining by

$$\mu_B(E,N) = -\frac{1}{\beta_B(E,N)}\frac{\partial \ln g_B}{\partial N}(E,N) \tag{2.14}$$

the *chemical potential* of the reservoir, we thereby obtain

$$\begin{aligned}\hat{\rho}_A &= \frac{1}{g}\exp\left[\ln g_B(E-\hat{H}_A, N-\hat{N}_A)\right] \\ &= \frac{g_B(E,N)}{g}\exp\left[-\beta_B(E,N)\hat{H}_A + \beta_B(E,N)\mu_B(E,N)\hat{N}_A\right]\,. \end{aligned} \tag{2.15}$$

Simplifying the notation and dropping the subsystem-specific indices yield the statistical density operator of the grand canonical ensemble

$$\hat{\rho} = \frac{1}{Y}e^{-\beta(\hat{H}-\mu\hat{N})}\,, \tag{2.16}$$

where the associated partition function

$$Y = \mathrm{Tr}\left[e^{-\beta(\hat{H}-\mu\hat{N})}\right] \tag{2.17}$$

can be inferred from requiring proper normalization of $\hat{\rho}$. This density operator acts within a quantum system whose Hamiltonian and particle number operator are given by $\hat{H}$ and $\hat{N}$, respectively. The reservoir to which it is coupled enters with two characteristic key properties, namely its temperature $T = 1/(k_B\beta)$ and its chemical potential μ. Fine tuning of those two parameters can effectively be used in order to control the energy and particle population within the system.

2.2 The Bose-Einstein distribution

Let us now more specifically consider a gas of bosonic atoms that do not interact with each other. For this particular case of an ideal Bose gas, the Hamiltonian of the system is constituted by one-body terms only, describing the kinetic energy of the atoms as well as their potential energy in the presence of external trapping configurations. It can be written as

$$\hat{H} = \sum_{k=0}^{\infty} E_k \hat{a}_k^\dagger \hat{a}_k \tag{2.18}$$

where $\hat{a}_k^\dagger$ and $\hat{a}_k$ are respectively the creation and annihilation operators associated with the eigenstate ϕ_k of the associated single-particle Hamiltonian, and E_k denotes the corresponding eigenenergy.

Expressing the particle number operator as

$$\hat{N} = \sum_{k=0}^{\infty} \hat{a}_k^\dagger \hat{a}_k \tag{2.19}$$

in this basis allows us to show that the density operator (2.16) of the grand canonical ensemble can be written as a product of individual density operators that are associated with the one-body eigenstates ϕ_k, as if those eigenstates represent independent thermodynamic systems that are connected to the same reservoir of energy and particles. Indeed, we have

$$e^{-\beta(\hat{H}-\mu\hat{N})} = \exp\left[-\beta \sum_{k=0}^{\infty} (E_k - \mu)\hat{a}_k^\dagger \hat{a}_k\right] = \prod_{k=0}^{\infty} e^{-\beta(E_k-\mu)\hat{a}_k^\dagger \hat{a}_k} \tag{2.20}$$

and hence

$$\langle n_0, n_1, \ldots | e^{-\beta(\hat{H}-\mu\hat{N})} | n_0', n_1', \ldots \rangle = \prod_{k=0}^{\infty} \delta_{n_k, n_k'} e^{-n_k \beta(E_k-\mu)} \tag{2.21}$$

for any pair of Fock states $|n_0, n_1, \ldots\rangle$ and $|n_0', n_1', \ldots\rangle$ defined with respect to the one-body eigenbasis. Consequently, using

$$\sum_{n_0, n_1, \ldots} \prod_{k=0}^{\infty} e^{-\beta(E_k-\mu)n_k} = \prod_{k=0}^{\infty} \left(\sum_{n_k} e^{-\beta(E_k-\mu)n_k} \right), \tag{2.22}$$

we can express the partition function of the grand canonical ensemble as

$$Y = \mathrm{Tr}\left[e^{-\beta(\hat{H}-\mu\hat{N})}\right] = \prod_{k=0}^{\infty} Y_k \tag{2.23}$$

with

$$Y_k = \sum_{n_k=0}^{\infty} e^{-\beta(E_k-\mu)n_k} = \frac{1}{1-e^{-\beta(E_k-\mu)}}\,, \tag{2.24}$$

where the latter identity is valid if $E_k > \mu$.

Owing to Eqs. (2.20) and (2.23), the density operator (2.16) of the grand canonical ensemble can be expressed as the product

$$\hat{\rho} = \prod_{k=0}^{\infty} \frac{1}{Y_k} e^{-\beta(E_k-\mu)\hat{a}_k^\dagger \hat{a}_k}\,. \tag{2.25}$$

Following Eq. (2.21), it is diagonal in the Fock basis defined with respect to the single-particle eigenstates, which implies that we have $\mathrm{Tr}[\rho \hat{a}_k^\dagger \hat{a}_{k'}] = 0$ for any pair of quantum numbers $k \neq k'$. The statistical average of the mean value of an operator

$$\hat{A} = \sum_{k,k'=0}^{\infty} A_{kk'} \hat{a}_k^\dagger \hat{a}_{k'} \tag{2.26}$$

that corresponds to a single-particle observable is then given by

$$\mathrm{Tr}[\hat{\rho}\hat{A}] = \sum_{k=0}^{\infty} \overline{\langle \hat{n}_k \rangle} A_{kk} \tag{2.27}$$

where

$$\overline{\langle \hat{n}_k \rangle} = \mathrm{Tr}[\hat{\rho} \hat{a}_k^\dagger \hat{a}_k] \tag{2.28}$$

is the average population of the one-body eigenstate ϕ_k. Using the identity

$$\hat{a}_k^\dagger \hat{a}_k \hat{\rho} = -\frac{1}{\beta Y_k} \frac{\partial}{\partial E_k} e^{-\beta(E_k-\mu)\hat{a}_k^\dagger \hat{a}_k} \prod_{k' \neq k} \frac{1}{Y_{k'}} e^{-\beta(E_{k'}-\mu)\hat{a}_{k'}^\dagger \hat{a}_{k'}} \tag{2.29}$$

we can calculate

$$\begin{aligned} \overline{\langle \hat{n}_k \rangle} &= \sum_{n_0, n_1, \ldots = 0}^{\infty} \langle n_0, n_1, \ldots | \hat{a}_k^\dagger \hat{a}_k \hat{\rho} | n_0, n_1, \ldots \rangle \\ &= -\frac{1}{\beta Y_k} \frac{\partial}{\partial E_k} \sum_{n_k=0}^{\infty} e^{-\beta(E_k-\mu)n_k} \prod_{k' \neq k} \left(\frac{1}{Y_{k'}} \sum_{n_{k'}=0}^{\infty} e^{-\beta(E_{k'}-\mu)n_{k'}} \right) \end{aligned} \tag{2.30}$$

and thus obtain with the definition (2.24) of the partial partition function associated with the state ϕ_k, provided we have $E_k > \mu$,

$$\overline{\langle \hat{n}_k \rangle} = -\frac{1}{\beta} \frac{\partial}{\partial E_k} \ln Y_k = \frac{1}{e^{\beta(E_k-\mu)} - 1}\,, \tag{2.31}$$

which is the celebrated *Bose-Einstein distribution*.

The statistical average of the total number of particles that are found within the system is then given by

$$\overline{\langle \hat{N} \rangle} = \sum_{k=0}^{\infty} \overline{\langle \hat{n}_k \rangle} = \sum_{k=0}^{\infty} \frac{1}{e^{\beta(E_k-\mu)} - 1}\,, \tag{2.32}$$

while we obtain

$$\overline{\langle \hat{H} \rangle} = \sum_{k=0}^{\infty} \overline{\langle \hat{n}_k \rangle} E_k = \sum_{k=0}^{\infty} \frac{E_k}{e^{\beta(E_k-\mu)} - 1}\,, \tag{2.33}$$

for the average value of the total energy that is contained within this ideal Bose gas. These two expressions implicitly rely on the requirement $\mu < E_k$ for all k that the chemical potential of the reservoir must fulfill in order for the grand canonical ensemble to yield meaningful results. Indeed, if the chemical potential exceeds one of those eigenenergies, say E_0, the expression (2.24) for the corresponding partition function diverges, and it is straightforward to show that the average population of the associated single-particle state ϕ_0, which one would now have to evaluate through the expression

$$\overline{\langle \hat{n}_k \rangle} = \frac{\sum_{n_k=0}^{\infty} n_k e^{-\beta(E_k-\mu)n_k}}{\sum_{n_k=0}^{\infty} e^{-\beta(E_k-\mu)n_k}}\,, \tag{2.34}$$

would diverge as well. Physically, this would mean that the system is flooded by an unlimited number of particles from the reservoir, which would give rise to an infinite population of the state ϕ_0. Obviously, the hypothesis of dealing with noninteracting particles, which may be a very good approximation for a rather dilute gas, will generally break down once the particle density within the system exceeds a certain threshold, and this will give rise to a modification of the minimal energy a particle needs to have in order to be ables to enter the system, usually in such a way that the influx of particles from the reservoir comes to a halt at some point.

Problems

2.1 Show that in the case of noninteracting fermionic atoms one obtains the *Fermi-Dirac distribution*

$$\overline{\langle \hat{n}_k \rangle} = \frac{1}{e^{\beta(E_k-\mu)} + 1} \tag{2.35}$$

for the average population of the single-particle eigenstate ϕ_k.

2.2 Calculate the variance of the particle number with respect to its statistical mean value (2.32). Under which conditions can the grand canonical ensemble be considered to yield identical predictions as the canonical ensemble, for observables that are a function of the particle number operator only?

2.3 Bose-Einstein condensation in free space

Let us now particularize for the specific case of a gas of noninteracting bosonic atoms that can freely move in D spatial dimensions, with $D = 1$, 2, or 3. For the case $D < 3$ we shall consider the presence of a tight transverse harmonic confinement in the remaining $3 - D$ dimensions, which is so strong that in the considered range of temperatures the atoms of the gas occupy the transverse ground mode only, whose associated ground mode energy is set to zero without loss of generality. This yields a purely kinetic single-particle Hamiltonian in D dimensions, written as

$$H = -\frac{\hbar^2}{2m}\frac{\partial^2}{\partial \mathbf{r}^2} \tag{2.36}$$

with $\mathbf{r} \equiv (r_1, \ldots, r_D) \in \mathbb{R}^D$ and m the mass of the atoms.

To render the eigenspectrum of this Hamiltonian discrete, we introduce an artificial *normalization volume* in terms of a D-dimensional hypercube (*i.e.*, a cube for $D = 3$, a square for $D = 2$, and a line for $D = 1$) exhibiting the length L and hence the hypervolume $V = L^D$ and featuring periodic boundary conditions. That is, a valid wavefunction ψ of this system has to fulfill the conditions $\psi|_{r_j+L} = \psi|_{r_j}$ for all $r_j \in \mathbb{R}$ and all $j = 1, \ldots, D$. The eigenfunctions of the Hamiltonian (2.36) satisfying these periodic boundary conditions are then given by the plane waves

$$\phi_{\mathbf{k}}(\mathbf{r}) = \frac{1}{\sqrt{V}} e^{i\mathbf{k}\cdot\mathbf{r}} \tag{2.37}$$

with $\mathbf{k} = (2\pi/L)\mathbf{l}$ where $\mathbf{l} \equiv (l_1, \ldots, l_D) \in \mathbb{Z}^D$ is the set of integers that represent the quantum numbers of this single-particle system. The associated eigenenergies are given by

$$E_{\mathbf{k}} = \frac{\hbar^2\mathbf{k}^2}{2m} = \frac{(2\pi\hbar)^2\mathbf{l}^2}{2mL^2} \tag{2.38}$$

with $\mathbf{l}^2 = l_1^2 + \ldots + l_D^2$.

Let us first evaluate the mean total population of the system, assuming that it is connected to a grand canonical particle and heat reservoir maintained at the temperature $T = 1/(k_B\beta)$ and the chemical potential μ. According to the Bose-Einstein distribution (2.31), this mean total population is, in analogy with Eq. (2.32), given by

$$\overline{\langle \hat{N} \rangle} = \sum\nolimits_{\mathbf{k}} \frac{1}{e^{\beta(E_{\mathbf{k}}-\mu)} - 1}\,, \tag{2.39}$$

where $\sum_{\mathbf{k}} \equiv \sum_{\mathbf{l}} = \sum_{l_1=-\infty}^{\infty} \cdots \sum_{l_D=-\infty}^{\infty}$ is a short-hand notation for the summation over all integer quantum numbers of the system. As we shall take the limit $L \to \infty$ in the end, to describe an infinitely extended system, we can safely consider that adjacent terms in the sum (2.39) are infinitesimally close to each other for any set of finite (*i.e.*, nonzero and non-infinite) values for β and μ. This

allows us to replace the summation $\sum_{\mathbf{l}}$ by an integration $\int d^D l = (2\pi)^{-D} V \int d^D k$, yielding

$$\overline{\langle \hat{N} \rangle} = \frac{V}{(2\pi)^D} \int d^D k \frac{1}{e^{\beta(E_{\mathbf{k}}-\mu)} - 1} \,. \tag{2.40}$$

Using the identity

$$\frac{1}{e^{\beta(E_{\mathbf{k}}-\mu)} - 1} = \frac{1}{1 - e^{-\beta(E_{\mathbf{k}}-\mu)}} - 1 = \sum_{l=1}^{\infty} e^{-l\beta(E_{\mathbf{k}}-\mu)} \,, \tag{2.41}$$

which is valid for $\mu < 0$ (since $E_{\mathbf{k}} > 0$ for all $\mathbf{k}$), we can evaluate Eq. (2.40) in terms of D Gaussian integrations, yielding

$$\overline{\langle \hat{N} \rangle} = \frac{V}{(2\pi)^D} \sum_{l=1}^{\infty} \sqrt{\frac{2\pi m}{l\hbar^2\beta}} e^{l\beta\mu} \,. \tag{2.42}$$

This latter expression can be rewritten in terms of the so-called *Bose function* which in the interval $0 \leq z < 1$ is defined by

$$g_p(z) = \sum_{l=1}^{\infty} \frac{z^l}{l^p} \tag{2.43}$$

for the parameter $p > 0$. Introducing the *thermal de Broglie wavelength* of the atomic gas as

$$\lambda_T = \frac{2\pi\hbar}{\sqrt{2\pi m k_B T}} \,, \tag{2.44}$$

we obtain

$$\overline{\langle \hat{N} \rangle} = \frac{V}{\lambda_T^D} g_{D/2}(e^{\beta\mu}) \tag{2.45}$$

for the mean population of the system, and hence

$$\bar{n} = \frac{\overline{\langle \hat{N} \rangle}}{V} = \frac{1}{\lambda_T^D} g_{D/2}(e^{\beta\mu}) \tag{2.46}$$

for the mean atom density.

Figure 2.1(a) shows the behaviour of the Bose function (2.43) in the interval of interest $0 \leq z < 1$ for various values of the parameter p. Independently of p we have the common scaling

$$g_p(z) \simeq z + O(z^2) \tag{2.47}$$

for small positive $z \ll 1$. For $p \leq 1$ the Bose function diverges in the opposite limit $z \to 1$ while it converges towards *Riemann's zeta function*

$$\zeta(p) = \sum_{l=1}^{\infty} \frac{1}{l^p} \tag{2.48}$$

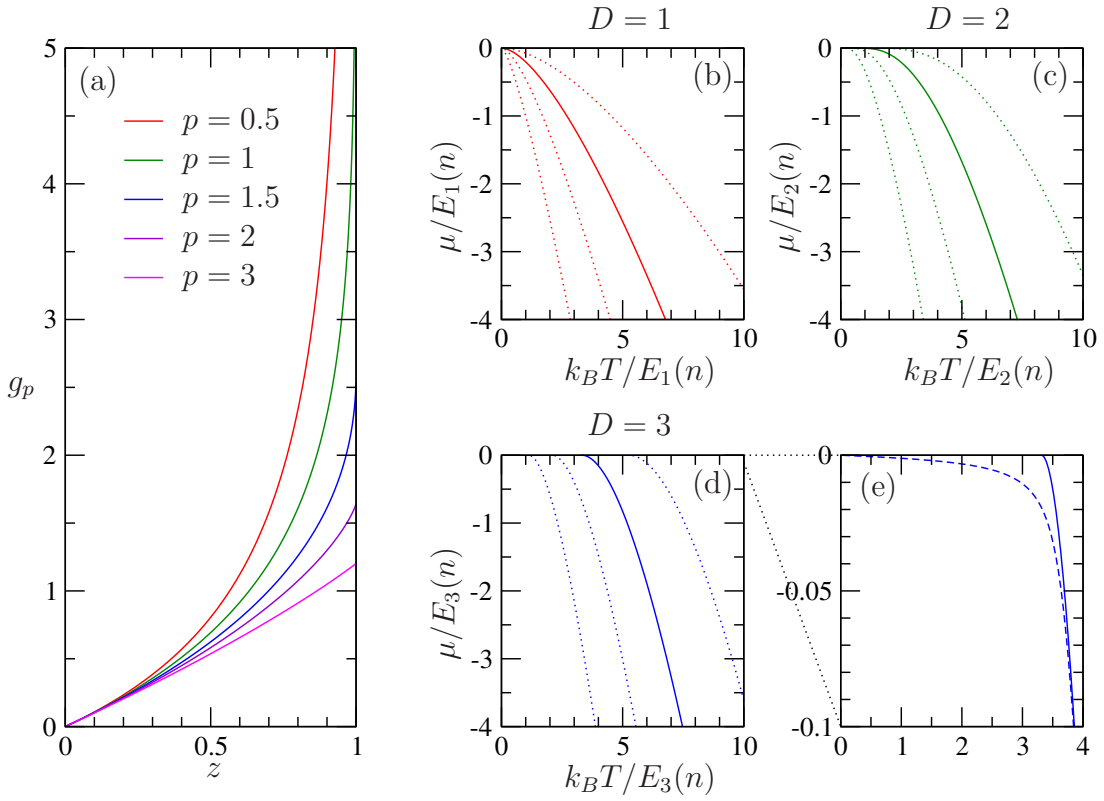

Figure 2.1: (a) Bose function (2.43) plotted for $p = 0.5$, 1, 1.5, 2, and 3. (b–d) Lines of constant atom density $\bar{n}$ plotted as a function of the temperature T and the chemical potential μ for (b) $D = 1$, (c) $D = 2$, and (d) $D = 3$ spatial dimensions. μ and k_BT are both given in units of the characteristic energy scale $E_D(n) = \hbar^2 n^{2/D}/m$ that is defined with respect to a given reference value n for the atom density. Solid lines show the case $\bar{n} = n$ within each panel, while dotted lines show, from left to right in the panels, the choices $\bar{n} = 0.2n$, $0.5n$, and $2n$. (d) Zoom onto the crossover towards Bose-Einstein condensation. The solid line shows the result that is from a numerical inversion of Eq. (2.46), while the dashed line is based on a numerical evaluation of Eq. (2.39) considering the case of $N = 1000$ atoms within the normalization volume.

if $p > 1$, yielding for the specific case $p = 3/2$

$$\lim_{z\to 1} g_{3/2}(z) = \zeta(3/2) \simeq 2.612375\,. \tag{2.49}$$

This observation indicates the existence of an upper limit for the mean density that the system can accomodate in three spatial dimensions at a given temperature, namely the density $\bar{n}_{\max} = \zeta(3/2)\lambda_T^{-3}$ that would be obtained from tuning the chemical potential close to zero.

This latter conclusion is valid in the strict thermodynamic limit, implying a strictly infinite normalization volume $V \to \infty$ (and hence, with a finite atom density $\bar{n}$, also an infinite total population of the system), and relies on the cooling process being truly conducted in the framework of a grand-canonical ensemble where the system's population and energy are controlled by the parameters T and μ of the heat and particle reservoir. It has to be amended, however, in the experimentally more common (and practically more efficient) situation that the atomic gas is cooled to ultralow temperatures by means of a pure heat reservoir, while impeding population exchange with its environment[1]. Being, in thermal equilibrium, identical to the one that is prepared in the heat reservoir, the temperature that the system thereby attains can become arbitrarily low for a sufficiently sophisticated control of the reservoir, ultimately limited only by the absolute zero of temperature. This would be in contradiction with the existence of a finite lower limit for the temperature at given total population of the system, as was obtained in the above considerations concerning a free three-dimensional Bose gas.

Indeed, relying on the equivalence of predictions made by the different statistical ensembles in the thermodynamic limit, we can describe such a canonical cooling process in the framework of the grand canonical ensemble, namely by considering a suitable variation of the chemical potential with the temperature which is such that the mean total population of the system remains constant during the cooling process. Figure 2.1(b–d) shows for $D = 1$, 2, and 3 how μ has to be tuned as a function of T in order to keep a constant mean atom density $\bar{n}$ in the system. A smooth crossover to the origin in the μ–T diagram is found for $D = 1$ and 2, reflecting the fact that in those two cases the $T^{D/2}$ scaling of the prefactor in Eq. (2.46) can be perfectly compensated by pushing μ sufficiently close to zero, and hence the argument of the Bose function in Eq. (2.46) sufficiently close to unity, in order to maintain a constant $\bar{n}$. This is no longer possible for $D = 3$ where there is an upper bound for $\bar{n}$ at given temperature.

[1]Technically, evaporative cooling, as discussed in the subsequent chapter, involves the coupling of the atomic gas to a particle reservoir maintained at very low chemical potential $\mu \to -\infty$. Note, however, that this coupling process is active only during a transient time scale that is needed to achieve sufficiently high phase-space densities for Bose-Einstein condensation to set in. Thermal equilibrium with that particle reservoir, which would imply the total depopulation of the atomic gas, is therefore, in practice, never attained in an evaporative cooling process.

Consequently, the curve of constant mean density $\bar{n}$ does, for $D = 3$, not seem to smoothly join the origin in the μ–T diagram but appears to terminate somewhere at the $\mu = 0$ axis, namely at the critical value

$$T_c = \frac{2\pi\hbar^2}{mk_B}\left(\frac{\bar{n}}{\zeta(3/2)}\right)^{2/3} \tag{2.50}$$

of the temperature corresponding to $\lambda_{T_c} = [\zeta(3/2)/\bar{n}]^{1/3}$.

This apparent paradox is resolved by re-examining the approximation that we made to evaluate the expression (2.39) for the mean population of the system, where the summation over single-particle eigenstates was replaced by an integration over the D-dimensional reciprocal space, yielding Eq. (2.40). That particular approximation is certainly valid in the thermodynamic limit $L \to \infty$ for any finite chemical potential μ since the absolute value of the latter will then clearly exceed the energy scale $\Delta E = (2\pi\hbar)^2/(2mL^2)$ that characterizes the spacing between adjacent levels in the single-particle eigenspectrum of the system. However, if in the $D = 3$ dimensional system a population-preserving cooling process is considered in which the temperature is lowered across T_c, the absolute value of chemical potential will then, for any large but finite size of the normalization volume, fall below the scale ΔE at some point. While adjacent terms in the summation in Eq. (2.39) can still be considered to be relatively close to each other in that case provided they are characterized by finite integer vectors $\mathbf{l} \neq \mathbf{0}$, the term associated with the single-particle ground state, corresponding to $\mathbf{l} = \mathbf{0}$, then attains a diverging value

$$N_0 = \frac{1}{e^{-\beta\mu} - 1} \simeq -\frac{1}{\beta\mu} + O[(\beta\mu)^0] \tag{2.51}$$

which for $-\mu \ll E_\Delta$ will be very different from the population $N_1 \simeq (\beta E_\Delta)^{-1}$ of one of the three first excited single-particle eigenstates. That ground-state term has therefore to be treated separately in the sum in Eq. (2.39), while for all other terms we can still justify, at least approximately, the replacement of the summation by an integration.

The sum over the populations of all excited states is thus still given by the expression (2.40), noting that for $D = 3$ the exclusion of a volume element of the size $(2\pi/L)^3$ from the integration domain has, for $L \to \infty$, no incidence on the value of the integral in Eq. (2.40). Using furthermore $g_D(e^{\beta\mu}) \simeq \zeta(D)$ for $-\beta\mu \ll 1$, we obtain for $T < T_c$ the expression

$$N = N_0 + \frac{V}{\lambda_T^3}\zeta(3/2) \tag{2.52}$$

for the total population N of the system. In combination with Eq. (2.51), we thereby obtain a linear scaling $\mu \simeq -k_B T/N_0 \simeq -k_B T/N$ of the chemical potential with the temperature in the ultracold regime $T \ll T_c$ for which we have $N - N_0 \ll N$.

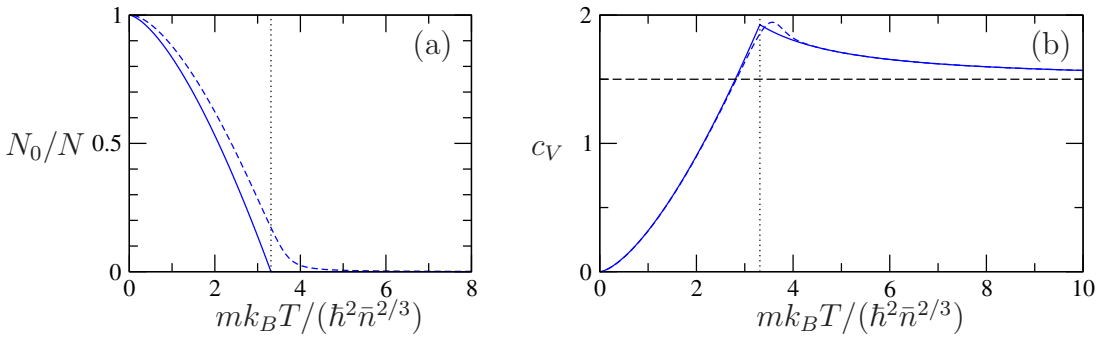

Figure 2.2: (a) Population N_0 of the single-particle ground state, normalized with respect to the total population N, and (b) specific heat, both plotted as a function of the temperature T. Solid lines show the behaviour of these observables for the infinite three-dimensional Bose gas, for which they exhibit kinks at the critical temperature T_c (marked by vertical dotted lines), while dashed lines illustrate what would be obtained for the case of a finite normalization volume containing altogether $N = 1000$ atoms.

Turned around, Eq. (2.52) can be rewritten to yield the population of the single-particle ground state as a function of the total population and the temperature according to

$$N_0/N = 1 - (T/T_c)^{3/2} \tag{2.53}$$

in the thermodynamic limit, where we use the expressions (2.50) for T_c and (2.44) for λ_T. This particular behaviour, displayed in Fig. 2.2(a), is indicative of a second-order *phase transition*, taking place at the critical temperature T_c. Like in the case of ferromagnetism, we can identify an order parameter, related here to the population of the single-particle ground state in this noninteracting bosonic many-body system, which is vanishingly small above the critical temperature and acquires macroscopically large values if the system is cooled below T_c. The second-order nature of this phase transition is manifested by the fact that the order parameter varies continuously in the entire temperature range, including the critical temperature T_c where it exhibits a kink.

The singular behaviour of the system at the critical temperature manifests itself not only in observables that are directly related to the ground-state population, but can be revealed also in more general susceptibilities, such as the *specific heat* defined through

$$c_V = \frac{1}{N}\frac{\partial}{\partial T}\overline{\langle \hat{H} \rangle}\,, \tag{2.54}$$

where the derivative of the system's mean total energy $\overline{\langle \hat{H} \rangle}$ with respect to the temperature is to be carried out at fixed total population N and fixed normalization volume V. The mean total energy of the system is straightforwardly

obtained via

$$\overline{\langle \hat{H} \rangle} = \sum\nolimits_{\mathbf{k}} \frac{E_{\mathbf{k}}}{e^{\beta(E_{\mathbf{k}}-\mu)}-1}\,, \tag{2.55}$$

in analogy with the corresponding expression (2.39) for the mean population. Above the critical temperature, for $T > T_c$, we can justify the replacement of the summation in Eq. (2.55) by an integration, yielding

$$\overline{\langle \hat{H} \rangle} = \frac{V}{(2\pi)^3} \int d^3k \frac{E_{\mathbf{k}}}{e^{\beta(E_{\mathbf{k}}-\mu)}-1} \tag{2.56}$$

in analogy with Eq. (2.40). Using the identity

$$\frac{E_{\mathbf{k}}}{e^{\beta(E_{\mathbf{k}}-\mu)}-1} = E_{\mathbf{k}} \sum_{l=1}^{\infty} e^{-l\beta(E_{\mathbf{k}}-\mu)} = -\frac{\partial}{\partial\beta} \sum_{l=1}^{\infty} \frac{1}{l} e^{-l\beta(E_{\mathbf{k}}-\mu)}\,, \tag{2.57}$$

Eq. (2.56) can be evaluated by means of Gaussian integrations, yielding

$$\overline{\langle \hat{H} \rangle} = \frac{3}{2} k_B T \frac{V}{\lambda_T^3} g_{5/2}(e^{\beta\mu})\,. \tag{2.58}$$

Below the critical temperature, this latter expression is amended as

$$\overline{\langle \hat{H} \rangle} = \frac{3}{2} k_B T \frac{V}{\lambda_T^3} \zeta(5/2)\,, \tag{2.59}$$

in analogy with Eq. (2.52), noting that the macroscopically populated single-particle ground state has vanishing energy.

The specific heat is then straightforwardly evaluated as

$$c_V = k_B \begin{cases} \dfrac{15}{4} \dfrac{k_B}{\lambda_T^3 \bar{n}} \zeta(5/2) & : \quad T < T_c \\ \dfrac{15}{4} \dfrac{g_{5/2}(e^{\beta\mu})}{\lambda_T^3 \bar{n}} - \dfrac{9}{4} \dfrac{\lambda_T^3 \bar{n}}{g_{1/2}(e^{\beta\mu})} & : \quad T > T_c \end{cases} . \tag{2.60}$$

As displayed in Fig. 2.2(b), c_V displays a power-law increase $\propto T^{3/2}$ up to the critical temperature T_c and then abruptly turns into a smooth decrease towards the asymptotic value $\frac{3}{2}k_B$ for $T \to \infty$. The latter represents the well-known specific heat for a classical ideal gas of free particles that do not exhibit internal (*i.e.*, rotational or vibrational) degrees of freedom. This confirms again that specific quantum features of this atomic gas become obsolete far above the critical temperature, respectively.

Problems

2.3 (a) Show that for $p = 1/2$ the Bose function diverges as

$$g_{1/2}(z) \simeq \sqrt{\frac{\pi}{1-z}} \tag{2.61}$$

for $0 < z < 1$ with $1 - z \ll 1$.

(b) Show that in one spatial dimension, $D = 1$, the chemical potential has to be tuned as

$$\mu \simeq -\frac{m(k_B T)^2}{2\hbar^2 \bar{n}^2} \tag{2.62}$$

as a function of the temperature T in order to maintain a fixed atom density $\bar{n}$ in the limit $T \to 0$.

2.4 (a) Show that for $p = 1$ the Bose function is given by

$$g_1(z) = -\ln(1 - z) \tag{2.63}$$

(b) Show that in two spatial dimensions, $D = 2$, the chemical potential has to be tuned as

$$\mu = k_B T \ln\left[1 - \exp\left(-\frac{2\pi\hbar^2\bar{n}}{mk_B T}\right)\right] \tag{2.64}$$

as a function of the temperature T in order to maintain a fixed atom density $\bar{n}$.

2.5 Show that the first derivative g_p' of the Bose function g_p satisfies the equation

$$g_p'(z) = \frac{g_{p-1}(z)}{z} \tag{2.65}$$

for all $p \in \mathbb{R}$ and all $0 < z < 1$.

2.6 Defining $p = 3/2$ and the energy scale $E_0 = 2\pi^2\hbar^2/(mV^{2/3})$, the total population and the mean total energy of the system can be written as

$$N = \begin{cases} N_0 + \left(\frac{k_B T}{E_0}\right)^p \zeta(p) : T < T_c \\ \left(\frac{k_B T}{E_0}\right)^p g_p(e^{\beta\mu}) \quad : T > T_c \end{cases} \tag{2.66}$$

and

$$E = pk_B T \left(\frac{k_B T}{E_0}\right)^p \begin{cases} \zeta(p+1) \ : T < T_c \\ g_{p+1}(e^{\beta\mu}) : T > T_c \end{cases}, \tag{2.67}$$

respectively, with the critical temperature

$$k_B T_c = [N/\zeta(p)]^{1/p} E_0 \,. \tag{2.68}$$

(a) Show that the specific heat is given by

$$c_V = pk_B \begin{cases} (p+1)\dfrac{\zeta(p+1)}{\zeta(p)}\left(\dfrac{T}{T_c}\right)^p & : T < T_c \\ (p+1)\dfrac{g_{p+1}(e^{\beta\mu})}{g_p(e^{\beta\mu})} - p\dfrac{g_p(e^{\beta\mu})}{g_{p-1}(e^{\beta\mu})} & : T > T_c \end{cases} \tag{2.69}$$

as a function of the temperature.

(b) Show that c_V is continous at the critical temperature for $p \leq 2$ and discontinuous otherwise.

(c) Show that c_V falls off as

$$c_V \simeq p k_B \left[1 + \frac{p-1}{2^{p+1}} N \left(\frac{E_0}{k_B T} \right)^p + O\left([N E_0^p / (k_B T)^p]^2 \right) \right] \tag{2.70}$$

for $T \to \infty$.

2.4 Bose-Einstein condensation in a harmonic trap

Let us now consider a more realistic modeling of the single-particle Hamiltonian describing a quantum gas, which requires some magnetic or optical trapping configuration in order to isolate the atoms of the gas from the surroundings. We therefore assume the presence of a harmonic confinement in D dimensions, centered about the origin and characterized by the oscillation frequencies $\omega_1, \ldots, \omega_D$. As in Section 2.3, the presence of a very tight confinement is considered in the remaining $3 - D$ dimensions, such that the atoms of the gas occupy only a single one-particle mode in those transverse dimensions, namely the transverse ground mode whose associated energy is set to zero. The single-particle Hamiltonian of this system is then given by the expression

$$H = -\frac{\hbar^2}{2m} \frac{\partial^2}{\partial \mathbf{r}^2} + V(\mathbf{r}) \tag{2.71}$$

with the potential energy

$$V(\mathbf{r}) = \frac{m}{2} \sum_{j=1}^{D} \omega_j^2 r_j^2 \,. \tag{2.72}$$

The eigenenergies of this one-body Hamiltonian (2.71) are straightforwardly evaluated as

$$E_{\mathbf{n}} = \sum_{j=1}^{D} (n_j + 1/2)\, \hbar \omega_j \tag{2.73}$$

with $\mathbf{n} \equiv (n_1, \ldots, n_D)$ and $n_j \in \{0, 1, 2, \ldots\}$ for all $j = 1, \ldots, D$. According to Eq. (2.32), we then obtain the mean total population of the system as

$$\overline{\langle \hat{N} \rangle} = \sum_{n_1, \ldots, n_D = 0}^{\infty} \frac{1}{e^{\beta(E_{\mathbf{n}} - \mu)} - 1} \tag{2.74}$$

in the presence of a heat and particle reservoir that is maintained at the temperature $T = 1/(k_B \beta)$ and the chemical potential $\mu < E_{\mathbf{0}}$.

In contrast to the case of free motion, we do not dispose here of an artificial regularization parameter, such as the size of the normalization volume introduced in Section 2.3, that would have to be set to infinity in the end and thereby allow us to transform the summations in Eq. (2.74) into integrals. To nevertheless justify this latter replacement, which is a necessary step in order to analytically calculate the mean population of the system, we have to assume that we are concerned with a specific hierarchy of energy scales implying the inequality $\beta\hbar\omega_j \ll 1$ for all $j = 1, \ldots, D$. In other words, the temperature to which we intend to cool down the system is ultralow (of the order of fractions of a microkelvin in practice) but not so low that its associated energy $k_B T$ becomes comparable to the energy scales $\hbar\omega_j$ characterizing the eigenstates of the trapping potential[2]. We anticipate here that those energy scales are actually considered to vanish, $\hbar\omega_j \to 0$, in the thermodynamic limit that we have to define in order to obtain a proper phase transition as in Section 2.3, in combination with a diverging population $N \to \infty$ of the system.

If this particular condition $\beta\hbar\omega_j \ll 1$ is satisfied for all $j = 1, \ldots, D$, we are entitled to approximate

$$\overline{\langle \hat{N} \rangle} \simeq \int_0^\infty dn_1 \cdots \int_0^\infty dn_D \frac{1}{e^{\beta(E_{\mathbf{n}} - \mu)} - 1} \,. \tag{2.75}$$

Using again Eq. (2.41) (now with $E_{\mathbf{n}}$ instead of $E_{\mathbf{k}}$), the above integrations are straightforwardly calculated via $\int_0^\infty e^{-\alpha_j n_j} dn_j = \alpha_j^{-1}$ for $\alpha_j > 0$. We then obtain

$$\overline{\langle \hat{N} \rangle} \simeq \left(\frac{k_B T}{\hbar\bar{\omega}} \right)^D g_D(e^{\beta\tilde{\mu}}) \,, \tag{2.76}$$

where g_D is again the Bose function (2.43),

$$\bar{\omega} = (\omega_1 \cdots \omega_D)^{1/D} \tag{2.77}$$

is the geometric mean of the oscillation frequencies in the trapping potential, and

$$\tilde{\mu} = \mu - \sum_{j=1}^{D} \frac{1}{2} \hbar\omega_j \tag{2.78}$$

corresponds to an effective redefinition of the chemical potential, done in such a way that we have the same constraint $\tilde{\mu} < 0$ as in the case of free motion.

Since for $D > 1$ the Bose function $g_D(z)$ approaches a finite value $\zeta(D)$ in the limit $z \to 1_-$, namely $\zeta(2) = \pi^2/6 \simeq 1.645$ for $D = 2$ and $\zeta(3) \simeq 1.202$ for

[2]More precisely, if we also assume the presence of a harmonic confinement in the $3 - D$ remaining dimensions, with the associated oscillation frequencies $\omega_{D+1}, \ldots, \omega_3$, then we have the hierarchy of energy scales $\hbar\omega_j \ll k_B T \ll \hbar\omega_k$ for all $1 \leq j \leq D$ and all $D < k \leq 3$.

$D = 3$, we can infer that Bose-Einstein condensation occurs in two- and three-dimensional harmonic trapping potentials. The associated critical temperature is evaluated from Eq. (2.76) as

$$T_c = \frac{\hbar\bar{\omega}}{k_B}\left(\frac{N}{\zeta(D)}\right)^{1/D} \tag{2.79}$$

for a given total population of N atoms in the trap. As in the case of free motion, the single-particle ground state of this system is macroscopically populated for $T < T_c$. Calculating the summation in Eq. (2.74) more carefully in the limit $\tilde{\mu} \to 0_-$, such that the ground-state contribution to that sum is singled out, we obtain, in perfect analogy with Eq. (2.52),

$$N = N_0 + \left(\frac{k_B T}{\hbar\bar{\omega}}\right)^D \zeta(D) \tag{2.80}$$

with $N_0 = -k_B T/\tilde{\mu}$ the ground-state population. This yields with Eq. (2.79)

$$N_0/N = 1 - (T/T_c)^D \ , \tag{2.81}$$

i.e., we obtain again a behaviour that is characteristic for a second-order phase transition.

As in the case of a free Bose gas, the singular behaviour of the system at this phase transition can be probed via the specific heat, defined by Eq. (2.54), where the derivative of the mean total energy with respect to temperature is here to be taken at fixed trap frequency parameters. The expression for the mean total energy,

$$\overline{\langle \hat{H} \rangle} = \sum_{n_1,\ldots,n_D=0}^{\infty} \frac{E_{\mathbf{n}}}{e^{\beta(E_{\mathbf{n}}-\mu)} - 1} \, , \tag{2.82}$$

can be evaluated in a perfectly analogous manner as in Section 2.3, using again the identity (2.57). We obtain

$$\overline{\langle \hat{H} \rangle} = \frac{N}{2}\sum_{j=1}^{D}\hbar\omega_j + Dk_B T\left(\frac{k_B T}{\hbar\bar{\omega}}\right)^2 \left\{ \begin{array}{c} \zeta(D+1) \ : T < T_c \\ g_{D+1}(e^{\beta\tilde{\mu}}) : T > T_c \end{array} \right. \tag{2.83}$$

below and above the critical temperature. The specific heat at constant trap frequency parameters is then yielded as

$$c_V = Dk_B \left\{ \begin{array}{c} (D+1)\dfrac{\zeta(D+1)}{\zeta(D)}\left(\dfrac{T}{T_c}\right)^D \qquad : T < T_c \\ (D+1)\dfrac{g_{D+1}(e^{\beta\tilde{\mu}})}{g_D(e^{\beta\tilde{\mu}})} - D\dfrac{g_D(e^{\beta\tilde{\mu}})}{g_{D-1}(e^{\beta\tilde{\mu}})} : T > T_c \end{array} \right. . \tag{2.84}$$

It increases as $\propto T^D$ below the critical temperature and approaches, for high temperatures $T \gg T_c$, the asymptotic value Dk_B that characterizes a classical

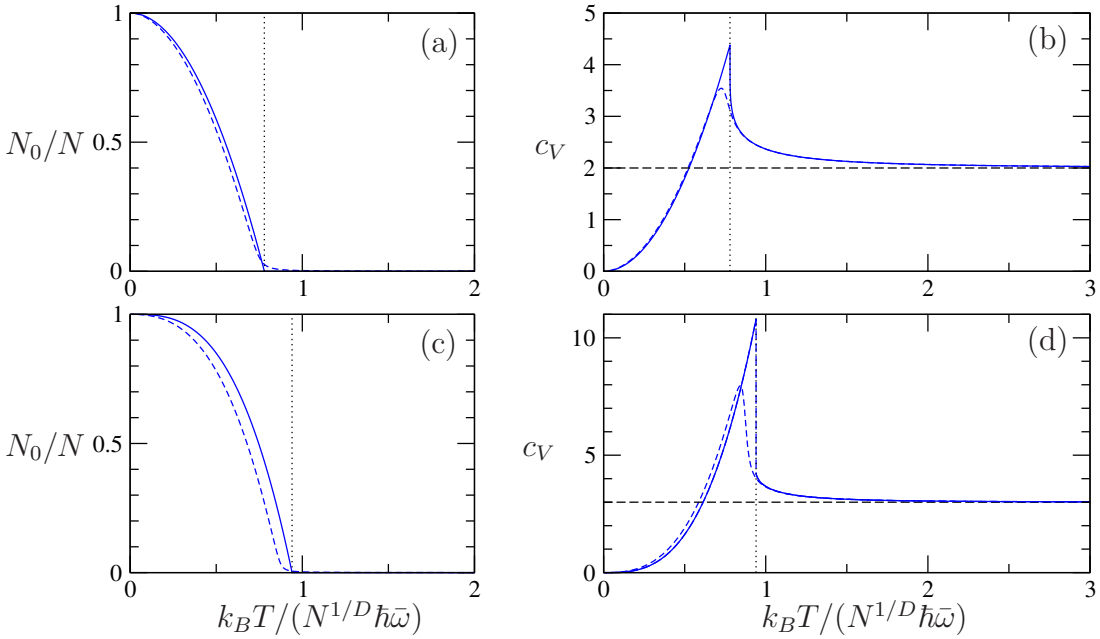

Figure 2.3: Temperature dependence of (a,c) the relative ground state population (normalized with respect to the total population N) and (b,d) the specific heat of a Bose gas in a harmonic trap defined in (a,b) $D = 2$ and (c,d) $D = 3$ spatial dimensions. Dashed lines show these observables for the specific case of $N = 1000$ atoms in the trap, while solid lines show the behaviour of these observables in a thermodynamic limit $N \to \infty$ which is defined such that the mean trap frequency scales as $\bar{\omega} \sim N^{-1/D}$. The critical temperature T_c that emerges in this limit is marked by vertical dotted lines. While for $D = 2$ the specific heat is continuous at T_c (even though it exhibits a diverging slope right above that temperature), it undergoes a discontinuous jump in $D = 3$ spatial dimensions when the temperature is varied across T_c.

ideal gas in a D-dimensional harmonic trap, as shown in Fig. (2.84). Since $g_{D-2}(z)$ diverges in the limit $z \to 1_-$ for $D \leq 2$ but attains a finite value in that limit for $D > 2$, the expression (2.84) for the specific heat is continuous at the critical temperature for $D = 2$, as in the case of free motion, whereas it undergoes a discontinuous drop at $T = T_c$ for $D = 3$.

Strictly speaking, the singular nature of this phase transition is never really manifested in experimentally realistic trapping potentials since the latter are most generally characterized by finite oscillation frequencies ω_j and can thus only host a finite number of atoms N when being put in contact with a grand-canonical reservoir maintained at finite chemical potential and finite temperature. Indeed, a phase transition can, from an academic point of view, only occur in the framework of a proper thermodynamic limit implying an infinite population

$N \to \infty$ of the system. In the case of free motion in three dimensions, this thermodynamic limit is most naturally obtained through the requirement of a diverging normalization volume, $V \to \infty$, thus yielding, for finite values of μ and T, a finite mean density $\bar{n} = N/V$ and hence, through Eq. (2.50), also a finite value for the critical temperature T_c. To get this latter property of a finite T_c also for the case of a trapped gas, we infer from Eq. (2.79) that the trap frequencies ω_j have to vanish in the thermodynamic limit, namely in such a way that we have the scaling $\bar{\omega} \sim N^{-1/D}$ for $N \to \infty$. For a harmonically trapped Bose-Einstein condensate at zero temperature, this would imply that both the atom density at the trap center and the occupied spatial volume in D dimensions diverge identically, namely as $\propto N^{1/2}$, in this particular thermodynamic limit.

The absence of an intrinsically defined pathway to reach the thermodynamic limit for trapped gases opens a possibility to justify the occurrence of Bose-Einstein condensation even in one-dimensional harmonic confinement potentials, despite the fact that for $D = 1$ the Bose function in Eq. (2.76) diverges for $\tilde{\mu} \to 0_-$. To show this, let us reconsider the calculation of the mean population in this particular limit. For $D = 1$ and $\tilde{\mu} \to 0_-$, the summation over the population of excited states according to Eq. (2.74) can be performed without the need to approximate it by an integral, namely through the asymptotic identity

$$\sum_{n=1}^{\infty} \frac{1}{e^{nx} - 1} \simeq \frac{-\ln x}{x} + O(x^{-1}) \tag{2.85}$$

for $0 < x \ll 1$. Substituting x with $\beta\hbar\omega$, we obtain from Eq. (2.74)

$$\overline{\langle \hat{N} \rangle} \simeq \frac{k_B T}{-\tilde{\mu}} + \frac{k_B T}{\hbar\omega} \ln\left(\frac{k_B T}{\hbar\omega}\right) \tag{2.86}$$

in the limit $\tilde{\mu} \to 0_-$. Identifying, as usual, the ground-state population with $N_0 = -k_B T/\tilde{\mu}$, we infer the expression for the macroscopic condensate fraction, valid below a certain critical temperature T_c, as

$$N_0/N = 1 - \frac{k_B T}{N\hbar\omega} \ln\left(\frac{k_B T}{\hbar\omega}\right) . \tag{2.87}$$

Clearly, if we defined the thermodynamic limit in the analogous manner as for multidimensional traps, namely through the scaling $\omega \sim N^{-1}$, the right-hand side of Eq. (2.87) would logarithmically diverge to the extent that $T_c = 0$ would be the only meaningful value for that critical temperature, thus excluding the occurrence of Bose-Einstein condensation. However, nothing prevents us from slightly amending the definition of the thermodynamic limit for this particular case of a one-dimensional trap, namely such that we have the scaling $\omega \sim N^{-1} \ln N$ for large N. Defining the trap frequency scale $\omega_0 = N\omega/\ln N$, which is thus supposed to remain constant in the limit $N \to \infty$, we rewrite Eq. (2.87) as

$$N_0/N = 1 - \frac{k_B T}{\hbar\omega_0} \left(1 - \frac{\ln(\beta\hbar\omega_0 \ln N)}{\ln N}\right) \overset{N\to\infty}{\simeq} 1 - \frac{k_B T}{\hbar\omega_0} \tag{2.88}$$

and thereby obtain a linear decrease of the condensate fraction with increasing T, up to the finite critical temperature

$$T_c = \frac{\hbar\omega_0}{k_B} = \frac{N\hbar\omega}{k_B \ln N}\,. \tag{2.89}$$

Bose-Einstein condensation can thus be achieved also in one-dimensional harmonic traps.

Problems

2.7 Show the validity of the series expansion

$$\sum_{n=1}^{\infty} \frac{1}{e^{nx}-1} = \frac{-\ln x + \gamma}{x} + \frac{1}{4} + O(x) \tag{2.90}$$

for $0 < x \ll 1$, where

$$\gamma = \lim_{N\to\infty} \left(\sum_{n=1}^{N} \frac{1}{n} - \ln N \right) \simeq 0.5772156649 \tag{2.91}$$

is the *Euler-Mascheroni constant*.

2.5 The condensate wavefunction

As in the case of a free Bose gas, the order parameter that characterizes Bose-Einstein condensation in a harmonic trap has to be related with the population of the single-particle ground mode of the trapping potential, whose temperature dependence, given by Eq. (2.81), features the typical characteristics of a second-order phase transition. In the case of a homogeneous Bose gas, this condensate population is readily evaluated owing to the fact that the single-particle ground mode is given by the stationary, zero-momentum component of the gas. In the presence of inhomogeneous confinement potentials, however, that ground mode would have to be determined *ex ante*, through an exquisite characterization of the trapping configuration at hand, in order to access its population in an experiment. In view of this technical complication, the concept of the order parameter may therefore appear difficult to use from a practical point of view.

Penrose and Onsager[3] found a way how to circumvent this problem. They proposed a definition of the order parameter that is more robust with respect to such experimental limitations and also encompasses the local character of order as

[3]O. Penrose and L. Onsager, *Bose-Einstein Condensation and Liquid Helium*, Phys. Rev. 104, 576 (1956).

well as the aspect of spontaneous symmetry breaking which is common to second-order phase transitions. Consider, for this purpose, an arbitrary basis $(\phi_k)_{k\in\mathbb{N}_0}$ of the one-body Hilbert space, which may or may not be close to the eigenbasis of the system's single-particle Hamiltonian. Denoting the associated creation and annihilation operators by $\hat{a}_k^\dagger$ and $\hat{a}_k$, we can form the so-called *reduced one-body density matrix* $(n_{kk'})_{k,k'\in\mathbb{N}_0}$ defined via

$$n_{kk'} = \overline{\langle \hat{a}_k^\dagger \hat{a}_{k'} \rangle} = \mathrm{Tr}[\hat{\rho}\hat{a}_k^\dagger \hat{a}_{k'}] \,. \tag{2.92}$$

This matrix is hermitian and positive, *i.e.*, we have $n_{kk'} = n_{k'k}$ for all $k, k' \in \mathbb{N}_0$ as well as $n_{kk} \geq 0$ for all $k \in \mathbb{N}_0$. Furthermore, its trace is evaluated as

$$\mathrm{Tr}(n_{kk'}) = \sum_{k=0}^{\infty} n_{kk} = \overline{\left\langle \sum_{k=0}^{\infty} \hat{a}_k^\dagger \hat{a}_k \right\rangle} = N \tag{2.93}$$

where N is the total number of particles populating the system. The eigenvalues of $(n_{kk'})$ are thus nonnegative and sum up to the total particle number N.

Following Penrose and Onsager, a Bose-Einstein condensate is realized if that reduced one-body density matrix exhibits one eigenvalue N_0 that is macroscopically large, *i.e.*, of the order of the total particle number. Denoting the associated normalized eigenvector by $(v_k)_{k\in\mathbb{N}_0}$, which thus satisfies $\sum_{k=0}^{\infty} |v_k|^2 = 1$ and solves the eigenvalue equations

$$\sum_{k'=0}^{\infty} n_{kk'} v_{k'} = N_0 v_k \tag{2.94}$$

for all k, the order parameter associated with the Bose-Einstein condensation is given by the *condensate wavefunction* defined through

$$\psi_0(\mathbf{r}) = \sqrt{N_0} \sum_{k=0}^{\infty} v_k \phi_k(\mathbf{r}) \,. \tag{2.95}$$

In the absence of interaction, we are, of course, entitled to represent the reduced one-body density matrix in the eigenbasis of the single-particle Hamiltonian, which is thus written as

$$\hat{H} = \sum_{k=0}^{\infty} E_k \hat{a}_k^\dagger \hat{a}_k \,. \tag{2.96}$$

The reduced one-body density matrix is then diagonal, $n_{kk'} = \delta_{kk'} N_k$, and its eigenvalues N_k are identical to the average populations of the system's single particle eigenstates, given the Bose-Einstein distribution (2.31). Denoting by ϕ_0 the ground state of the system, such that we have $E_0 < E_k$ for all $k > 0$, we obtain the condensate wavefunction as

$$\psi_0(\mathbf{r}) = \sqrt{N_0} \phi_0(\mathbf{r}) \,. \tag{2.97}$$

Its square modulus $|\psi_0(\mathbf{r})|^2$ thus yields the spatial density of condensed atoms.

Order, below the critical temperature, is thus a local concept, being highest in the trap center and decreasing towards the edges of the atomic cloud. Furthermore, this concept involves an element of spontaneous symmetry breaking, namely concerning the $U(1)$ gauge symmetry, due to the fact that the eigenvectors of the reduced one-body density matrix, as well as the eigenfunctions of the single-particle Hamiltonian, are defined up to arbitrary phase factors $e^{i\varphi}$. Let us also stress that no knowledge about the system's Hamiltonian is required to define and evaluate the order parameter according to Penrose and Onsager. We even do not need to exclude the presence of atom-atom interaction since, as a matter of fact, the elements (2.92) of the reduced one-body density matrix can be evaluated also for interacting systems. The above concept of the order parameter is thus applicable to interacting systems as well. Incidentally, it allows one to formally define the notion of a Bose-Einstein condensate in the presence of interaction, namely via the condensate wavefunction (2.95).

It is instructive to evaluate the reduced one-body density matrix in position representation. Using the field operator $\hat{\psi}(\mathbf{r}) = \sum_{k=0}^{\infty} \phi_k(\mathbf{r})\hat{a}_k$, we obtain

$$n(\mathbf{r},\mathbf{r}') = \overline{\left\langle \hat{\psi}^\dagger(\mathbf{r})\hat{\psi}(\mathbf{r}') \right\rangle} = \sum_{k,k'=0}^{\infty} n_{kk'}\phi_k^*(\mathbf{r})\phi_{k'}(\mathbf{r}')\,, \tag{2.98}$$

which shows that this particular observable can also be seen as a measure for long-range coherence within the atomic cloud. In the absence of interaction, we can choose $(\phi_k)_{k\in\mathbb{N}_0}$ to be the eigenbasis of the single-particle Hamiltonian, thus yielding $n_{kk'} = \delta_{kk'}N_k$ with N_k given by the Bose-Einstein distribution (2.31). Equation (2.98) then simplifies to

$$n(\mathbf{r},\mathbf{r}') = \sum_{k=0}^{\infty} \frac{\phi_k^*(\mathbf{r})\phi_k(\mathbf{r}')}{e^{\beta(E_k-\mu)}-1}\,. \tag{2.99}$$

Let us now specifically evaluate these spatial one-body density matrix elements for the case of a homogeneous noninteracting Bose gas in three dimensions. As was discussed in Section 2.3, the single-particle eigenfunctions of this system are given by the plane waves $\phi_{\mathbf{k}}(\mathbf{r}) = V^{-1/2}e^{i\mathbf{k}\cdot\mathbf{r}}$ whose wave vectors $\mathbf{k}$ are such that $\phi_{\mathbf{k}}$ fulfills the periodic boundary conditions imposed by the presence of the normalization volume V. We thus have $\phi_{\mathbf{k}}^*(\mathbf{r})\phi_{\mathbf{k}}(\mathbf{r}') \propto e^{i\mathbf{k}\cdot(\mathbf{r}'-\mathbf{r})}$ and can infer that $n(\mathbf{r},\mathbf{r}')$ depends only on the distance between the two points $\mathbf{r}$ and $\mathbf{r}'$, *i.e.*, $n(\mathbf{r},\mathbf{r}') \equiv n(\mathbf{r}-\mathbf{r}')$. Following the calculation steps undertaken in Section 2.3, we replace the sum over those quantized wave vectors by an integral in reciprocal space, singling out the contribution of the $\mathbf{k}=\mathbf{0}$ component for $T < T_c$. This then yields the spatial one-body density matrix as a Fourier transform

$$n(\mathbf{r}-\mathbf{r}') = \frac{1}{V}\int d^3p\, \tilde{n}(\mathbf{p})e^{i\mathbf{p}\cdot(\mathbf{r}-\mathbf{r}')/\hbar} \tag{2.100}$$

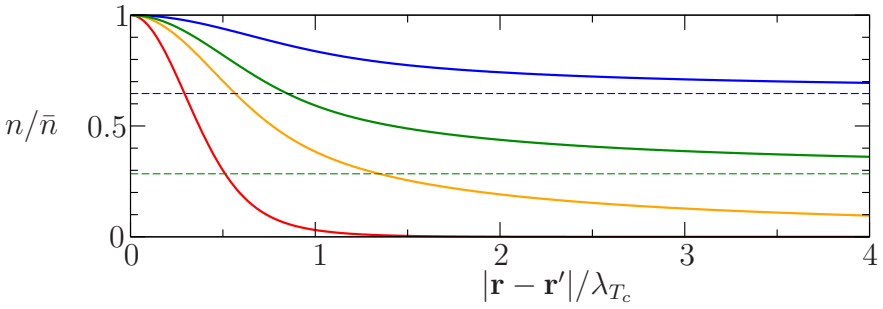

Figure 2.4: Off-diagonal long-range order for a three-dimensional homogeneous Bose gas. Plotted are (from above to below) the spatial one-body density matrix elements $n(\mathbf{r}-\mathbf{r}')$ (given in units of the total atom density $\bar{n}$) as a function of $|\mathbf{r}-\mathbf{r}'|$ (given in units of the thermal de Broglie wavelength λ_{T_c} at critical temperature T_c) for $T = 0.5T_c$ (blue curve), $T = 0.8T_c$ (green curve), $T = T_c$ (orange curve), and $T = 2T_c$ (red curve). While above the critical temperature the spatial long-range coherence $n(\mathbf{r},\mathbf{r}')$ decreases to zero for $|\mathbf{r}-\mathbf{r}'| \to \infty$, it attains a finite value $n_0 = N_0/V$ (marked by horizontal dashed lines) for $T < T_c$, which corresponds to the condensate population N_0.

of the particle density in momentum space $n(\mathbf{p})$, the latter being evaluated as

$$\tilde{n}(\mathbf{p}) = \begin{cases} \dfrac{V}{(2\pi\hbar)^3}\dfrac{1}{e^{\beta[p^2/(2m)-\mu]}-1} & : \quad T > T_c \\ \dfrac{V}{(2\pi\hbar)^3}\dfrac{1}{e^{\beta p^2/(2m)}-1} + N_0\delta(\mathbf{p}) & : \quad T < T_c \end{cases} . \tag{2.101}$$

Figure 2.4 shows the behaviour of the spatial one-body density matrix elements $n(\mathbf{r}-\mathbf{r}')$, as evaluated via Eqs. (2.100) and (2.101), as a function of the distance $|\mathbf{r}-\mathbf{r}'|$ below, at, and above the critical temperature T_c. While for $T > T_c$ this particular measure for spatial coherence rapidly decreases to zero at large distances, a finite asymptotic value is attained below the critical temperature. It is obvious from Eqs. (2.100) and (2.101) that this asymptotic value arises from the contribution of the Bose-Einstein condensate, *i.e.*, we have

$$\lim_{|\boldsymbol{\rho}|\to\infty} n(\boldsymbol{\rho}) = N_0/V \tag{2.102}$$

with N_0 the macroscopic population of the single-particle ground state. The presence of such a condensate thus gives rise to a nonvanishing *off-diagonal long-range order* across the atomic cloud, which in homogeneous systems can serve as an alternative measure for the order parameter that is associated with Bose-Einstein condensation.

Problems

2.8 Show that the spatial one-body density matrix element, as evaluated through Eqs. (2.100) and (2.101), asymptotically decays as

$$n(\boldsymbol{\rho}) \simeq \begin{cases} N_0/V + \dfrac{1}{\lambda_T^2 \rho} & : \quad T \leq T_c \\ \dfrac{1}{\lambda_T^2 \rho} \exp\left(-2\sqrt{-\pi\beta\mu}\rho/\lambda_T\right) & : \quad T > T_c \end{cases} \tag{2.103}$$

for large $\rho/\lambda_T \to \infty$, with λ_T the thermal de Broglie wavelength (2.44) and $\beta\mu$ the solution of the equation $g_{3/2}(e^{\beta\mu}) = \lambda_T^3 N/V$.

Chapter 3

Ultracold atoms

3.1 The hyperfine spectrum of alkali atoms

Alkali atoms, which constitute the leftmost column of the periodic table, are ideally suited candidates for the realization of Bose-Einstein condensates using ultracold quantum gases. As they are characterized by a set of entirely closed shells together with an extra unpaired electron that occupies an otherwise empty s shell, they feature a finite magnetic momentum which is associated with the spin of this unpaired electron. This allows one to confine them within magnetic traps. Noble gases such as helium, which would be much more obvious a choice in view of creating a Bose-Einstein condensate with an ideal gas, are rather unsuited from this point of view, since they do not exhibit unpaired electrons giving rise to a finite magnetic momentum in their ground state.

Another asset of alkali atoms, in particular in contrast to hydogen, is that the energetic level difference between the electronic ground state and the first excited state to which a dipole transition from the ground state is allowed lies in the optical regime and can therefore be accessed with standard lasers. This allows one to confine alkali atoms in optical dipole traps and to cool them using laser cooling techniques. In the case of hydrogen, which owing to its theoretical simplicity would also be a much more obvious choice for an atomic species to be used for realizing a Bose-Einstein condensate, this energy difference is approximately 10.2 eV. It would correspond to a wavelength of about 120 nm that a laser should have in order to induce a resonant transition between the ground state of hydrogen and its first excited p state. While it is not strictly impossible to generate coherent electromagnetic radiation in this ultraviolet regime, it requires much more technical effort than for laser light in the visible or infrared regime.

Last but not least, alkali atoms weakly interact with each other, mainly owing, again, to the presence of the unpaired electron. While the presence of a finite atom-atom interaction should, at first glance, have to be considered as a nuisance in view of experimentally reproducing the process of Bose-Einstein condensation

that we discussed in the previous chapter, it is nowadays seen as an important resource that opens the door towards the general exploration of interaction effects within complex many-body systems in a highly controlled manner, to the extent that ultracold quantum gases represent suitable candidates for engineering *quantum simulators* of complex many-body physics. Moreover, the presence of interaction between the atoms of the gas allows one to reduce the temperature of the latter via evaporative cooling techniques, as we shall briefly discuss in the subsequent section.

The most frequently used atomic species for creating Bose-Einstein condensates is Rubidium 87, *i.e.*, ^{87}Rb, as it is commonly abbreviated. Indeed, the first successful experimental realization of a Bose-Einstein condensate with ultracold quantum gases was done with ^{87}Rb atoms, namely in 1995 at the *Joint Institute for Laboratory Astrophysics* (JILA) of the University of Colorado in Boulder[1]. Other pioneering experiments on Bose-Einstein condensation carried out in the same year at the *Massachusetts Institute of Technology* (MIT)[2] and the Rice University in Houston[3] respectively used sodium 23 atoms, abbreviated as ^{23}Na, as well as lithium 7 atoms, abbreviated as ^{7}Li. Clearly, the choice of the isotope has to be such that the atomic species under consideration is bosonic and features an even number of fermionic elementary particles. This implies for alkali atoms, which have an odd number of electrons, that the number of their nucleons is also odd.

By now, Bose-Einstein condensates have been realized also with potassium and cesium atoms as well with atomic species that are not belonging to the alkali column of the periodic table, such as calcium, strontium, chromium, dysprosium, erbium, ytterbium, as well as the technically more challenging atomic species hydrogen and helium (the latter in the long-lived mestastable triplet state corresponding to orthohelium, which allows one to magnetically trap the atoms and to apply evaporative cooling). A key interest in performing experiments on Bose-Einstein condensates with atomic species belonging to the "bulk" of the periodic table resides in the possibility to explore strong interaction effets in such condensates. This is particularly the case for atoms belonging to the group of transition metals which feature a long-range dipolar interaction. Evidently, the presence of a strong atom-atom interaction can give rise to significant complications in the conception of the experimental protocol to be used in order to trap the gas and cool it below the condensation temperature. It would be rather hard, if not im-

[1]M. H. Anderson, J. R. Ensher, M. R. Matthews, C. E. Wieman, and E. A. Cornell, *Observation of Bose–Einstein Condensation in a Dilute Atomic Vapor*, Science 269, 198 (1995).

[2]K. B. Davis, M.-O. Mewes, M. R. Andrews, N. J. van Druten, D. S. Durfee, D. M. Kurn, and W. Ketterle, *Bose–Einstein condensation in a gas of sodium atoms*, Phys. Rev. Lett. 75, 3969 (1995).

[3]C. C. Bradley, C. A. Sackett, J. J. Tollett, and R. G. Hulet, *Evidence of Bose-Einstein Condensation in an Atomic Gas with Attractive Interactions*, Phys. Rev. Lett. 75, 1687 (1995).

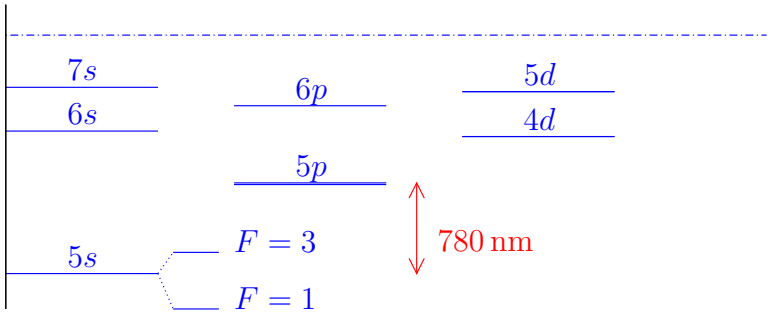

Figure 3.1: Level scheme of the ground state $5s$ and some of the lowest excited states of ^{87}Rb, plotted as a function of their energies (vertical axis). The label denotes the atomic shell in which the unpaired valence electron is located. The dash-dotted line indicates the location of the single ionization threshold of ^{87}Rb. The energetic distance ΔE between the ground state $5s$ and the first excited state $5p$ corresponds to the infrared wavelength $\lambda = hc/\Delta E \simeq 780\,\mathrm{nm}$. Note that every p and d state features a fine structure splitting into sublevels due to the spin-orbit coupling of the valence electron. On a much smaller scale, the ground level exhibits a hyperfine splitting due to the interaction of the magnetic moments of the electron spin and the nuclear spin. This hyperfine splitting gives rise to two sublevels characterized by the total spin quantum numbers $F = 1$ and $F = 2$, the energetic distance δE between which (not drawn to scale here) corresponds to the transition frequency $\nu = \delta E/h \simeq 6.8\,\mathrm{GHz}$.

possible, to do that *e.g.* for carbon atoms which are so reactive that they rather quickly form molecular aggregates.

Figure 3.1 shows a scheme of the energy levels of the electronic ground state and some of the lowest excited states of ^{87}Rb. All those levels correspond to electronic configurations with closed $1s^2 2s^2 2p^6 3s^2 3p^6 3d^{10} 4s^2 4p^6$ shells and one unpaired valence electron in an additional shell (indicated by the label in Fig. 3.1). Contrary to hydrogen, the degeneracy between the $5s$, $5p$, and $5d$ levels is lifted on a rather large energy scale. This phenomenon, dubbed *quantum defect*, is a consequence of the fact that states with high angular momentum quantum numbers, such as $5f$ or $5g$, correspond to valence electron wavefunctions that have very little amplitude inside the core region that is occupied by the closed shells of the atom. In those states, the valence electron is therefore effectively exposed to the attractive Coulomb potential resulting from a uniformly charged sphere with the charge e, which means that their energies are nearly identical to their counterparts in hydrogen. Low angular momentum states such as $5s$ or $5p$, on the other hand, do feature a finite probability of presence of the valence electron inside the core region, which implies that the effective charge of the core as it is effectively experienced by the valence electron is significantly larger

than for hydrogen. Consequently, the associated energy levels are significantly lower than their counterparts in hydrogen, and this reduction of energy is mostly pronounced for the s states which have the highest probability of presence of the valence electron inside the core region. Owing to this quantum defect, the dipole allowed transitions between the ground state ns and the first excited state np of alkali atoms lie in the optical or near-infrared regime in which lasers are commonly available.

All states with nonvanishing angular momentum quantum number feature a splitting into two sublevels, due to the spin-orbit coupling of the valence electron. While s states are not concerned by this fine structure effect, they also exhibit splitting into two sublevels, albeit on a much smaller energy scale. This *hyperfine splitting* arises from the interaction of the magnetic moments associated with the electron spin and the nuclear spin.

A simple model for this hyperfine structure of states with vanishing angular momentum quantum number is provided by the effective Hamiltonian

$$H_{\mathrm{HF}} = A\vec{I}\cdot\vec{S} \tag{3.1}$$

defined in terms of an energy constant A, where $\vec{S}$ denotes the spin of the electron and $\vec{I}$ the one of the nucleus. This hyperfine Hamiltonian (3.1) can be diagonalized through the introduction of the total spin $\vec{F} = \vec{I} + \vec{S}$ in terms of which we can rewrite the expression (3.1) as

$$H_{\mathrm{HF}} = \frac{A}{2}\left(\vec{F}^2 - \vec{I}^2 - \vec{S}^2\right) . \tag{3.2}$$

The eigenbasis of H_{HF} is then given in terms of the common eigenstates $|I, F, m_F\rangle$ of $\vec{I}^2$, $\vec{S}^2$, and $\vec{F}^2$, which can be parametrized in terms of the nuclear spin quantum number I, the total spin quantum number F, as well as the magnetic quantum number m_F associated with the total spin, which corresponds to its z component. Knowing that the nuclear spin quantum number for ^{87}Rb is $I = 3/2$ and that we have $S = 1/2$ for the electron spin, we obtain, through the rules of the addition of angular momenta, the two possibilities $F = 1$ or $F = 2$ for the quantum number associated with the total spin F. This gives rise to the two eigenenergies

$$\begin{aligned} E_F &= \frac{A}{2}[F(F+1) - I(I+1) - S(S+1)] = \frac{A}{2}[F(F+1) - 9/2] \\ &= \begin{cases} -5A/4 : F = 1 \\ 3A/4 \ : F = 2 \end{cases} \end{aligned} \tag{3.3}$$

associated with the eigenstates $|I, F, m_F\rangle$ of the Hamiltonian (3.1).

The prefactor A characterising the energy scale of the hyperfine interaction in the expressions (3.1–3.3) is given by

$$A = \frac{2}{3}\mu_0 g_e \mu_B g_N \mu_N \rho_0 . \tag{3.4}$$

Here, $\mu_0 = 4\pi \times 10^{-7}\,\mathrm{Vs/Am}$ is the vacuum permeability,

$$\mu_B = \frac{e\hbar}{2m_e}\,, \tag{3.5}$$

$$\mu_N = \frac{e\hbar}{2m_p} \tag{3.6}$$

are Bohr's magneton and the nuclear magneton, respectively, defined in terms of the masses m_e and m_p of the electron and the proton, $g_e \simeq 2$ and g_N denote the electronic and nuclear Landé factor, respectively, and ρ_0 represents the electronic density of the $5s$ orbital, hosting the unpaired electron, at the position of the nucleus. The expression (3.4) can be calculated via the evaluation of the magnetic field

$$\vec{B}_0 = -\frac{2}{3}\mu_0 g_e \mu_B \rho_0 \vec{S} \tag{3.7}$$

that is created by the unpaired electron in the $5s$ shell at the position of the nucleus. We then obtain the Hamiltonian (3.1) through the energy $H_{\mathrm{HF}} = -\vec{\mu}\cdot\vec{B}_0$ of the nuclear magnetic moment $\vec{\mu} = g_N \mu_N \vec{I}$ in the presence of this magnetic field (3.7). The maximal value of this magnetic moment is specifically obtained as $\mu = I g_N \mu_N \simeq 2.751 \mu_N$ for ^{87}Rb. This altogether yields a hyperfine splitting

$$E_{F=2} - E_{F=1} = 2A = h\nu_{\mathrm{HF}} \tag{3.8}$$

that corresponds to the microwave frequency $\nu_{\mathrm{HF}} \simeq 6.8\,\mathrm{GHz}$ in the case of ^{87}Rb.

Problems

3.1 Show that the magnetic field created by an electron that is contained within a spatially isotropic s orbital is, in leading nonrelativistic order, evaluated as

$$\vec{B}(0) = -\frac{2}{3}\mu_0 \mu_B |\psi(0)|^2 \vec{e}_s$$

at the position of the nucleus, where $\psi(r)$ denotes the s orbital as a function of the distance r from the nucleus and $\vec{e}_s$ is the unit vector along the orientation of the electron spin.

3.2 Magnetic traps

In the presence of an external magnetic field $\vec{B}$, the hyperfine Hamiltonian (3.1) is modified according to

$$H = A\vec{I}\cdot\vec{S} + g_e\mu_B\vec{B}\cdot\vec{S} - g_N\mu_N\vec{B}\cdot\vec{I}\,, \tag{3.9}$$

such that it also accounts for the energies of the electronic and nuclear magnetic moments within this external field. Since according to Eqs. (3.5) and (3.6) we

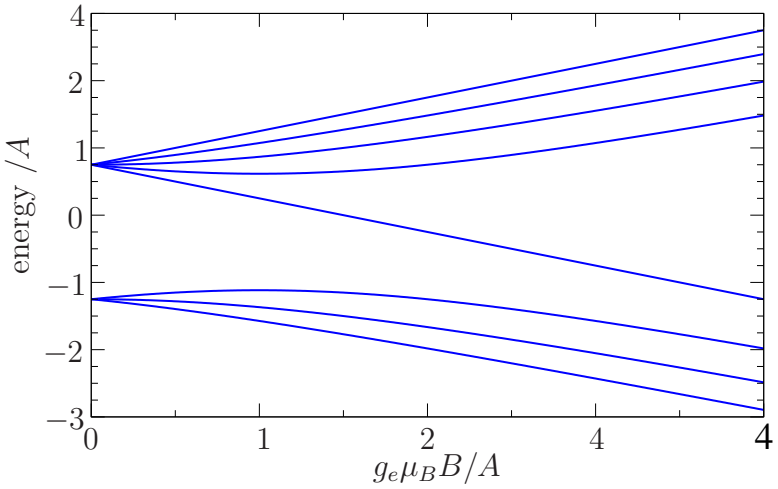

Figure 3.2: Hyperfine levels of ^{87}Rb as a function of the magnetic field B, plotted in units of the energy scale A given by Eq. (3.4).

have $\mu_N/\mu_B = m_e/m_p \simeq 5.44 \times 10^{-4} \ll 1$, the last term on the right-hand side of Eq. (3.9) can safely be neglected as compared to the second last term. Assuming that the magnetic field is oriented along the z axis of the coordinate system, *i.e.*, $\vec{B} = |\vec{B}|\vec{e}_z$, we can therefore simplify the internal Hamiltonian of the atom as

$$H = A\vec{I}\cdot\vec{S} + CS_z \tag{3.10}$$

with $C = g_e\mu_B|\vec{B}|$.

Figure 3.2 shows the $4I+2$ eigenvalues of this simplified Hamiltonian (3.10) as a function of the magnetic field strength $B = |\vec{B}|$ for the special case of ^{87}Rb featuring $I = 3/2$. They are generally calculated as

$$E_I^{\pm} = \frac{AI \pm C}{2} \tag{3.11}$$

as well as

$$E_{m_I}^{\pm} = -\frac{A}{4} \pm \frac{1}{2}\sqrt{A^2(I+1/2)^2 + C^2 + AC(2m_I+1)} \tag{3.12}$$

for all $m_I \in \{-I, -I+1, \ldots, I-1\}$. In the limit of a weak magnetic field, such that we have $C \ll A$, Eq. (3.12) is approximately evaluated as

$$E_{m_I}^{\pm} \simeq -\frac{A}{4} \pm \frac{(2I+1)A}{4} \pm \frac{2m_I+1}{2(2I+1)}C \tag{3.13}$$

in linear order in C/A. This is the *Zeeman effect* which describes the splitting of the $F = 1$ and $F = 2$ hyperfine states into $2F+1$ sublevels due to the presence of

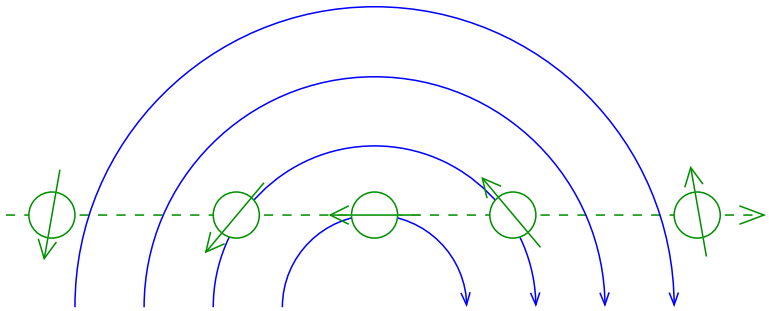

Figure 3.3: An atom that is moving along a straight line across a spatial region in which the external magnetic field (indicated by the blue field lines) is inhomogeneous will keep the (antiparallel, in this case) orientation of its magnetic moment with respect to the local direction of the magnetic field throughout this motion, provided the latter is sufficiently slow such that the adiabaticity condition, relating the effective speed of change of the magnetic field at the position of the atom with the Zeeman splitting of its hyperfine sublevels, remains valid along the entire trajectory of the atom.

the magnetic field. This Zeeman splitting can be perturbatively evaluated within the eigenstates $|I, F, m_F\rangle$ of the hyperfine Hamiltonian (3.1) that we introduced in the previous section. We obtain for the case of ^{87}Rb with $I = 3/2$

$$E_{F=2,m_F} \simeq \frac{3}{4}A + \frac{1}{4}m_F C\,, \tag{3.14}$$

$$E_{F=1,m_F} \simeq -\frac{5}{4}A - \frac{1}{4}m_F C\,. \tag{3.15}$$

In the opposite limit of a very strong magnetic field, with $C \gg A$, we approximately evaluate Eq. (3.12) as

$$E^{\pm}_{m_I} \simeq \pm\frac{C}{2} \pm \frac{A}{4}(2m_I + 1 \mp 1)\,. \tag{3.16}$$

This is the *Paschen-Back* effect. It expresses the fact that in a strong magnetic field the hyperfine part (3.1) of the Hamiltonian (3.10) represents a small perturbation as compared to the CS_z term corresponding to the energy of the electronic magnetic moment within the external magnetic field.

While an external magnetic field that is generated by a set of coils and/or current-carrying wires in a laboratory cannot be considered to be strictly homogeneous, it typically varies on length scales that are much larger than the Bohr radius which is the characteristic length scale for the atom. Approximating it by a homogeneous field is therefore very well justified as long as the atom is at rest. If the atom is moving in space, it will, as is illustrated in Fig. 3.3, still experience a magnetic field that is approximately homogeneous, but the orientation of this

field and its absolute strength at the instantaneous position of the atom will effectively vary with time. As long as this variation is slow as compared to the time scale that is given by the inverse of the Zeeman splitting $C/4$ between adjacent hyperfine sublevels (or, in the case of a very strong magnetic field, by the inverse of the Paschen-Back splitting $A/2$), the adiabatic theorem of quantum mechanics ensures that the hyperfine spin state of the atom is unchanged in the course of its motion. That is, if the atom is initially prepared within an eigenstate of the Hamiltonian (3.10), it will remain in that eigenstate during its motion. What will vary, however, is the notion of the z axis in Eq. (3.10), which will be such that it adiabatically adapts to the local orientation of the external magnetic field. In addition, the modulus of the magnetic field, determining the energy scale C that characterizes the eigenvalues (3.11) and (3.12), will vary as well during this motion.

We can therefore infer that the presence of a spatially inhomogeneous profile of the external magnetic field translates into an *effective potential* for the moving atom. In the Zeeman regime of a comparatively weak magnetic field, this effective potential can, up to a global constant, be written as

$$V(\vec{r}) = -\vec{\mu} \cdot \vec{B}(\vec{r}) \,, \tag{3.17}$$

where the effective magnetic moment $\vec{\mu}$ of the atom has a fixed projection onto the local magnetic field axis, or, more precisely, as

$$V(\vec{r}) = \frac{m_{\text{eff}} g_e \mu_B}{2I+1} |\vec{B}(\vec{r})| \tag{3.18}$$

according to Eq. (3.13), with a fixed magnetic quantum number m_{eff}. Note that the latter does not flip from an energetically unfavorable (*e.g.*, positive) to a more favorable (*e.g.*, negative) value as long as the adiabaticity condition discussed above is fulfilled. This implies in particular that an atom whose magnetic moment is initially antiparallel to the local direction of the external magnetic field will maintain this antiparallel orientation in the course of its motion, which is very different from what would happen for a classical magnetic dipole.

This insight allows one to conceive magnetic field configurations whose associated effective potentials exhibit a local minimum at some point in space, about which atoms of the considered species can therefore be confined. While it is impossible to create magnetic field configurations that exhibit a finite local maximum in its abolute strength $|\vec{B}|$, a local minimum of $|\vec{B}|$ can be generated. It is thereby possible to realize magnetic traps for atoms whose hyperfine spin states are such that their corresponding magnetic moment is antiparallel to the direction of the external magnetic field. In the case of ^{87}Rb atoms, this trapping property is effectively fulfilled for the hyperfine states $|F = 2, m_F = 2\rangle$ and $|F = 2, m_F = 1\rangle$, as well as for the state $|F = 1, m_F = -1\rangle$ as long as we have $g_e \mu_B |\vec{B}(\vec{r})| < A$ for all $\vec{r}$.

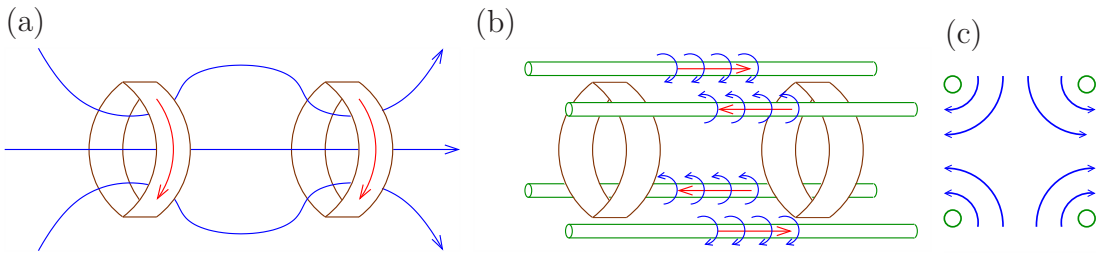

Figure 3.4: (a) Magnetic field lines (blue arrows) created by a pair of symmetric coils in which circulates an electric current of the same magnitude in the same orientation (red arrows). If the distance between the coils exceeds their radius, a local minimum in the intensity of the magnetic field along the symmetry axis occurs at the geometric centre of the configuration. (b) To ensure that the geometric centre represents a local minimum of $|\vec{B}|$ also with respect to the two transverse directions perpendicular to the symmetry axes, the two Helmholtz coils can be enclosed in a square-shaped cage of four parallel wires in which circulates an electric current in alternating directions, as shown by the red arrows. (c) As shown by the cross section, the magnetic field that this cage generates within the perpendicular plane becomes minimal on the symmetry axis.

Figure 3.4 shows an example for such a trapping configuration, which is named *Ioffe-Pritchard trap*. It consists of two symmetric coils, oriented parallel to each other, in which circulates an electric current of the same magnitude in the same orientation. Contrary to the Helmholtz configuration, the distance between the coils is not identical to their radius but exceeds the latter. A local minimum in the intensity of the magnetic field along the symmetry axis is then induced at the geometric centre of the configuration. To ensure that at this centre the intensity of the magnetic field is minimal also with respect to the two transverse directions perpendicular to the symmetry axes, the two Helmholtz coils can be enclosed in a square-shaped cage of four parallel wires in which circulates an electric current in alternating directions, as shown in Fig. 3.4(b). We thereby obtain an effective trapping potential for atoms whose magnetic moment is oriented antiparallel to the direction of the magnetic field. Near the geometric centre (which we identify with the origin of the coordinate system, with the z axis being oriented along the symmetry axis of the configuration), this trapping potential can, up to an unimportant global constant, be approximated by an anisotroic three-dimensional parabolic confinement of the form

$$V(\vec{r}) = \frac{1}{2}k_{\perp}\left(x^2 + y^2\right) + \frac{1}{2}k_{||}z^2\,, \tag{3.19}$$

where the two (positive) spring constants $k_{||}$ and $k_{\perp}$ can respectively be tuned by the currents circulating within the two coils as well as within the four cage wires.

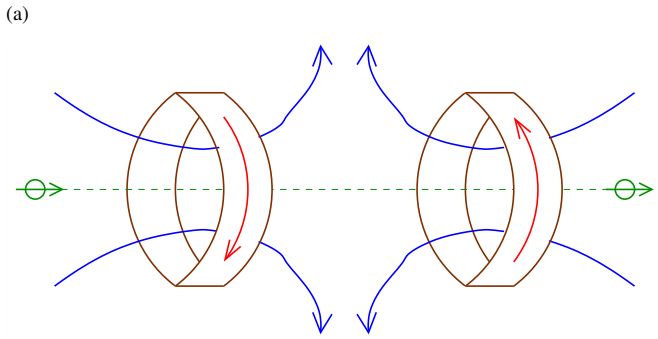

Figure 3.5: Anti-Helmholtz configuration of two coils, giving rise to a node of the magnetic field in the geometric centre. As a consequence, the adiabaticity condition cannot be granted within this configuration. An atom that moves along the symmetry axis and has its magnetic moment polarized parallel to this axis will, when passing across the geometric centre, undergo a sudden change of the orientation of its magnetic moment with respect to the direction of the external magnetic field, simply becaues the latter suddenly changes its sign at this point. This anti-Hemlholtz configuration is therefore unsuited to magnetically confine ultracold atoms.

Naively, one might consider that an opposite orientation of the currents circulating in the two coils, as shown in Fig. 3.5, should give rise to an even easier possibility to realize a magnetic trap, since in that case the magnetic field exactly vanishes in the geometric centre of the configuration. However, a vanishing magnetic field implies that the condition for the validity of the adiabatic theorem, namely that the time scale on which the orientation and strength of the magnetic field at the position of the atom effectively vary is slow compared to the inverse of the Zeeman splitting, can no longer be granted, since the hyperfine sublevels become degenerate at the point where $\vec{B}$ vanishes. If we consider, *e.g.*, an atom that propagates along the symmetry axis and has its magnetic moment polarized parallel to this axis, the orientation of this magnetic moment with respect to the direction of the external magnetic field suddenly changes when the atom passes across the geometric centre of the configuration, trivially because the direction of the magnetic field suddenly changes sign at that point.

As a consequence, the anti-Helmholtz configuration of the two coils depicted in Fig. 3.5 cannot be used to magnetically trap atoms. In combination with laser beams, it can nevertheless be employed to conceive *magneto-optical traps* which allow one to confine atoms and reduce their temperature via laser cooling techniques. However, those magneto-optical traps are unsuited to reach ultracold temperatures yielding Bose-Einstein condensation of the atomic gas since the permanent absorption and re-emission of laser photons that takes place in such a trap introduce an intrinsic lower bound for the temperature that can be reached

through laser cooling.

Problems

3.2 Show the validity of Eqs. (3.11) et (3.12).

3.3 Interaction with a laser

Trapping configurations for ultracold alkali atoms can be created not only by external magnetic fields but also by laser radiation the photon energy of which lies close to the (dipole allowed) intra-atomic transition from the ground state to the first excited p state of the atom. This can be shown from first principles. We start, for this purpose, from the effective two-body Hamiltonian

$$\mathcal{H} = \frac{1}{2m}\left(\vec{p} - e\vec{A}(\vec{r},t)\right)^2 + \frac{1}{2m_e}\left(\vec{p}_e + e\vec{A}(\vec{r}_e,t)\right)^2 + \mathcal{V}(\vec{r}_e - \vec{r}) \tag{3.20}$$

describing the mutual interaction between the unpaired valence electron and the atomic core as well as their respective interactions with the electromagnetic field induced by the laser. Here, $\vec{r}_e$ and $\vec{r}$ represent the positions of the valence electron and the atomic nucleus, respectively, and $\vec{p}_e$ and $\vec{p}$ are their associated momentum operators. Their mutual electron-core interaction energy is modeled by an effective potential $\mathcal{V}$ which in practice depends only on the distance between the electron and the nucleus. Using the Coulomb gauge, the laser field is represented in terms of the vector potential $\vec{A}$, which allows one to determine the associated electric and magnetic fields according to

$$\vec{E}(\vec{r},t) = -\frac{\partial}{\partial t}\vec{A}(\vec{r},t)\,, \tag{3.21}$$

$$\vec{B}(\vec{r},t) = \vec{\nabla}\times\vec{A}(\vec{r},t) \tag{3.22}$$

for all $(\vec{r},t)$. In the case of optical or infrared laser beams with not too strong intensities, we can neglect the effect of the magnetic field as compared to the electric one and use the fact that spatial variations of the field amplitudes take place on length scales that are much larger than the Bohr radius, which amounts to performing the so-called *dipole approximation*. This allows one to derive, through a suitable gauge transformation of the atomic wavefunction, the effective single-particle Hamiltonian

$$H = -\frac{\hbar^2}{2m}\frac{\partial^2}{\partial\vec{\rho}^2} + \mathcal{V}(\vec{\rho}) + e\vec{E}(\vec{r},t)\cdot\vec{\rho} \tag{3.23}$$

describing the dynamics in the intra-atomic relative coordinate $\vec{\rho} = \vec{r}_e - \vec{r}$, where the position $\vec{r}$ of the nucleus enters as a parameter.

For the sake of simplicity, we assume for the following that the considered laser beam is monochromatic and linearly polarized. The electric field that it generates is therefore modeled as

$$\vec{E}(\vec{r},t) = \vec{\mathcal{E}}_0(\vec{r}) \cos\left(\omega t - \varphi(\vec{r})\right) \tag{3.24}$$

with a spatially dependent vectorial amplitude $\vec{\mathcal{E}}_0$ and a scalar phase function φ, which can both be considered to be locally constant on a scale that is comparable to Bohr's radius. In view of defining an optical potential with this laser beam, we furthermore assume its photon energy to be close to the energy of a dipole allowed intra-atomic transition, typically from the electronic ground state to the first excited p state of the alkali atom, *i.e.*, we have $\hbar\omega \simeq E_1 - E_0$, where E_0 and E_1 are the energies of the involved electronic ground state $|0\rangle$ and excited state $|1\rangle$, respectively. In the case of ^{87}Rb, those two states would be characterized by the quantum numbers $n = 5$, $l = 0$, $m_l = 0$ as well as $n = 5$, $l = 1$, $m_l = 0$, respectively, where the z axis that effectively defines the notion of the magnetic quantum number m_l is identified with the local direction of the electric field amplitude vector $\vec{\mathcal{E}}_0(\vec{r})$ at the position $\vec{r}$ of the atom. Note that we have to exclude the case of an *exact* resonance with the intra-atomic transition, in order not to significantly populate the excited state via this laser radiation. The laser photon energy is therefore slightly detuned from the energy difference $E_1 - E_0$, and this on a scale that exceeds the natural linewidth of the excited energy level.

The application of time-dependent perturbation theory under these conditions yields that the ground state is not appreciably depopulated in the presence of the laser beam, but undergoes a shift $E_0 \mapsto E_0 + \Delta E_0$ in its effective eigenenergy. This shift is explicitly evaluated as

$$\Delta E_0 = -\frac{|\langle 1|e\vec{\rho}\cdot\vec{e}_z|0\rangle|^2}{E_1 - E_0 - \hbar\omega}\,\frac{I(\vec{r})}{2\epsilon_0 c} \equiv V(\vec{r}) \tag{3.25}$$

in lowest nonvanishing order in the laser field amplitude $\vec{\mathcal{E}}_0(\vec{r})$, where

$$I(\vec{r}) = \frac{1}{2}\epsilon_0 c|\vec{\mathcal{E}}_0(\vec{r})|^2 \tag{3.26}$$

denotes the intensity of the laser at the position $\vec{r}$ of the atom. The spatial intensity profile of the laser therefore translates into an effective potential $V(\vec{r})$ governing the motion of the atom, which is defined by Eq. (3.25). In contrast to the analogous effective potential (3.18) that is obtained in the presence of a magnetic field, the (positive or negative) sign of this effective potential is not *a priori* fixed for a given choice for the atomic hyperfine state, but can be changed by properly tuning the laser frequency. Most specifically, an overall attractive effective potential, with $V(\vec{r}) \leq 0$ for all $\vec{r}$, is obtained if the laser is *red-detuned* with respect to the intra-atomic transition, *i.e.*, if $\hbar\omega < E_1 - E_0$, while a *blue-detuned* laser, with $\hbar\omega > E_1 - E_0$, leads to an overall repulsive effective potential, with $V(\vec{r}) \geq 0$ for all $\vec{r}$.

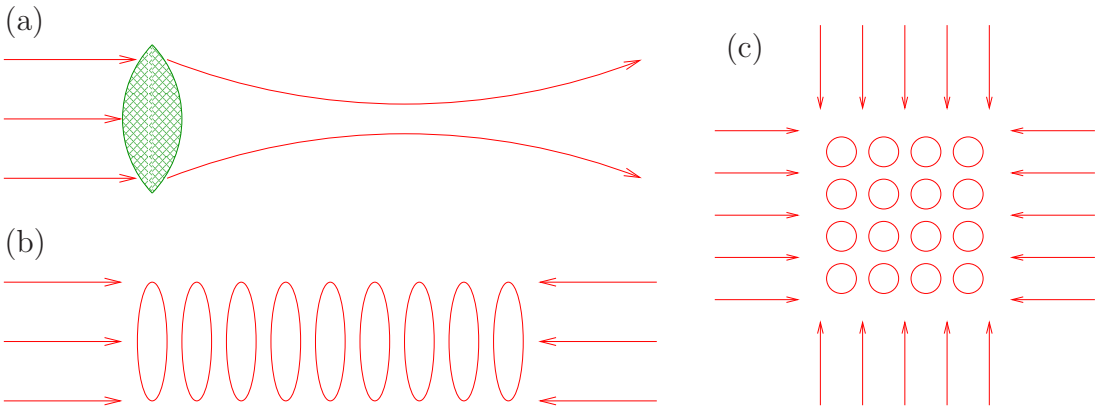

Figure 3.6: Sketch of various optical trapping configurations induced by laser beams: (a) optical dipole trap, created by a focused red-detuned laser beam; (b) one-dimensional optical lattice, created by a pair of two counterpropagating laser beams with the same wavelength; (c) two-dimensional optical lattice, created by two orthogonal pairs of counterpropagating laser beams with the same wavelength. Curved lines, ellipses, and circles show the equipotential levels of the effective optical potential that the atoms are exposed to within such laser beam configurations.

This insight allows one to conceive trapping potentials for ultracold atoms using optical means. The simplest way to create such an optical trap consists in directing a red-detuned laser beam onto a circularly shaped focusing lens. As illustrated in Fig. 3.6(a), a local maximum of the laser intensity is then induced at the focal point behind the lens. Owing to the fact that the laser is red-detuned, this local intensity maximum corresponds to a local minimum of the effective potential (3.25) about which the atoms can consequently be trapped. Very similarly to the local potential (3.19) that we obtained for the magnetic Ioffe-Pritchard trap, this *optical dipole trap* gives rise to an anisotroic three-dimensional parabolic confinement of the form

$$V(\vec{r}) = \frac{1}{2}k_{\perp}\left(x^2 + y^2\right) + \frac{1}{2}k_{||}z^2 \tag{3.27}$$

in the near vicinity of the trap centre, where we identify the origin with the focal point and the z axis with the propagation direction of the laser field (and omit an unimportant global constant). The spring constants $k_{||}$ and $k_{\perp}$ can be tuned by the varying the laser beam intensity and by changing the focal characteristics of the lens.

Using pairs of counterpropagating laser beams with the same frequency (which, in practice, can be generated from a single laser beam by means of beam splitter devices and mirrors), we can generate an *optical lattice* corresponding to a spatially periodic potential with a period that equals half the wavelength of the

laser, owing to the the periodic intensity profile of the standing wave that results from the superposition of the two laser beams. Such an optical lattice can be attractive or repulsive, depending on the detuning of the laser frequency. As illustrated in Fig. 3.6(b), a single pair of counterpropagating laser beams gives rise to a one-dimensional optical lattice defined along the axis of beam propagation, whose transverse extent is effectively determined by the waist of the laser beams and can consequently be reduced by subjecting those beams to focusing, as explained above for the optical dipole trap. Two or three pairs of counterpropagating laser beams, defined along mutually perpendicular axes, give rise to two- or three-dimensional lattice potentials, respectively. Note that it would be extremely hard to engineer such lattices, which are defined with spatial periods in the submicron regime, by magnetic fields that are generated from coils and current-carrying electric wires.

Lasers can not only be used to create trapping configurations for a gas of cold alkali atoms, but also to cool such a trapped gas. A simple strategy to achieve this goal consists in exposing the atoms to a couple of laser beams which irradiate the gas from different directions with a frequency that is slightly red-detuned with respect to the intra-atomic transition from the electronic ground state to the excited p state. Due to the Doppler effect, atoms moving against such a laser beam will, in their inertial reference frame, effectively see a blue-shift of the associated photon frequency, which implies that the latter gets closer to the intra-atomic transition frequency. Resonant transitions between the ground state of the atom and its first excited p state can then occur at specific positive velocity components in the direction against the propagation of the laser beam. The recoil that the atom experiences after the absorption of a laser photon therefore diminishes the speed of the atom and thence gives rise to a reduction of its kinetic energy.

More sophisticated laser cooling techniques that are more effective than this *Doppler cooling* reside on a spatial tuning of the intra-atomic transition frequency, which can be achieved within magneto-optical traps. As for Doppler cooling, those techniques are concerned with a fundamental lower limit for the temperature that can thereby be reached. This limit is given by the recoil energy $\hbar^2 k_{\mathrm{photon}}^2/(2m)$ that an atom receives after the spontaneous re-emission of the absorbed laser photon into some arbitrary direction. Generally, the temperatures that can thereby be reached are of the order of $\sim 10\,\mu$K, which is not sufficiently low to yield Bose-Einstein condensation.

To further reduce the temperature of an atomic gas below this recoil limit, an alternative technique has to be employed, which effectively amounts to performing an *evaporative cooling* process. To this end, we consider that the atoms are, after a preliminary laser cooling stage, exposed to a magnetic trapping potential which, as was described in the previous section, provides a confinement for atoms whose magnetic moment is antiparallel to the direction of the external magnetic field. A spin-polarized sample of trapped atoms that are prepared in a specific hyperfine

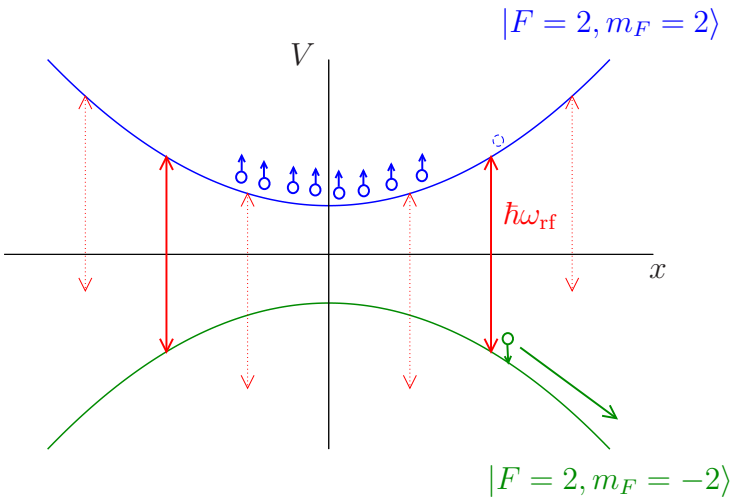

Figure 3.7: Sketch of the working principle of evaporative cooling. Spin-polarized atoms in a hyperfine state (*e.g.*, $|F = 2, m_F = 2\rangle$ for ^{87}Rb) in which the orientation of the magnetic moment is antiparallel to the external magnetic field are confined within a magnetic field configuration that exhibits a finite local minimum in space. A radio-frequency field can induce spin-flips of such atoms to an untrapped hyperfine state (*e.g.*, $|F = 2, m_F = -2\rangle$ for ^{87}Rb) at positions where the energy difference between the trapped and the untrapped state equals $\hbar\omega_{\mathrm{rf}}$ with ω_{rf} the frequency of this electromagnetic radiation. By tuning this frequency such that those resonant transitions occur suitably far away from the trap centre, atoms exhibiting high kinetic energies can thereby be removed from the trap. The gas of remaining atoms is then cooled through re-thermalization.

state featuring this antiparallel orientation (*e.g.*, $|F = 2, m_F = 2\rangle$ for ^{87}Rb) is then exposed to an electromagnetic field in the radio-frequency regime (*i.e.*, with a frequency of the order of $\sim$ MHz) which is tuned such that it induces resonant transitions to an untrapped hyperfine state (*e.g.*, to $|F = 2, m_F = -2\rangle$ for ^{87}Rb) at positions that are off-centre with respect to the magnetic trap and therefore correspond to an enhanced potential energy. As sketched in Fig. 3.7, atoms with relatively high kinetic energies will therefore, at some point during their motion within the trap, come across spatial regions where a flip of their magnetic moment from a trapped to an untrapped orientation is induced by the radio-freqency field, which implies that they are ejected from the trap. The thermal distribution of the spin-polarized sample within the magnetic trap is therefore cut off at high energies by this "radio-frequency knife". Provided the atoms of the gas interact with each other on reasonable time scales, this cut-off gives rise to a re-thermalization of the gas, with the effect that its temperature is lowered. High phase-space densities at temperatures below $1\,\mu$K can thereby be reached without loosing too many atoms, which is sufficient to trigger Bose-Einstein condensation.

Problems

3.3 Show how effective one-body Hamiltonian in the dipole approximation (3.23) can be derived from the two-body Hamiltonian (3.20) by means of a suitable gauge transformation of the wavefunction. Assume, for this purpose, that the vector potential varies slowly on a scale corresponding to Bohr's radius and that the magnetic field resulting from this vector potential can be neglected.

3.4 Show how Eq. (3.25) can be derived using time-dependent perturbation theory.

3.4 The Born-Oppenheimer approximation

Atoms in a trapped quantum gas do not only interact with external electric and magnetic fields but also with each other. As they are electrically neutral particles that do not exhibit an intrinsic permanent dipole moment, the effect of this atom-atom interaction is relatively weak in absolute terms, to the extent that the basic statistical assumptions leading to classical and quantum ergodicity, as discussed in Chapter 1, can safely be considered to be valid. Nevertheless, the presence of atom-atom interaction can by no means be totally neglected for Bose-Einstein condensates made of alkali atoms. It gives rise to a number of properties that are characteristic for such condensates, including, in particular, their superfluidity.

It is therefore mandatory to develop a simplified but quantitative model for describing the interaction between atoms in a quantum gas. We start, for this purpose, from a microscopic *first-principles* theory of the quantum gas, for which we take into account that each atom in the gas is constituted by Z electrons with negative electric charge $-e$ and spin $1/2$ (with Z being an odd number for alkali atoms) as well as by a point-like nucleus with the positive charge Ze and a nuclear spin I. Neglecting the presence of external magnetic or optical confinement potentials for the moment, we can formulate this microscopic first-principles theory of a gas of N neutral atoms in terms of the Hamiltonian

$$\begin{aligned} H &= \sum_{i=1}^{N} \frac{1}{2m} \vec{p}_i^{\,2} + \sum_{j=1}^{ZN} \frac{1}{2m_e} \vec{p}_{e,j}^{\,2} + \sum_{i=1}^{N} \sum_{j=1}^{ZN} V_{eN}\left(X_i, \xi_j\right) \\ &\quad + \sum_{i=2}^{N} \sum_{i'=1}^{i-1} V_{NN}\left(X_i, X_{i'}\right) + \sum_{j=2}^{ZN} \sum_{j'=1}^{j-1} V_{ee}\left(\xi_j, \xi_{j'}\right) . \end{aligned} \tag{3.28}$$

Here, $\vec{p}_i$ and $\vec{p}_{e,j}$ represent the momentum operators of the ith nucleus and the jth electron, respectively, and m and m_e denote their corresponding masses. The potential energy is expressed in terms of the generalized coordinates $X_i \equiv (\vec{r}_i, \Sigma_i)$ and $\xi_j \equiv (\vec{r}_{e,j}, \sigma_j)$ for the ith nucleus and the jth electron, respectively, where

$\vec{r}_i$ and $\vec{r}_{e,j}$ represent their position operators while $\Sigma_i \in \{-I, -I+1, \ldots, I\}$ and $\sigma_j \in \{-1/2, 1/2\}$ denote their spin states with respect to a given reference axis in the spatial coordinate system. Taking into account the fact that the interaction between the involved particles is dominated by electrostatic Coulomb attraction or repulsion, we can justify the first-order approximations

$$V_{eN}(X_i, \xi_j) \simeq -\frac{Ze^2}{4\pi\epsilon_0 |\vec{r}_i - \vec{r}_{e,j}|}, \tag{3.29}$$

$$V_{NN}(X_i, X_{i'}) \simeq \frac{Z^2 e^2}{4\pi\epsilon_0 |\vec{r}_i - \vec{r}_{i'}|}, \tag{3.30}$$

$$V_{ee}(\xi_j, \xi_{i'}) \simeq \frac{e^2}{4\pi\epsilon_0 |\vec{r}_{e,j} - \vec{r}_{e,j'}|} \tag{3.31}$$

for the electron-nucleus, nucleus-nucleus, and electron-electron interaction potentials, respectively, where ϵ_0 denotes the vacuum permittivity. The above expressions (3.29)–(3.31) ought to be amended by spin-dependent terms, such as spin-spin interaction and spin-orbit coupling, in order to carry out numerically accurate atomic and molecular structure calculations on the basis of the Hamiltonian (3.28).

Equation (3.28) can be rewritten as

$$H = \sum_{i=1}^{N} \frac{1}{2m} \vec{p}_i^{\,2} + H_{\rm el} \tag{3.32}$$

where we introduce by

$$\begin{aligned} H_{\rm el} = & \sum_{j=1}^{ZN} \frac{1}{2m_e} \vec{p}_{e,j}^{\,2} + \sum_{i=1}^{N} \sum_{j=1}^{ZN} V_{eN}(X_i, \xi_j) + \sum_{j=2}^{ZN} \sum_{j'=1}^{j-1} V_{ee}(\xi_j, \xi_{j'}) \\ & + \sum_{i=2}^{N} \sum_{i'=1}^{i-1} V_{NN}(X_i, X_{i'}) \end{aligned} \tag{3.33}$$

an electronic Hamiltonian which parametrically depends on the nuclear coordinates $X_1, \ldots, X_N$. This Hamiltonian can be diagonalized in the electronic coordinates. We thereby obtain its normalized fermionic eigenstates $|\Phi_n\rangle$ (*i.e.*, the eigenstates that are fully antisymmetric in the electronic coordinates) satisfying $H_{\rm el}|\Phi_n\rangle = U_n|\Phi_n\rangle$ with the associated eigenenergies U_n. Both eigenstates and eigenvalues parametrically depend on the positions and spins of the nuclei, *i.e.* we have $U_n \equiv U_n(\vec{r}_1\Sigma_1, \ldots, \vec{r}_N\Sigma_N)$ and can express the associated wavefunctions as

$$\langle \xi_1, \ldots, \xi_{ZN} | \Phi_n \rangle = \Phi_n(\vec{r}_{e,1}\sigma_1, \ldots, \vec{r}_{e,ZN}\sigma_{ZN}; \vec{r}_1\Sigma_1, \ldots, \vec{r}_N\Sigma_N) . \tag{3.34}$$

Having thereby formally solved the electronic problem for all possible choices for the positions and spins of the nuclei, we can decompose the wavefunction Ψ of the many-body system in the above electronic eigenbasis. This yields

$$\begin{aligned}\Psi\left(X_1,\ldots,X_N,\xi_1,\ldots,\xi_{ZN},t\right) &= \sum\!\!\!\!\!\!\int_n \psi_n\left(X_1,\ldots,X_N,t\right) \\ &\quad \times\Phi_n\left(\xi_1,\ldots,\xi_{ZN};X_1,\ldots,X_N\right)\,, \quad (3.35)\end{aligned}$$

where the thereby introduced nuclear wavefunctions ψ_n can be obtanied from the projections of Ψ to the electronic eigenstates Φ_n. As the latter are of mixed discrete and continuous nature at high energies, the above decomposition generally involves a combination of sums and integrals. Projecting now the many-body Schrödinger equation $i\hbar\frac{\partial}{\partial t}\Psi = H\Psi$ onto the electronic eigenstates Φ_n gives then rise to a system of coupled time evolution equations

$$\begin{aligned}i\hbar\frac{\partial}{\partial t}\psi_n\left(X_1,\ldots,X_N\right) &= \left(\sum_{i=1}^{N}\frac{1}{2m}\vec{p}_i^{\,2} + U_n\left(X_1,\ldots,X_N\right)\right)\psi_n\left(X_1,\ldots,X_N\right) \\ &\quad + \sum\!\!\!\!\!\!\int_{n'}\sum_{i=1}^{N}\frac{1}{m}\vec{p}^{\,(i)}_{nn'}\left(X_1,\ldots,X_N\right)\cdot\vec{p}_i\psi_{n'}\left(X_1,\ldots,X_N\right) \\ &\quad + \sum\!\!\!\!\!\!\int_{n'} T_{nn'}\left(X_1,\ldots,X_N\right)\psi_{n'}\left(X_1,\ldots,X_N\right) \quad (3.36)\end{aligned}$$

with the coupling coefficients

$$\begin{aligned}\vec{p}^{\,(i)}_{nn'}\left(X_1,\ldots,X_N\right) &= \sum_{\sigma_1\cdots\sigma_{ZN}}\int d^3r_{e,1}\cdots d^3r_{e,ZN}\Phi_n^*\left(\xi_1,\ldots,\xi_{ZN};X_1,\ldots,X_N\right) \\ &\quad \times\frac{\hbar}{i}\frac{\partial}{\partial\vec{r}_i}\Phi_{n'}\left(\xi_1,\ldots,\xi_{ZN};X_1,\ldots,X_N\right)\,, \quad (3.37) \\ T_{nn'}\left(X_1,\ldots,X_N\right) &= \sum_{\sigma_1\cdots\sigma_{ZN}}\int d^3r_{e,1}\cdots d^3r_{e,ZN}\Phi_n^*\left(\xi_1,\ldots,\xi_{ZN};X_1,\ldots,X_N\right) \\ &\quad \times\sum_{i=1}^{N}\frac{-\hbar^2}{2m}\frac{\partial^2}{\partial\vec{r}_i^{\,2}}\Phi_{n'}\left(\xi_1,\ldots,\xi_{ZN};X_1,\ldots,X_N\right)\,. \quad (3.38)\end{aligned}$$

The *Born-Oppenheimer approximation* essentially consists in neglecting within Eq. (3.36) the second and third lines containing the coupling terms between different electronic states, such that the nuclear wavefunctions evolve according to

$$\begin{aligned}i\hbar\frac{\partial}{\partial t}\psi_n\left(X_1,\ldots,X_N\right) &\simeq \sum_{i=1}^{N}\frac{1}{2m}\vec{p}_i^{\,2}\psi_n\left(X_1,\ldots,X_N\right) \\ &\quad + U_n\left(X_1,\ldots,X_N\right)\psi_n\left(X_1,\ldots,X_N\right)\,. \quad (3.39)\end{aligned}$$

This approximation is very well justified since the nuclear mass is much larger than the electron mass, *i.e.*, we have $m/m_e \gg 1$. Indeed, we can infer from the structure of the electronic Hamiltonian (3.33) in combination with the Coulomb interaction potentials (3.29)–(3.31) that the electronic eigenfunctions Φ_n vary in both their electronic and nuclear coordinates on length scales that are typically of the order of Bohr's radius $a_B = 4\pi\epsilon_0\hbar^2/(m_e e^2)$ (eventually to be amended by a prefactor of the order of $1/Z$ for tightly bound core-shell electrons). The coefficients that induce the couplings between different electronic levels within Eq. (3.36) scale then as $\vec{p}^{(i)}_{nn'} \sim \hbar/a_B$ as well as $T_{nn'} \sim \hbar^2/(2ma_B^2) = m_e R/m$ according to Eqs. (3.37) and (3.38), respectively, where we introduce by $R = \hbar^2/(2m_e a_B^2)$ Rydberg's unit of energy. As the latter represents the characteristic scale of the associated eigenenergies U_n, we can through simple dimensional considerations infer the length scale $\hbar/\sqrt{2mR}$ on which the nuclear wavefunctions ψ_n typically vary according to Eq. (3.39). The effective coupling matrix elements between different electronic levels consequently scale as $\sim \sqrt{m_e/m}R$ according to the second line of Eq. (3.36), while the third line induces couplings of the order of $(m_e/m)R$. Those couplings are thus significantly smaller than the typical spacing $|U_n - U_{n'}| \sim R$ between different electronic energy levels and can therefore safely be neglected unless two such energy levels happen to accidentally coincide, *i.e.*, unless $U_n(X_1, \ldots, X_N) = U_{n'}(X_1, \ldots, X_N)$, at some specific configuration $(X_1, \ldots, X_N)$ of the nuclear coordinates.

Of particular relevance is the electronic ground state Φ_0 of the gas, which is generally attained at low temperatures. Its associated nuclear wavefunction ψ_0 evolves, in the framework of the above Born-Oppenheimer approximation, according to the Schrödinger equation (3.39) which is defined in terms of the effective N-body interaction potential $U_0(X_1, \ldots, X_N)$. In the case of a dilute gas in which close atom-atom encounters involving inter-nuclear distances of the order of few Bohr radii are rather rare, the latter N-body potential can be approximately represented by a superposition of two-body interaction terms according to

$$U_0(X_1, \ldots, X_N) \simeq \sum_{i=2}^{N} \sum_{i'=1}^{i-1} U_0(|\vec{r}_i - \vec{r}_{i'}|)\,, \tag{3.40}$$

where the *Born-Oppenheimer potential curve* U_0 describes the effective interaction energy of two atoms as a function of the interatomic distance $r = |\vec{r}_i - \vec{r}_{i'}|$. For large $r \to \infty$ we are effectively dealing with two independent neutral atoms and therefore trivially obtain $U_0(r) \simeq 2E_0$ where E_0 is the (negative) ground-state energy of a single atom. As the atoms are moved closer to each other, a spontaneous polarisation of the electronic cloud within one of them can induce a weak electric field at the position of the other atom, which in turn polarizes the electronic cloud of that other atom as well. This induced dipole-dipole interaction, which is also termed *van der Waals interaction*, gives rise to a weak attractive potential between the atoms. It asymptotically scales as $U_0(r) - 2E_0 \simeq -C/r^6$

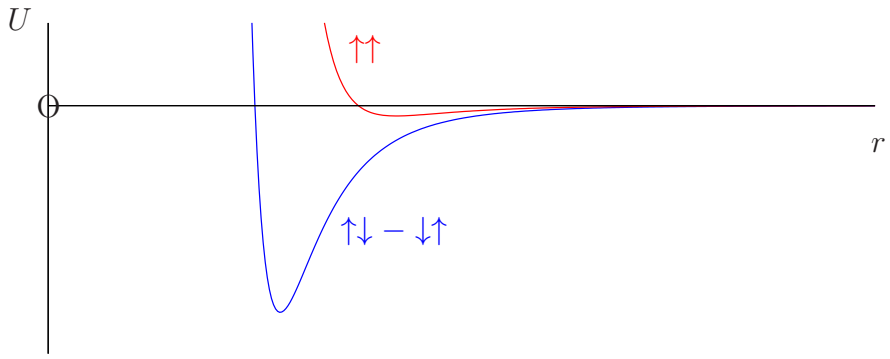

Figure 3.8: Qualitative sketch of the two-body van der Waals interaction potential between two identical alkaline atoms as a function of their distance r, for both the singlet (blue curve) and the triplet configuration (red curve) of the electronic spin state.

for large distances r between the atoms[4], where the associated van der Waals coefficient C is found to lie in the range $10^3 < a_B^6 C/(2R) < 10^4$ for alkali atoms. At extremely short distances $r \ll a_B$, on the other hand, the two-body potential trivially diverges due to Coulomb repulsion between the nuclei, which in that case can no longer be screened by the electrons due to Heisenberg's uncertainty principle. The local and global minimum that is located in between these two extremal situations corresponds to the formation of a diatomic molecule.

Figure 3.8 shows a qualitative sketch of the two-body van der Waals interaction potential $U(r) = U_0(r) - 2E_0$ as a function of r for both the spin-singlet and the spin-triplet configuration of the two valence electrons. Contrary to hydrogen, not only the singlet but also the triplet configuration features a bonding state of the two atoms, albeit with a much more shallow potential minimum than for the singlet. In absolute terms, the depth of this triplet potential miminum is equivalent to a few hundred Kelvin in the case of ^{87}Rb, which is many orders of magnitude larger than the typical temperatures characterizing an ultracold quantum gas, and the singlet potential well has a depth of about 6×10^3 K. The precise knowledge of the shape of this Van der Waals interaction potential is therefore not necessarily required in order to describe the effect of atom-atom interaction within an ultracold dilute quantum gas where the absolute and relative kinetic energies are of the order of μK. We can, for this purpose, permit ourselves to replace it by a simplified model potential which is chosen such that it correctly reproduces the low-energy two-body collision processes between the atoms of the gas.

[4] At extremely large inter-atomic distances which are typically not relevant in trapped gases, this scaling law is to be amended due to the relativistic *Casimir effect* which accounts for the finite propagation speed of electromagnetic radiation. This gives rise to a decrease of the interaction potential proportional to $-r^{-7}$ for very large r.

Problems

3.5 Show that the Van der Waals interaction potential $U_0(r)-2E_0$ scales asymptotically as $U_0(r)-2E_0 \simeq -C/r^6$ for large inter-atomic distances r. Assume for this purpose that only the valence electrons of the two atoms effectively participate at the interaction process, while the inner core-shell electrons of each one of the atoms are not appreciably affected by the presence of the other atom.

3.5 Two-body scattering

To develop a simple model for the atom-atom interaction that correctly describes the collision between two atoms in the ultracold gas, it is useful to theoretically study such two-body collision processes. We therefore start from the Schrödinger equation

$$i\hbar\frac{\partial}{\partial t}\Psi(\vec{r}_1,\vec{r}_2,t) = -\frac{\hbar^2}{2m}\left(\frac{\partial^2}{\partial\vec{r}_1^{\,2}}+\frac{\partial^2}{\partial\vec{r}_2^{\,2}}\right)\Psi(\vec{r}_1,\vec{r}_2,t)+U(\vec{r}_1-\vec{r}_2)\Psi(\vec{r}_1,\vec{r}_2,t) \quad (3.41)$$

which describes two identical alkali atoms with the mass m and the mutual interaction energy $U(\vec{r}_1-\vec{r}_2)$. The latter is, in practice, given by the energetically lowest Born-Oppenheimer potential curve that effectively results from restricting the atoms to a given hyperfine sublevel within a magnetic trap. It would correspond to the triplet curve (sketched in red in Fig. 3.8) in the presence of a very strong magnetic field for which trapping is achieved by polarizing the spins of the two valence electrons along the magnetic field axis.

A first simplification of the two-body problem is achieved by introducing the centre-of-mass and relative coordinates

$$\vec{R} = \frac{1}{2}(\vec{r}_1+\vec{r}_2)\ , \quad (3.42)$$

$$\vec{r} = \vec{r}_1-\vec{r}_2 \quad (3.43)$$

in which the Schrödinger equation (3.41) separates. More precisely, inserting the Fourier series ansatz

$$\Psi(\vec{r}_1,\vec{r}_2,t) = \Psi(\vec{R}+\vec{r}/2,\vec{R}-\vec{r}/2,t) = \int d^3K\psi^{(\vec{K})}(\vec{r},t)e^{i\vec{K}\cdot\vec{R}} \quad (3.44)$$

into Eq. (3.41) and using the relation

$$\frac{\partial^2}{\partial\vec{r}_1^{\,2}}+\frac{\partial^2}{\partial\vec{r}_2^{\,2}} = \frac{1}{2}\frac{\partial^2}{\partial\vec{R}^{\,2}}+2\frac{\partial^2}{\partial\vec{r}^{\,2}} \quad (3.45)$$

yields that the Fourier components $\psi^{(\vec{K})}$, which are associated with plane-wave states of the centre-of-mass motion with a fixed total momentum $\hbar\vec{K}$, are not

coupled with each other and evolve independently according to the effective one-body Schrödinger equation

$$i\hbar\frac{\partial}{\partial t}\psi^{(\vec{K})}(\vec{r},t) = \left(-\frac{\hbar^2}{2m_r}\frac{\partial^2}{\partial\vec{r}^2} + U(\vec{r}) + \frac{\hbar^2K^2}{4m}\right)\psi^{(\vec{K})}(\vec{r},t)\,, \tag{3.46}$$

where we introduced by

$$m_r = \frac{m}{2} \tag{3.47}$$

the *reduced mass* associated with the motion in the relative coordinates. The two-body collision problem posed in this section is thereby reduced to an effective one-body scattering problem in the relative coordinates, which is to be solved for each one of the Fourier components $\psi^{(\vec{K})}$.

To this end, we first perform the gauge transformation

$$\psi^{(\vec{K})}(\vec{r},t) \equiv \psi(\vec{r},t)e^{-iE_Kt/\hbar} \tag{3.48}$$

with $E_K = \hbar^2K^2/(4m)$ for all $\vec{r},t$, such that the transformed wavefunction ψ (in which we leave out the $\vec{K}$ label for the sake of simplicity) evolves according to the Schrödinger equation

$$i\hbar\frac{\partial}{\partial t}\psi(\vec{r},t) = -\frac{\hbar^2}{2m_r}\frac{\partial^2}{\partial\vec{r}^2}\psi(\vec{r},t) + U(\vec{r})\psi(\vec{r},t) \tag{3.49}$$

in the presence of the central scattering potential U that asymptotically vanishes for large distances from the origin[5], *i.e.*, we have $U(\vec{r}) \to 0$ for $r \to \infty$. The initial state of this wavefunction in the case of a scattering problem corresponds to a wave packet that is prepared asymptotically far away from the origin and moves towards it. Since the presence of a scattering potential U that has finite support only in the immediate vicinity of the origin is not relevant for the initial evolution of such a wave packet, we can represent the solution of the Schrödinger equation (3.49) as

$$\psi(\vec{r},t_0) = \int d^3k\,\alpha(\vec{k})e^{i\vec{k}\cdot\vec{r}}e^{-iE_kt_0/\hbar} \tag{3.50}$$

for times $t_0 \to -\infty$ sufficiently far in the asymptotic past, with $\alpha(\vec{k})$ the Fourier components of the wavefunction, corresponding to its momentum distribution, and

$$E_k = \frac{\hbar^2k^2}{2m_r}\,. \tag{3.51}$$

[5]In the case that the Born-Oppenheimer potential U is defined such that it asymptotically tends to a nonzero constant $-2E_0$ for large distances, this latter constant ought to be factored out as well by the gauge transformation (3.48), *i.e.*, we would define $E_K = \hbar^2K^2/(4m) - 2E_0$ in that case.

According to quantum scattering theory, the initial wavefunction (3.50) evolves according to

$$\psi(\vec{r},t) = \int d^3k\, \alpha(\vec{k}) \psi_{\vec{k}}(\vec{r}) e^{-iE_k t/\hbar} \tag{3.52}$$

for finite times t at which parts of the wave packet move across the origin of the coordinate system, where the scattering wavefunction $\psi_{\vec{k}}$ satisfies the *Lippmann-Schwinger equation*

$$\psi_{\vec{k}}(\vec{r}) = e^{i\vec{k}\cdot\vec{r}} - \frac{m_r}{2\pi\hbar^2} \int d^3r' \frac{e^{ik|\vec{r}-\vec{r}'|}}{|\vec{r}-\vec{r}'|} U(\vec{r}') \psi_{\vec{k}}(\vec{r}')\,. \tag{3.53}$$

The latter describes the coherent superposition of an incident plane wave and all outgoing spherical waves that emanate from the positions $\vec{r}'$ at which the scattering potential is nonvanhishing, whose weight in this superposition is proportional to $U(\vec{r}')\psi_{\vec{k}}(\vec{r}')$. It is a straightforward exercise to verify that the self-consistent expression (3.53) for the scattering wavefunction solves the stationary Schrödinger equation

$$-\frac{\hbar^2}{2m_r} \frac{\partial^2}{\partial \vec{r}^2} \psi_{\vec{k}}(\vec{r}) + U(\vec{r}) \psi_{\vec{k}}(\vec{r}) = E_k \psi_{\vec{k}}(\vec{r}) \tag{3.54}$$

and can therefore be seen as an integral representation of the latter.

We now make use of the fact that the two-body interaction potential displays a spherical symmetry, such that we can write it as $U(\vec{r}) \equiv u(|\vec{r}|)$, and falls off to zero very rapidly, namely according to $u(r) \sim -r^{-6}$, for large distances $r \to \infty$ from the origin. In that case, the asymptotic behaviour of the scattering wavefunction can be approximately expressed as

$$\psi_{\vec{k}}(\vec{r}) \simeq e^{i\vec{k}\cdot\vec{r}} - \frac{a(\theta)}{r} e^{ikr} \tag{3.55}$$

for large $|\vec{r}| \to \infty$, with a scattering amplitude $a(\theta)$ that depends on the polar angle θ defined with respect to the wave vector $\vec{k}$, such that we have $\vec{k}\cdot\vec{r} = kr\cos\theta$. By means of a Taylor series expansion in the integral on the right-hand side of Eq. (3.53), this scattering amplitude is obtained as

$$a(\theta) \simeq \frac{m_r}{2\pi\hbar^2} \int d^3r' u(r') \psi_{\vec{k}}(\vec{r}') e^{-ik\vec{e}_r\cdot\vec{k}} \left(1 + O(r'/r)\right) \tag{3.56}$$

up to corrections that scale as r'/r, where $\vec{e}_r = \vec{r}/r$ is the unit vector in the direction $\vec{r}$. A perturbative approach, in the spirit of the Born series, would consist in solving Eq. (3.55) through iteratively inserting more and more refined approximations for $\psi_{\vec{k}}$ into the right-hand side of Eq. (3.56). However, this approach requires the scattering potential to be globally small, *i.e.*, such that $|u(r)|$ can be bounded from above by a perturbative parameter, which is clearly not the case for the Van der Waals interaction potential of two alkali atoms.

We therefore pursue a different approach to determine $a(\theta)$, which consists in decomposing the solution $\psi_{\vec{k}}$ of the stationary Schrödinger equation (3.54) in spherical harmonics, using the fact that U exhibits spherical symmetry. As we know already from Eq. (3.55) that $\psi_{\vec{k}}$ does not depend on the azimutal angle defined with respect to the $\vec{k}$ axis, this decomposition simplifies to

$$\psi_{\vec{k}}(\vec{r}) = \sum_{l=0}^{\infty} P_l(\cos\theta)\frac{\chi_l(r)}{r} \tag{3.57}$$

where P_l is the Legendre polynomial of degree l. Inserting this ansatz into Eq. (3.54) yields the one-dimensional Schrödinger equation

$$-\frac{\hbar^2}{2m_r}\chi_l''(r) + U_{\text{eff}}(r)\chi_l(r) = E_k\chi_l(r) \tag{3.58}$$

with

$$U_{\text{eff}}(r) = u(r) + \frac{l(l+1)\hbar^2}{2m_r r^2} \tag{3.59}$$

that the radial wavefunction χ_l has to fulfill, in combination with the boundary condition $\chi_l(0) = 0$ that is needed in order not to give rise to a singularity of $\psi_{\vec{k}}$ at the origin. As we have $U_{\text{eff}}(r) \to 0$ for $r \to \infty$, the asymptotic behaviour of this radial wavefunction can generally be written as

$$\chi_l(r) = A_l \sin(kr - l\pi/2 + \delta_l) \tag{3.60}$$

for some amplitude $A_l \in \mathbb{C}$ and some phase shift $\delta_l \in \mathbb{R}$, the latter being defined such that it would vanish if the scattering potential u was not there, *i.e.*, such that we would have $\delta_l = 0$ for all l if $u(r) \equiv 0$ for all r. This choice becomes obvious from an analogous decomposition of the incident plane wave according to

$$e^{i\vec{k}\cdot\vec{r}} = \sum_{l=0}^{\infty} i^l(2l+1)P_l(\cos\theta)j_l(kr) \tag{3.61}$$

with the *spherical Bessel function* j_l which is approximately evaluated as

$$j_l(kr) \simeq \frac{1}{kr}\sin(kr - l\pi/2) \tag{3.62}$$

for large distances $kr \gg 1$. Inserting the expressions (3.57) and (3.61) in combination with Eqs. (3.60) and (3.62) into the asymptotic expression (3.55) for the scattering wavefunction yields the equation

$$A_l = \frac{i^l}{k}(2l+1)e^{i\delta_l} \tag{3.63}$$

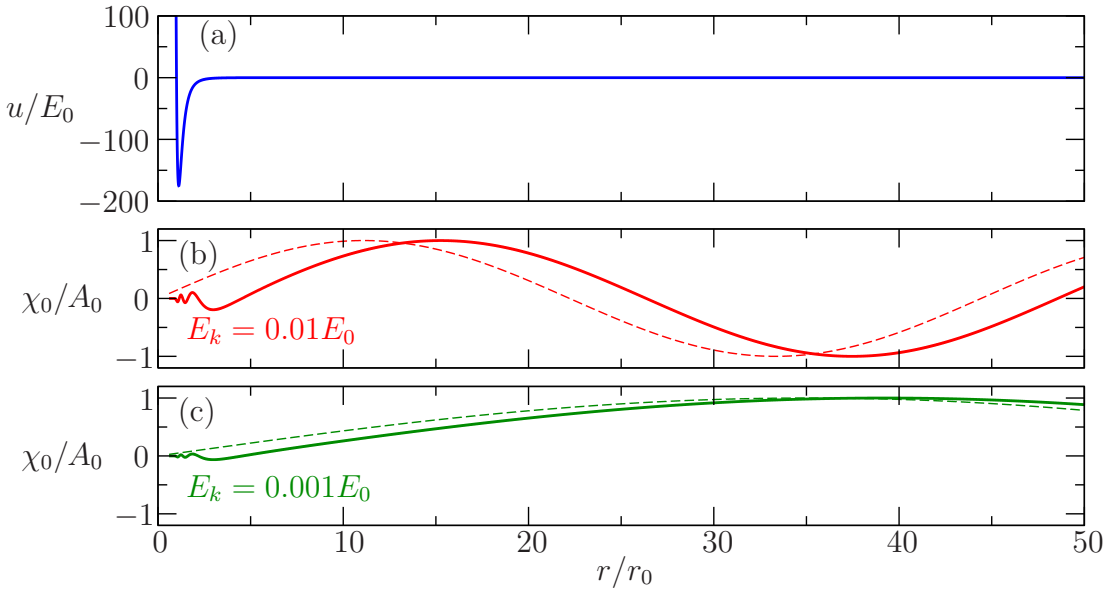

Figure 3.9: Radial profiles of the s-wave component χ_0 of the scattering wavefunction in the presence of the Lennard-Jones potential (3.66) with $\mathcal{A} = 700$, displayed in panel (a). The scattering wavefunctions were calculated for the energies (b) $E_k = 0.01E_0$ and (c) $E_k = 0.001E_0$. The dashed lines in the panels (b) and (c) show the radial profiles $\chi_0(r) = A_0 \sin(kr)$ that would result for $\mathcal{A} = 0$, *i.e.*, if the scattering potential was not there ($u \equiv 0$). An s-wave scattering length of the order of $a_s \simeq 5r_0$ is obtained for both scattering wavefunctions.

for the radial wave amplitude, from which we obtain the expression

$$a(\theta) = -\frac{1}{k}\sum_{l=0}^{\infty}(2l+1)\sin\delta_l e^{i\delta_l}P_l(\cos\theta)\,, \tag{3.64}$$

for the scattering amplitude. The latter is therefore fully determined in terms of the *scattering phases* δ_l which encode the characteristics of the potential u and its effect onto the scattering process under consideration.

We can now make use of the fact that the two-body collision process takes place at ultra-low centre-of-mass and relative kinetic energies, which implies that k^{-1} is by far the largest length scale of the problem. We can therefore permit ourselves to evaluate the expression (3.64) in the formal limit $k \to 0$. To this end, it can be shown that for scattering potentials falling off as $u(r) \sim -r^{-n}$ with $n > 3$ for large $r \to \infty$ the associated scattering phases scale as

$$\delta_l \propto \begin{cases} k^{2l+1} : 2l+1 < n-2 \\ k^{n-2} : 2l+1 \geq n-2 \end{cases} \tag{3.65}$$

in the limit $k \to 0$. This is illustrated in Figs. 3.9 and 3.10 for the case of the

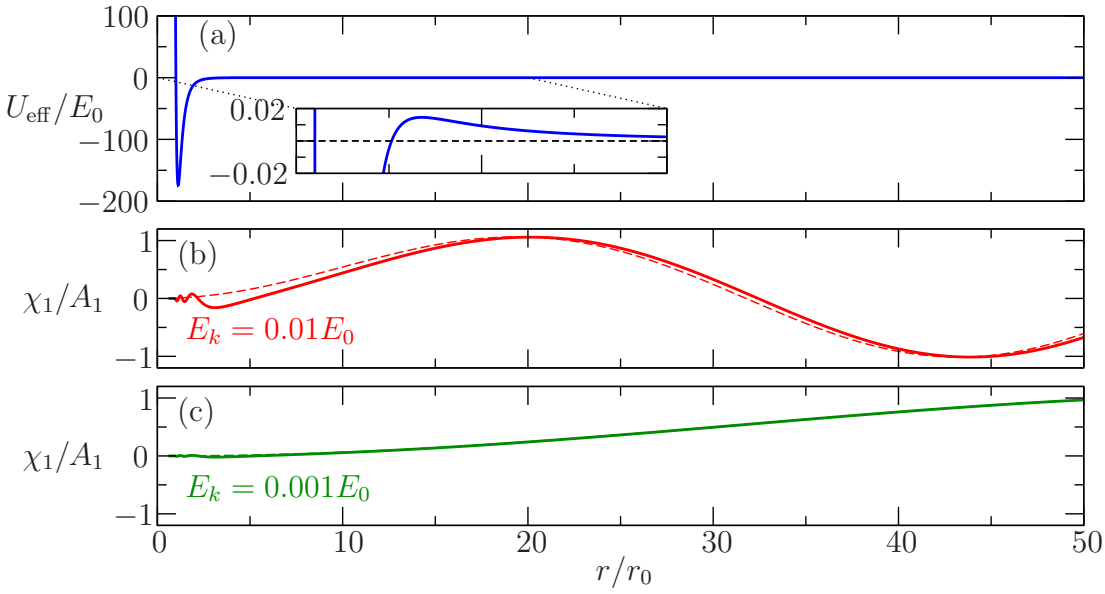

Figure 3.10: Same as Fig. (3.9) for the p-wave components χ_1. Panel (a) shows the effective potential (3.59) composed by the Lennard-Jones potential (3.66) with $\mathcal{A} = 700$ and the angular momentum barrier $\hbar^2/(m_r r^2)$ for $l = 1$. The dashed lines in the panels (b) and (c) show the radial profiles that would result for $\mathcal{A} = 0$. While a tiny displacement between the radial part of the true scattering wavefunction and the unperturbed radial function can still be seen for $E = 0.01E_0$, the two wave profiles become practically indistinguishable for $E = 0.001E_0$.

Lennard-Jones potential

$$u(r) = \mathcal{A}E_0 \left[\left(\frac{r_0}{r}\right)^{12} - \left(\frac{r_0}{r}\right)^{6} \right] \tag{3.66}$$

with $E_0 = \hbar^2/(m_r r_0^2)$ and $\mathcal{A} = 700$. As we see in Fig. 3.9, the spatial displacement between the radial wavefunction χ_0 associated with the s-wave and the corresponding unperturbed radial wavefunction, given by $\chi_0(r) = A_0 \sin(kr)$ in the case of the s-wave, does not significantly vary in absolute terms with the wave number k. Consequently, the corresponding scattering phase δ_0, which one can identify with the *relative* spatial displacement normalized with respect to the inverse wave number k^{-1}, scales linearly with k for small k. This scaling is stronger than linear for the p-wave, as can be seen in Fig. 3.10. Indeed, a finite tunneling barrier arises for $l = 1$ as well as for higher angular momenta, the spatial extent of which increases with decreasing energy. Consequently, any difference that arises between the radial wavefunction χ_l and its unperturbed counterpart close to the origin becomes strongly suppressed on the outer side of this tunneling barrier, and this suppression becomes more effective with decreasing wave number.

We can therefore set $\sin\delta_l \simeq \delta_l$ for all $l \in \mathbb{N}_0$ and hence obtain, via the scaling laws (3.65),

$$\frac{1}{k}\sin\delta_l \propto \begin{cases} k^0 : l = 0 \\ k^2 : l = 1 \\ k^3 : l \geq 2 \end{cases} \tag{3.67}$$

for the Van der Waals potential describing the two-body interaction between neutral atoms, featuring the exponent $n = 6$ within Eq. (3.65). In the formal limit $k \to 0$, the expression (3.64) for the scattering amplitude therefore simplifies to

$$a(\theta) = -\frac{1}{k}\delta_0 e^{i\delta_0} + O(k^2) \tag{3.68}$$

up to terms that scale quadratically with k. Defining by

$$a_s = -\frac{\delta_0}{k} \tag{3.69}$$

the *s-wave scattering length*, we can rewrite Eq. (3.68) as

$$a(\theta) = a_s(1 - ika_s) + O(k^2) = a_s + O(k)\,. \tag{3.70}$$

The low-energy collision between two atoms is therefore dominantly described by the isotropic s-wave component of the corresponding scattering process in the relative coordinate, giving therefore rise to the scattering wavefunction

$$\psi_{\vec{k}}(\vec{r}) \simeq e^{i\vec{k}\cdot\vec{r}} - \frac{a_s}{r}e^{ikr} \tag{3.71}$$

that features a perfectly spherical scattered wave emanating from the origin. The expression (3.71) simplifies to

$$\psi_{\vec{k}}(\vec{r}) \simeq 1 - \frac{a_s}{r} \tag{3.72}$$

in the formal limit $k \to 0$ where we are dealing with the hierarchy of length scales $r_0 \ll r \ll 1/k$, with r_0 being the intrinsic length scale characterizing the two-body atom-atom interaction potential.

It is rather instructive to analytically calculate this s-wave scattering length for the case of a simple piecewise constant scattering potential of the form

$$u(r) = \begin{cases} -U_0 : r < r_0 \\ 0 \quad : r \geq r_0 \end{cases}\,. \tag{3.73}$$

The solution of the radial Schrödinger equation (3.58) for $l = 0$ is locally obtained as

$$\chi_0(r) = A_0 \begin{cases} \alpha_k \sin(\kappa_k r) & : r < r_0 \\ \sin(kr - \delta_0) & : r > r_0 \end{cases} \tag{3.74}$$

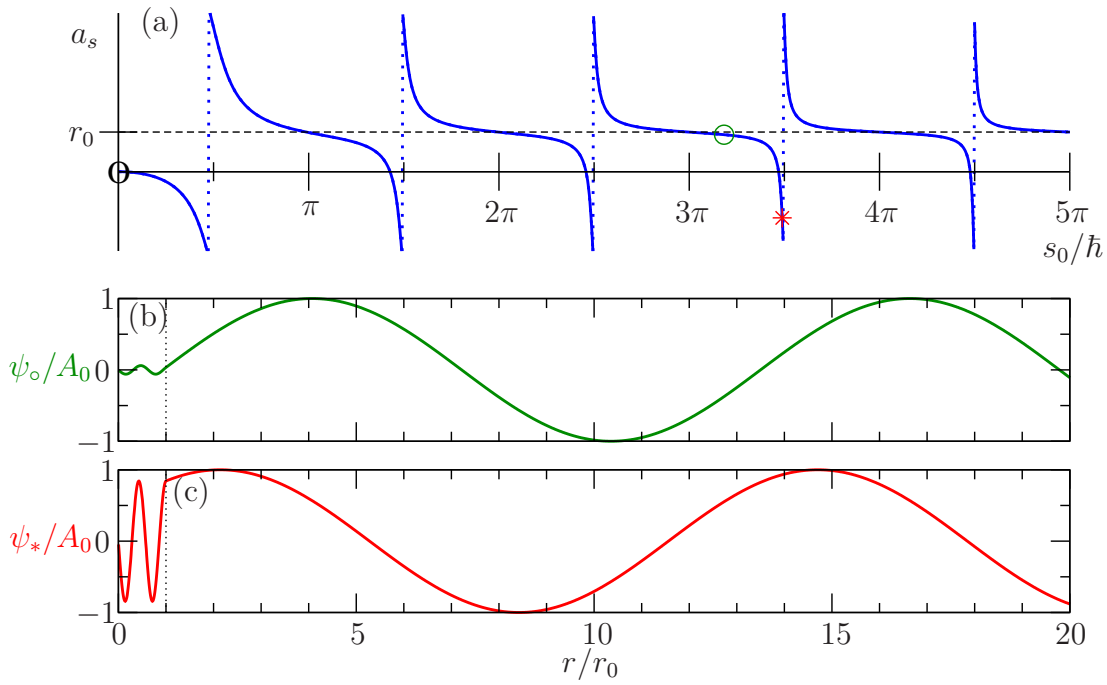

Figure 3.11: (a) s-wave scattering length (3.77) for the box potential (3.73), calculated for $kr_0 = 0.5$ as a function of $s_0/\hbar$ with s_0 being defined through Eq. (3.79). For large $s_0/\hbar \gg 1$, wide plateaus at the value $a_s \simeq r_0$ are encountered. The panels (b) and (c) show the scattering wavefunctions (3.74) corresponding to $s_0/\hbar = 10$ (green circle) and $s_0/\hbar = 10.96$ (red star), respectively, with the associated values $a_s \simeq 0.933483 r_0$ and $a_s \simeq -1.16598 r_0$.

with

$$\alpha_k = \frac{\sin(kr_0 - \delta_0)}{\sin(\kappa_k r_0)}, \tag{3.75}$$

$$\kappa_k = \sqrt{k^2 + 2m_r U_0/\hbar^2}, \tag{3.76}$$

and the s-wave scattering length

$$a_s = r_0 - \frac{1}{k} \arctan\left[\frac{k}{\kappa_k} \tan(\kappa_k r_0)\right]. \tag{3.77}$$

In the limit $k \to 0$ we obtain

$$a_s \overset{k\to 0}{=} r_0 \left(1 - \frac{\hbar}{s_0} \tan\frac{s_0}{\hbar}\right), \tag{3.78}$$

where we have introduced by

$$s_0 = \sqrt{2m_r U_0} r_0 \tag{3.79}$$

the classical action associated with half a round-trip within the potential well at zero total energy. In the presence of a deep potential well that can accomodate a large number of bound quantum states, we have $s_0 \gg \hbar$. Hence, for a randomly chosen potential depth U_0 which is much larger than $\hbar^2/(m_r r_0^2)$ one most probably finds an s-wave scattering length that is very close to spatial extent of the well, *i.e.*, $a_s \simeq r_0$, unless $s_0/\hbar$ is close to an odd multiple of $\pi/2$ where the tangent function features a singularity. This is illustrated in Fig. 3.11(a) which shows a_s as a function of $s_0/\hbar$ for $kr_0 = 0.5$. Wide plateaus at the value $a_s \simeq r_0$ are encountered for large $s_0/\hbar \gg 1$. s-wave scattering lengths that strongly deviate from this most probable value, in particular those that are negative, occur only within a very small parameter window about the singularities of the tangent function.

The panels (b) and (c) of Fig. 3.11 show the scattering wavefunctions (3.74) that are respectively associated with a positive and a negative value of the s-wave scattering length. A remarkable difference between these two wavefunctions occurs in the spatial region $0 < r < r_0$ within the potential well. While the wavefunction $\psi_\circ$ associated with the positive scattering length $a_s \simeq r_0$ features only a marginal probability density within the potential well, the wavefunction ψ_* that is associated with the negative scattering length has a large amplitude within the interval $[0, r_0]$. Translated back to the two-body collision problem that we originally posed in this section, this would imply that it would generally be rather unlikely to actually encounter the two atoms very close to each other during their collision, unless their s-wave scattering length is negative or, more generally, strongly deviates from the reference value r_0.

Certainly, the box potential (3.73) represents a rather simplistic model for the two-body interaction between alkali atoms, which means that we are not really in a position to draw the above conclusions concerning two-body collision processes of alkali atoms. To get a more realistic insight into the general behaviour of the s-wave scattering length as a function of the depth of the Van der Waals potential well, we show in Fig. 3.12 analogous radial profiles of scattering wavefunctions that were numerically calculated for the Lennard-Jones model (3.66), namely for the total energy $E = \hbar^2 k^2/(2m_r) = 0.0001\, E_0$ and the values $\mathcal{A} \in \{500, 510, 520, \ldots, 990\}$ of the parameter $\mathcal{A}$ that characterizes the effective depth of the potential well. We see in panel (c) that an s-wave scattering length of the order of $a_s \simeq 10\, r_0$ is most generally encountered, in which case the associated wavefunction exhibits a very weak probability for the two atoms to be found close to each other as compared to this particular length scale. As is also seen in panel (c), significantly high probabilities for close atom-atom encounters mainly arise if the s-wave scattering length is negative or much larger than the above reference scale $\sim 10\, r_0$ for a_s. These numerical results corroborate our findings and conclusions that we obtained for the box potential.

The enhancement of the probability for close atom-atom encounters that arises in the case of a negative s-wave scattering length has a detrimental impact on the

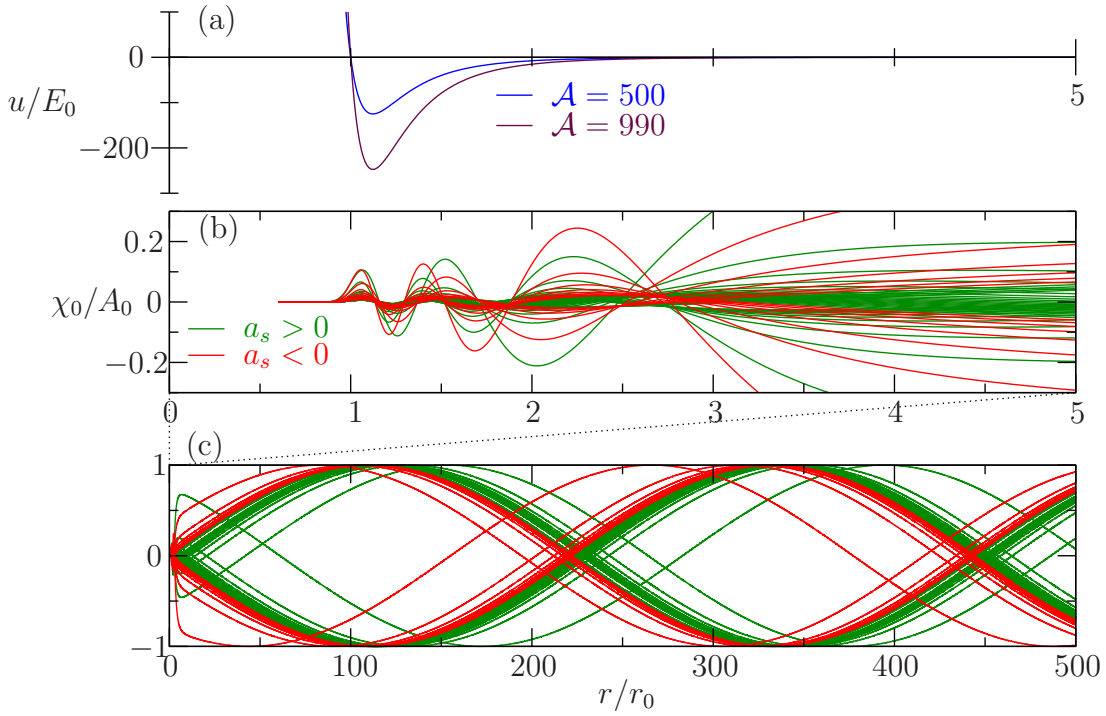

Figure 3.12: (b,c) Radial profiles of the scattering wavefunctions for the Lennard-Jones potential (3.66) for the prefactors $\mathcal{A} \in \{500, 510, 520, \ldots, 990\}$ and the total energy $E = \hbar^2 k^2/(2m_r) = 0.0001\, E_0$. Each line corresponds to a different value of $\mathcal{A}$. It is coloured in green if the associated s-wave scattering length is positive, and in red otherwise. Panel (a) shows the Lennard-Jones potential (3.66) for $\mathcal{A} = 500$ and $\mathcal{A} = 990$.

stability of the ultracold atomic quantum gas insofar as it favours the formation of diatomic molecules. Owing to the kinetic constraints that are imposed by the conservation of the total momentum and the total energy of the colliding atom pair, such molecules cannot result from two-body collision processes. However, they can be formed in the rarer case of a *three-body collision*, where three atoms of the quantum gas happen to be close to each other at a given instant. In that case, the excess energy that results from the formation of a molecular bound state between two of the colliding atoms can be taken away by the degree of freedom that describes the relative motion between this freshly formed diatomic molecule and the third atom, giving rise to an enhancement of their kinetic energies. Those two particles are therefore prone to leave the trap and/or to heat up other atoms via further collisions that occur along their trajectories, which accelerates the destruction of the quantum gas[6].

[6]In analogy with a supernova, the resulting collapse of the quantum gas and its disintegration into a number of molecules, metal clusters, and hot atoms is termed *bosenova*.

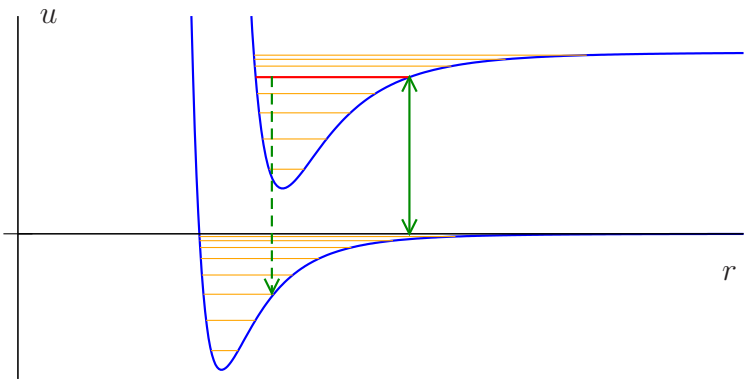

Figure 3.13: Sketch of the principle of photoassociation spectroscopy. A laser field, whose photon energy is displayed by the green solid arrow, induces a resonant transition of the ultracold two-body scattering state to a vibrational mode (indicated by the red line) that is associated with an excited electronic state. This transition takes place at a specific distance from the origin, namely where the energy of the excited Born-Oppenheimer curve, as defined with respect to the dissociation threshold of the diatomic molecule, equals the photon energy of the laser. Its effectiveness is therefore proportional to the modulus square of the scattering wavefunction at that distance. A stable molecule can be formed via the subsequent spontaneous emission of a photon, which gives rise to a de-excitation of the electronic state (as indicated by the dashed arrow).

Hence, to quantitatively assess whether or not a Bose-Einstein condensate made of ultracold alkali atoms can be formed and maintained on reasonably long time scales, it is of vital importance to determine the positive or negative sign of the s-wave scattering length charaterizing the atomic species under consideration. This task is very hard to do via numerical calculations. Indeed, the Born-Oppenheimer potential curves that describe the interaction of a pair of identical alkali atoms in their electronic ground state generally exhibit a large number of bound molecular states. Those curves therefore have to be computed with very high numerical precision in order to accurately determine the s-wave scattering length, namely such that the action integral evaluated at the dissociation threshold is precise on a scale that is small compared to $\hbar$ (see Fig. 3.11 for the case of the box potential). Especially for heavy alkali atoms such as rubidium, the nonrelativistic approximation that is inherent in the Schrödinger equation is not sufficient for this purpose, and one has to resort to methods based on the Dirac equation in order to solve this problem.

As it stands, s-wave scattering lengths of atomic species are most conveniently determined experimentally, namely through ultracold *photoassociation spectroscopy*. To this end, a resonant laser transition is induced from the electronic ground state of the colliding atom pair to an excited state featuring stable

	H	^{7}Li	^{23}Rb	^{39}K	^{41}K	^{85}Rb	^{87}Rb	^{133}Cs
singlet a_s/a_B	0.41	33	66	140	85	2400	90	280
triplet a_s/a_B	1.2	-28	20	-20	65	-370	106	2400

Table 3.1: s-wave scattering lengths of hydrogen and a number of bosonic alkali isotopes, for both the singlet and the triplet configuration of the valence electrons. Note the negative values of the triplet s-wave scattering lengths in the case of the isotopes ^{7}Li, ^{39}K, and ^{85}Rb.

vibrational motion of the two atoms, as is sketched in Fig. 3.13. Owing to the *Franck-Condon principle*, this transition takes place at a specific inter-atomic distance r, namely where the energy of the Born-Oppenheimer potential curve associated with the excited electronic state, as defined with respect to the dissociation threshold of the diatomic molecule, equals the photon energy of the laser. Its effectiveness is therefore proportional to the modulus square of the scattering wavefunction at that distance r. The formation of the diatomic molecule is completed via the spontaneous emission of a photon, which induces a de-excitation from the excited to the ground-state Born-Oppenheimer curve, with a finite probability for the atom pair to end up in a stable vibrational mode. By monitoring the yield of the thereby associated diatomic molecules as a function of the laser frequency, one can experimentally trace the radial profile of the scattering wavefunction associated with the dynamics in the relative motion of the colliding atom pair, which in turn allows one to determine the s-wave scattering length.

Table 3.1 shows a list of the thereby determined s-wave scattering lengths of hydrogen and a number of bosonic alkali isotopes, for both the singlet and the triplet configuration of the valence electrons. While the s-wave scattering length for most of those atomic species is found to be positive, negative values for a_s do occur as well, namely specifically for the isotopes ^{7}Li, ^{39}K, and ^{85}Rb. As was discussed above, those isotopes consequently feature an enhanced rate for the formation of diatomic molecules via three-body collisions. They are therefore inappropriate for the creation of a Bose-Einstein condensate that is supposed to exist over a reasonably long lifetime. Note that this is particularly the case for one of the atomic species, namely ^{7}Li, that was studied in one of the three pioneering experiments on Bose-Einstein condensation with ultracold atoms[7]. This particular experiment did therefore yield a much less convincing evidence for the occurrence of Bose-Einstein condensation than the other two pioneering experiments which were dealing with ^{87}Rb and ^{23}Na atoms.

[7]C. C. Bradley, C. A. Sackett, J. J. Tollett, and R. G. Hulet, *Evidence of Bose-Einstein Condensation in an Atomic Gas with Attractive Interactions*, Phys. Rev. Lett. 75, 1687 (1995).

Problems

3.6 Show the validity of Eq. (3.45).

3.7 Show that the position representation of the retarded Green function

$$G_0(E) = \left(E - \frac{\hbar^2}{2m_r} \frac{\partial^2}{\partial \vec{r}^2} + i\epsilon \right)^{-1} \tag{3.80}$$

describing the free motion in the relative coordinate (with $\epsilon \to 0_+$) is given by

$$\langle \vec{r} | G_0(E) | \vec{r}\,' \rangle = -\frac{m_r}{2\pi\hbar^2} \frac{e^{ik_E|\vec{r}-\vec{r}\,'|}}{|\vec{r}-\vec{r}\,'|} \tag{3.81}$$

with $k_E = \sqrt{2mE}/\hbar$ for all $\vec{r}$ and $\vec{r}\,'$.

3.8 Show that the expression (3.52) in combination with the Lippmann-Schwinger equation (3.53) represents the unique solution of the Schrödinger equation (3.49) for an initial wave profile (3.50) which is such that it has no significant common overlap with the scattering potential at the initial time $t = t_0$, *i.e.*, we can safely set $\psi(\vec{r}, t_0)U(\vec{r}) = 0$ for all $\vec{r}$.

3.9 Show that the the wavefunction $\psi_{\vec{k}}$ satisfying the Lippmann-Schwinger equation (3.53) solves the stationary Schrödinger equation (3.54).

3.10 Show how Eqs. (3.63) and (3.64) result from inserting the expressions (3.57), (3.60), (3.61), and (3.62) into Eq. (3.55).

3.11 Show that for a scattering potential falling off as $u(r) \sim -r^{-n}$ with $n > 3$ for large $r \to \infty$ the scattering phases scale, in the limit $k \to 0$, as $\delta_l \propto k^{2l+1}$ for $2l + 3 < n$ and as $\delta_l \propto k^{n-2}$ for $2l + 3 \geq n$.

3.12 Show the validity of Eqs. (3.74–3.77).

3.6 The replacement potential

Having established that the s-wave scattering length a_s is the only relevant parameter characterizing two-body collisions in a gas of ultracold neutral atoms, we can now permit ourselves to replace the rather intricate Van der Waals interaction potential that is associated with the energetically lowest Born-Oppenheimer curve by a technically simpler model potential which is designed such that it exhibits the same value for a_s as the actual two-body interaction. We shall opt for an effective potential that is globally weak, as weak as possible, such that it does not exhibit any bound state, contrary to a typical interaction potential of an alkali atom species. While loss processes due to three-body collisions are thereby

ruled out within such a model potential, its weakness allows us to employ perturbative approaches that facilitate the task of performing many-body calculations of the ground state and the excited states of the atomic gas.

More specifically, we shall consider a spherically symmetric effective interaction potential $U(\vec{r}) \equiv u(|\vec{r}|)$ whose strength is sufficiently small that the Lippmann-Schwinger equation (3.53) can be solved by a convergent Born series. The latter is obtained by iteratively inserting the expression (3.53) for the scattering wavefunction on the right-hand side of this equation, yielding

$$\begin{aligned} \psi_{\vec{k}}(\vec{r}) &= e^{i\vec{k}\cdot\vec{r}} - \frac{m_r}{2\pi\hbar^2}\int d^3r' \frac{e^{ik|\vec{r}-\vec{r}'|}}{|\vec{r}-\vec{r}'|}u(r')e^{i\vec{k}\cdot\vec{r}'} \\ &\quad + \Big(\frac{m_r}{2\pi\hbar^2}\Big)^2 \int d^3r' \int d^3r'' \frac{e^{ik|\vec{r}-\vec{r}'|}}{|\vec{r}-\vec{r}'|}\frac{e^{ik|\vec{r}'-\vec{r}''|}}{|\vec{r}'-\vec{r}''|}u(r')u(r'')e^{i\vec{k}\cdot\vec{r}''} + O(u^3) \end{aligned} \tag{3.82}$$

up to corrections that scale cubically with the scattering potential. The scattering amplitude that defines the asymptotic behaviour (3.55) of the wavefunction, given by $\psi_{\vec{k}}(\vec{r}) \simeq e^{i\vec{k}\cdot\vec{r}} - a(\theta)e^{ikr}/r$, is then yielded as

$$\begin{aligned} a(\theta) &= \frac{m_r}{2\pi\hbar^2}\int d^3r' u(r') e^{i(\vec{k}-k\vec{e}_r)\cdot\vec{r}'} \\ &\quad - \Big(\frac{m_r}{2\pi\hbar^2}\Big)^2 \int d^3r \int d^3r'' \frac{u(r')u(r'')}{|\vec{r}'-\vec{r}''|} e^{ik(|\vec{r}'-\vec{r}''|-\vec{e}_r\cdot\vec{r}')}e^{i\vec{k}\cdot\vec{r}''} + O(u^3) \end{aligned} \tag{3.83}$$

as a function of the polar angle $\theta = \arccos[\vec{k}\cdot\vec{r}/(kr)]$.

As detailed in the previous section, s-wave scattering is obtained in the low-energy limit $k \to 0$, yielding the series

$$a_s = \frac{m_r}{2\pi\hbar^2}\int d^3r u(r) - \Big(\frac{m_r}{2\pi\hbar^2}\Big)^2 \int d^3r \int d^3r' \frac{u(r)u(r')}{|\vec{r}-\vec{r}'|} + O(u^3)\,. \tag{3.84}$$

Defining

$$g = \int u(r) d^3r\,, \tag{3.85}$$

we obtain in first-order Born approximation, *i.e.* neglecting the $O(u^2)$ contributions in Eq. (3.84), the expression

$$a_s \simeq \frac{m_r g}{2\pi\hbar^2} \tag{3.86}$$

for the s-wave scattering length of this effective potential. Hence, the scattering potential has to be conceived such that its integral over space matches

$$g \simeq \frac{2\pi\hbar^2 a_s}{m_r}\,. \tag{3.87}$$

It will be very useful and instructive to evaluate leading-order corrections to this expression. We introduce for this purpose the length scale

$$\rho = g^2 \left(\int d^3r \int d^3r' \frac{u(r)u(r')}{|\vec{r} - \vec{r}'|} \right)^{-1} , \tag{3.88}$$

which characterizes the spatial extent over which this effective potential is defined. An evaluation of Eq. (3.84) in the second-order Born approximation, neglecting contributions of the order $O(u^3)$, yields

$$a_s = \frac{m_r g}{2\pi\hbar^2} - \left(\frac{m_r g}{2\pi\hbar^2} \right)^2 \frac{1}{\rho} . \tag{3.89}$$

Hence, the expression (3.87) is to be amended as

$$g = \frac{2\pi\hbar^2 a_s}{m_r} + \frac{m_r g}{2\pi\hbar^2 \rho} \tag{3.90}$$

$$\simeq \frac{2\pi\hbar^2 a_s}{m_r} \left(1 + \frac{a_s}{\rho} + O[(a_s/\rho)^2] \right) . \tag{3.91}$$

This clearly indicates that $a_s < \rho$ is a necessary (though not sufficient) condition for the Born series to converge, *i.e.*, the effective replacement potential has to be defined with a characteristic spatial extent ρ that significantly exceeds the s-wave scattering length of the atomic species under consideration.

While we could, at this stage, further particularize the specific (*e.g.*, gaussian, or piecewise constant) functional form of U, we content ourselves with requiring that this replacement potential be sufficiently well-behaved and non-pathological such that it indeed falls off rapidly for distances exceeding ρ. Consequently, its Fourier transform coefficients, which are defined by

$$g_k = \int u(r) e^{i\vec{k}\cdot\vec{r}} d^3r , \tag{3.92}$$

do not feature a significant dependence on k for wave numbers below ρ^{-1}, such that one can safely approximate $g_k \simeq g_0 = g$ for $0 < k \ll \rho^{-1}$. Hence, as long as the wavefunction describing the ultracold gas varies on length scales ξ that are far greater than the s-wave scattering length of the atomic species under consideration, *i.e.* such that the hierarchy of scales $a_s \ll \rho \ll \xi$ can be satisfied for the spatial extent ρ characterizing the replacement potential, we can use the effective approximation

$$U(\vec{r}) = g\delta(\vec{r}) \tag{3.93}$$

with δ the three-dimensional delta function. In physical terms, the intricate Van der Waals potential describing the two-body interaction in a gas of atoms can be safely replaced by a rather structureless contact potential provided this gas is ultracold and dilute, *i.e.*, provided the atoms move with extremely low kinetic energies and have a mean interparticle distance that significantly exceeds the s-wave scattering length characterizing the interaction potential.

Problems

3.13 Scattering is most conventionally described in terms of the T *matrix* whose matrix elements in position space are given by the selfconsistent solution of the Lippmann-Schwinger equation

$$T_k(\vec{r},\vec{r}\,') = U(\vec{r})\delta(\vec{r}-\vec{r}\,') - \frac{m_r U(\vec{r})}{2\pi\hbar^2}\int d^3r'' \frac{e^{ik|\vec{r}-\vec{r}\,''|}}{|\vec{r}-\vec{r}\,''|} T_k(\vec{r}\,'',\vec{r}\,')\,. \qquad (3.94)$$

(a) Show that

$$\psi_{\vec{k}}(\vec{r}) = e^{i\vec{k}\cdot\vec{r}} - \frac{m_r}{2\pi\hbar^2}\int d^3r'' \frac{e^{ik|\vec{r}-\vec{r}\,''|}}{|\vec{r}-\vec{r}\,''|}\int d^3r' T_k(\vec{r}\,'',\vec{r}\,') e^{i\vec{k}\cdot\vec{r}\,'} \qquad (3.95)$$

solves the Lippmann-Schwinger equation (3.53) for the scattering wavefunction.

(b) Consider now a globally weak spherically symmetric scattering potential $U(\vec{r}) \equiv u(|\vec{r}|)$. Show that the T matrix fulfills the properties

$$\int d^3r \int d^3r' T_k(\vec{r},\vec{r}\,')\vec{r} \;=\; 0\,, \qquad (3.96)$$

$$\int d^3r \int d^3r' T_k(\vec{r},\vec{r}\,')\vec{r}\,' \;=\; 0\,. \qquad (3.97)$$

(c) Show that in that case the scattering amplitude, as defined through Eq. (3.55), is given by the expression

$$a(\theta) = \frac{m_r}{2\pi\hbar^2}\int d^3r \int d^3r' T_k(\vec{r},\vec{r}\,') + O(k^2) \qquad (3.98)$$

for low wave numbers k.

(d) Using this expression, show that one recovers the k-scaling expressed in Eq. (3.70), *i.e.*,

$$a(\theta) = a_s(1 - ika_s) + O(k^2)\,, \qquad (3.99)$$

with

$$a_s = \frac{m_r}{2\pi\hbar^2}\int d^3r \int d^3r' T_0(\vec{r},\vec{r}\,')\,. \qquad (3.100)$$

3.14 Show that the length scale ρ, as defined in Eq. (3.88), can be rewritten as

$$\rho = 2\pi^2 g^2 \left(\int \frac{g_k^2}{k^2} d^3k\right)^{-1} \qquad (3.101)$$

in terms of the Fourier coefficients (3.92) of the replacement potential.

Chapter 4

The interacting Bose-Einstein condensate

4.1 The Gross-Pitaevskii equation

Let us now consider a gaz of N ultracold bosonic atoms that are confined in a magnetic or optical trapping potential. We assume that the atoms belong to a single isotopical alkaline species (*e.g.*, ^{87}Rb) and are spin-polarized, *i.e.*, they are all prepared in the same hyperfine state, which would be a natural outcome of magnetic trapping as was discussed in Section 3.2. Using the formalism of second quantization (see also Eq. (1.67)), the Hamiltonian of this quantum system is written as

$$\begin{aligned} \hat{H} &= \int d^3r \hat{\psi}^\dagger(\vec{r}) \left(-\frac{\hbar^2}{2m}\frac{\partial^2}{\partial \vec{r}^2} + V(\vec{r}) \right) \hat{\psi}(\vec{r}) \\ &\quad + \frac{1}{2} \int d^3r \int d^3r' U(\vec{r}-\vec{r}') \hat{\psi}^\dagger(\vec{r}) \hat{\psi}^\dagger(\vec{r}') \hat{\psi}(\vec{r}') \hat{\psi}(\vec{r}) \end{aligned} \tag{4.1}$$

in terms of the bosonic field operators $\hat{\psi}(\vec{r}), \hat{\psi}^\dagger(\vec{r})$, where m is the mass of the atoms, $V(\vec{r})$ is the trapping potential at position $\vec{r}$, and $U(\vec{r}-\vec{r}')$ describes the interaction potential between two atoms located at the positions $\vec{r}$ and $\vec{r}'$. Note that this expression (4.2), which is commonly presented as starting point for the theoretical description of a generic spin-polarized single-species quantum gas, already involves an *a priori* approximation insofar as it is based on the assumption (which is very well justified at low densities) that the interaction between the atoms in this gas can be described by means of a two-body potential.

At ultralow temperatures of the gas, which imply ultralow kinetic energies of the atoms, we are entitled to replace the actual Van der Waals interaction between two atoms by a simpler effective potential which is perturbatively small. As was discussed in Section 3.6, this replacement potential has to be chosen such that it reproduces the correct outcome of an ultracold two-body collision

process, the latter being entirely parametrized in terms of the s-wave scattering length a_s of the isotopical species under consideration. On length scales that exceed $|a_s|$ by far, and on energy scales that are far below the extremal values of that replacement potential, we can safely approximate the latter by a three-dimensional Dirac distribution, namely through

$$U(\vec{r} - \vec{r}\,') = g\delta(\vec{r} - \vec{r}\,') \tag{4.2}$$

with the prefactor

$$g = \frac{4\pi\hbar^2 a_s}{m}\,. \tag{4.3}$$

In the framework of this replacement potential, a positive s-wave scattering length, $a_s > 0$, is thus associated with an effectively repulsive interaction between the atoms in the gas, while a negative $a_s < 0$ would lead to an effective attraction between them (keeping in mind, however, that the actual Van der Waals interaction potential between the atoms has both attractive and repulsive features). As was pointed out in Section 3.6, this particular approximation requires a specific diluteness condition to be valid, namely that the mean interparticle distance in the gas is much larger than a_s. Note that one thereby totally neglects the impact of three-body collisions, normally giving rise to the formation of diatomic molecules in the gas, since the replacement potential does, by construction, not feature any bound state even if it is globally attractive.

While the high-temperature properties of the gas are only weakly affected by atom-atom interaction, the presence of the latter has a dramatic impact on ultracold thermal states far below the condensation temperature. In particular, the ground state $|\mathrm{GS}\rangle$ of this many-body system is drastically modified with respect to the case of a noninteracting Bose gas, where it would be simply given by a single Fock state having N atoms in the single-particle orbital that corresponds to the lowest energy eigenstate of the one-body kinetic-plus-potential Hamiltonian. An exact analytical calculation of the many-body ground state is impossible if interaction is present. However, excellent approximations of the ground state $|\mathrm{GS}\rangle$ can be obtained through the application of the *variational principle*, stating that the mean value $\langle \mathrm{GS}|\hat{H}|\mathrm{GS}\rangle$ is stationary with respect to variations of this state $|\mathrm{GS}\rangle$ under the constraint $\langle \mathrm{GS}|\mathrm{GS}\rangle = 1$, owing to the fact that $|\mathrm{GS}\rangle$ minimizes the expectation value of $\hat{H}$ in the bosonic many-body Hilbert space.

In practice, the variational principle is not applied in the entire many-body Hilbert space but only within a restricted submanifold thereof. This submanifold is usually defined such that it allows for a simplified (ideally analytical) treatment of the problem and that its optimal approximation for the ground state can be reasonably considered to lie rather close to the true ground state $|\mathrm{GS}\rangle$ in the Hilbert space. In the case of a weakly interacting Bose gas (or, more precisely, a Bose gas whose effective interaction can be accurately modeled in terms of a globally weak potential), a convenient choice for this submanifold is

given by the *Hartree ansatz* where it is assumed that all atoms of the condensate share the same single-particle orbital. As pointed out above, this Hartree ansatz (which is actually identical to a Hartree-Fock approximation for bosons) precisely corresponds to the ground-state configuration of the ideal Bose gas, and it can therefore be expected that it yields an excellent approximation of the ground state also for the weakly interacting gas if the single-particle orbital that hosts the atoms is optimally chosen.

The Hartree approximation for the ground state can be written as

$$|\mathrm{GP}\rangle = |N, 0, 0, \ldots\rangle \tag{4.4}$$

in the Fock-space representation that is defined with respect to an orthonormal single-particle basis $(\phi_0, \phi_1, \phi_2, \ldots)$ whose first member ϕ_0 corresponds to the orbital to be optimized. Defining, according to Eq. (2.95), the condensate wavefunction associated with this Hartree ansatz as

$$\psi_0(\vec{r}) = \sqrt{N}\phi_0(\vec{r})\,, \tag{4.5}$$

one has

$$\hat{\psi}(\vec{r})|N, 0, 0, \ldots\rangle = \psi_0(\vec{r})|N-1, 0, 0, \ldots\rangle \tag{4.6}$$

and can thus straightforwardly evaluate the mean value of the Hamiltonian (4.2) as

$$\begin{aligned} \langle \mathrm{GP}|\hat{H}|\mathrm{GP}\rangle &= \int d^3r \left[\psi_0^*(\vec{r})\left(-\frac{\hbar^2}{2m}\Delta + V(\vec{r})\right)\psi_0(\vec{r}) + \frac{g}{2}|\psi_0(\vec{r})|^4\right] \\ &\equiv E_{\mathrm{GP}}[\psi_0] \end{aligned} \tag{4.7}$$

for large $N \gg 1$ for which one can justify the approximation $N - 1 \simeq N$. The constraint

$$\int |\psi_0(\vec{r})|^2 d^3r = N \tag{4.8}$$

can be incorporated into the optimization problem through the introduction of a Lagrange multiplier μ, such that one has to find a stationary point of the expression $E_{\mathrm{GP}}[\psi_0] - \mu\left(\int |\psi_0(\vec{r})|^2 d^3r - N\right)$. Formally, this latter functional is defined for two *a priori* independent complex functions ψ_0 and ψ_0^*, which upon solution of the variational problem turn out to be the complex conjugate of one another. Performing the variational principle with respect to ψ_0^*, according to

$$\frac{\delta}{\delta\psi_0^*(\vec{r})}\left[E_{\mathrm{GP}}[\psi_0] - \mu\left(\int |\psi_0(\vec{r})|^2 d^3r - N\right)\right] = 0\,, \tag{4.9}$$

yields the celebrated *Gross-Pitaevskii equation*[1]

$$-\frac{\hbar^2}{2m}\Delta\psi_0(\vec{r}) + V(\vec{r})\psi_0(\vec{r}) + g|\psi_0(\vec{r})|^2\psi_0(\vec{r}) = \mu\psi_0(\vec{r})\,. \tag{4.10}$$

[1] E. P. Gross, *Structure of a quantized vortex in boson systems*, Nuovo Cimento 20, 454 (1961); L. P. Pitaevskii, *Vortex Lines in an Imperfect Bose Gas*, Sov. Phys. JETP 13, 451 (1961).

Equation (4.10) can be intepreted as an effective stationary Schrödinger equation constituted by the various kinetic and potential terms that contribute to the total energy of an individual atom in the condensate. The nonlinear term $g|\psi_0(\vec{r})|^2$ can be seen as an additional contribution to the effective potential experienced by an atom, which arises from its interaction with all other atoms of the condensate. The total energy μ of the atom, appearing on the right-hand side of Eq. (4.10), represents the *chemical potential* of the gas, *i.e.*, the energy that an individual particle has when being added to or extracted from the gas. It must not be confused with the mean total energy per particle of the gas, given by $E_{\rm GP}[\psi_0]/N$, but can be obtained from

$$\mu = \frac{d}{dN} E_{\rm GP}[\psi_0] = \frac{1}{N} \int d^3r \psi_0^*(\vec{r}) \left(-\frac{\hbar^2}{2m}\Delta + V(\vec{r}) + g|\psi_0(\vec{r})|^2 \right) \psi_0(\vec{r}) \,, \quad (4.11)$$

where on the right-hand side we use the normalization condition (4.8) as well as the fact that ψ_0 fulfills the Gross-Pitaevskii equation (4.10).

Standard solution techniques for the Schrödinger equation that are based on the superposition principle cannot be applied here, due to the presence of the nonlinearity, and exact analytical solutions of Eq. (4.10) can be obtained only under very specific circumstances. In the presence of a spatially constant potential $V(\vec{r}) \equiv V_0$ the Gross-Pitaevskii equation (4.10) is exactly solved by the homogeneous condensate wavefunction $\psi(\vec{r}) = \sqrt{n}$ for all $\vec{r}$, provided the system has infinite spatial extension or is defined within a normalization volume featuring periodic boundaries. Owing to Eq. (4.10), the atom density n is then related to the chemical potential μ via

$$gn = \mu - V_0 \,. \quad (4.12)$$

In the case of a repulsive effective interaction between the atoms, $g > 0$, it can be straightforwardly shown that this homogeneous wavefunction minimizes both the kinetic and the interaction energy of the atoms and thus yields the optimal Hartree approximation for the many-body ground state of the gas.

While periodic boundary conditions cannot be experimentally realized in three dimensions, it is possible to engineer, via suitably designed blue-detuned laser field configurations, homogeneous confinement potentials that are delimited by hard-wall boundaries. Consider the presence of two hard-wall boundaries parallel to the $x-y$ plane, placed at $z = 0$ and $z = L$ with L being much larger than any other characteristic length scale of the system. The condensate wavefunction then features a z dependence and satisfies the one-dimensional Gross-Pitaevskii equation

$$-\frac{\hbar^2}{2m}\psi_0''(z) + g|\psi_0(z)|^2\psi_0(z) = (\mu - V_0)\psi_0(z) \quad (4.13)$$

for $0 < z < L$, with the boundary conditions $\psi_0(0) = \psi_0(L) = 0$ (assuming that periodic boundaries still exist along the x and y directions). For large $L \to \infty$

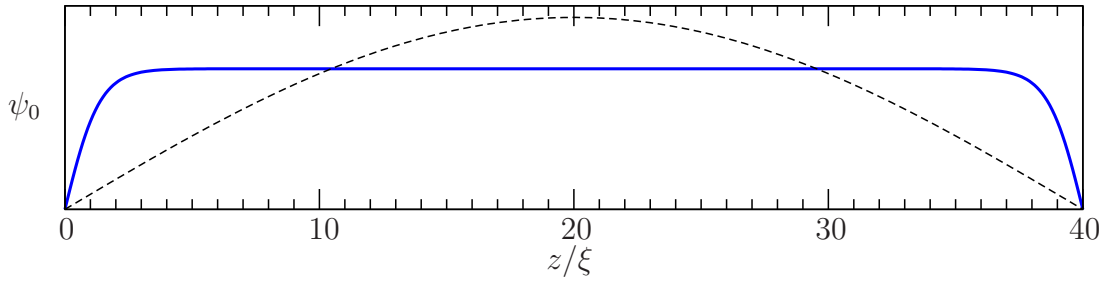

Figure 4.1: Condensate wavefunction (solid blue line) for a repulsively interacting Bose gas in the presence of a homogeneous potential and hard-wall boundary conditions at $z = 0$ and $z = L = 40\xi$, with ξ the healing length of the atomic gas defined according to Eq. (4.15). The dashed black line shows the (sinusoidal) wavefunction that would be obtained in the absence of interaction, for the same total population of the gas.

and finite z, with $0 < z \ll L$, Eq. (4.13) is solved by

$$\psi_0(z) = \sqrt{n}\tanh\left(\frac{z}{\sqrt{2}\xi}\right) \tag{4.14}$$

with

$$\xi = \frac{\hbar}{\sqrt{2mgn}}\,, \tag{4.15}$$

where the asymptotic condensate density n is related to the chemical potential via Eq. (4.12). The length scale (4.15) is dubbed *healing length* since it characterizes the spatial distance within which the presence of any type of perturbation in the potential configuration is annihilated within the profile of the condensate wavefunction. Taking into account the second hard-wall boundary condition at $z = L$, the condensate wavefunction can be approximately expressed as

$$\psi_0(z) \simeq \sqrt{n}\tanh\left(\frac{z}{\sqrt{2}\xi}\right)\tanh\left(\frac{L-z}{\sqrt{2}\xi}\right)\,, \tag{4.16}$$

which for $\xi \ll L$ resembles closely the true condensate wavefunction shown in Fig. 4.1. Quite intuitively, this particular wavefunction profile represents a compromise between minimizing the interaction energy, through flattening and levelling out the density distribution, and minimizing the kinetic energy, through avoiding very steep slopes of the wavefunction.

The relation (4.12) gives us an indication how to proceed in order to determine an approximate expression for the condensate density $n(\vec{r})$ in the presence of a nonuniform potential $V(\vec{r})$ that features a weak spatial dependence. Given the fact that the chemical potential μ has to be constant throughout the entire spatial extension of the condensate, we obtain from generalizing Eq. (4.12)

$$gn(\vec{r}) = \mu - V(\vec{r})\,. \tag{4.17}$$

This is the *Thomas-Fermi approximation*. More rigorously, Eq. (4.17) can be obtained from the Gross-Pitaevskii equation (4.10) through neglecting the kinetic energy term. This yields the equation

$$\left(V(\vec{r}) + g|\psi_0(\vec{r})|^2\right)\psi_0(\vec{r}) = \mu\psi_0(\vec{r}) \tag{4.18}$$

which is straightforwardly solved as

$$\psi_0(\vec{r}) = \begin{cases} \sqrt{\frac{1}{g}\left(\mu - V(\vec{r})\right)} & : \quad \mu > V(\vec{r}) \\ 0 & : \quad \text{otherwise} \end{cases} . \tag{4.19}$$

Quite intuitively, as is also shown in Fig. 4.2, the density profile $n(\vec{r})$ resulting from this expression is such that it gives rise to a spatially homogeneous effective potential energy $V(\vec{r}) + gn(\vec{r})$ each atom of the condensate experiences (pretty much as for a lake in which the water molecules redistribute themselves such as to flatten the surface and thereby minimize the total potential energy).

The chemical potential in the above expression (4.19) is determined from the normalization condition (4.8) $\int d^3r|\psi_0(\vec{r})|^2 = N$. For the case of an anisotropic harmonic trapping potential

$$V(\vec{r}) = \sum_{j=1}^{3} \frac{1}{2} m\omega_j^2 r_j^2 \tag{4.20}$$

this calculation yields

$$\mu = \left(\frac{15}{8\pi}Ng\right)^{2/5} \left(\frac{m\bar{\omega}^2}{2}\right)^{3/5} , \tag{4.21}$$

where

$$\bar{\omega} = (\omega_1\omega_2\omega_3)^{1/3} \tag{4.22}$$

represents the geometric average of the oscillation frequencies ω_j characterizing the trapping potential. Using the relation (4.3) between the interaction strength g and the s-wave scattering length a_s, and introducing the mean oscillator length

$$\bar{a} = \sqrt{\frac{\hbar}{m\bar{\omega}}} , \tag{4.23}$$

Eq. (4.21) can be rewritten as

$$\mu = \frac{1}{2}\left(15Na_s/\bar{a}\right)^{2/5}\hbar\bar{\omega} \equiv \mu(N) . \tag{4.24}$$

With Eq. (4.11) the total energy contained in the condensate is then yielded as

$$E_{\rm GP} = \int_0^N \mu(N')dN' = \frac{5}{7}N\mu(N) \simeq 1.055N\left(Na_s/\bar{a}\right)^{2/5}\hbar\bar{\omega} . \tag{4.25}$$

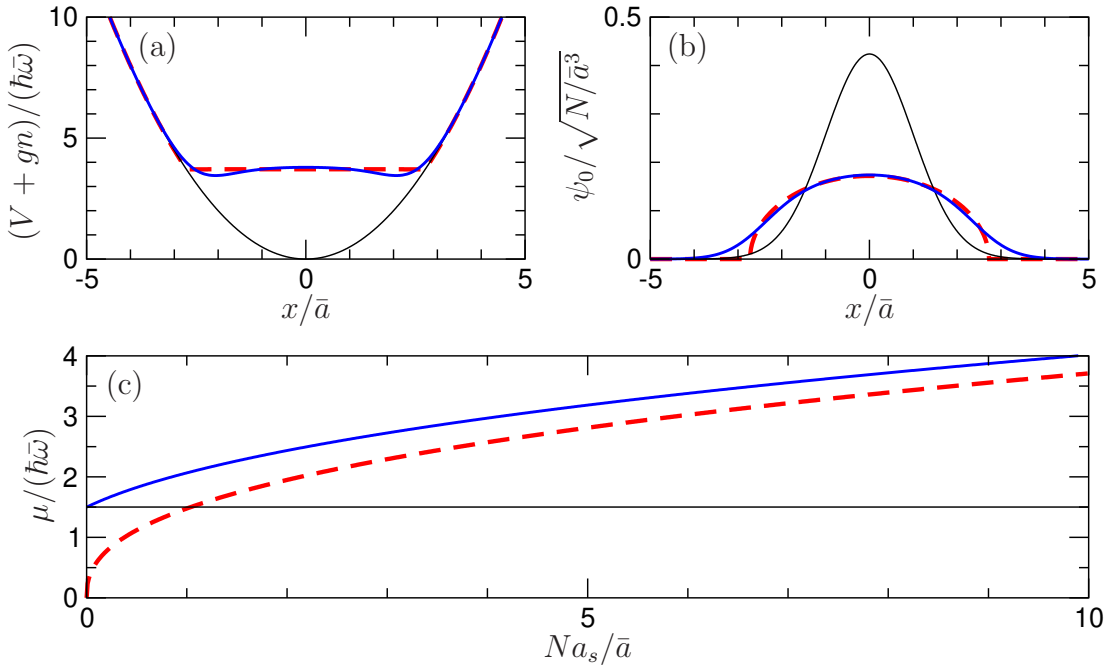

Figure 4.2: Thomas-Fermi approximation for the case of an isotropic three-dimensional harmonic oscillator, characterized by the oscillator length $\bar{a}$. Panels (a) and (b) respectively show, for $Na_s/\bar{a} = 10$, the effective potential energy $V + gn$ (a) as well as the condensate wavefunction (b) as a function of one of the three coordinates x, with the other two coordinates y, z being set to zero. Panel (c) shows the chemical potential as a function of $Na_s/\bar{a}$. Thin black curves correspond to the noninteracting case $a_s = 0$, thick dashed red curves result from the Thomas-Fermi approximation, and blue curves show the behaviours that are obtained from an exact numerical solution of the Gross-Pitaevskii equation (4.10).

Quite intriguingly, $E_{\rm GP}$ features much weaker a scaling with N, namely $\propto N^{7/5}$, than what would have been expected if the orbital ϕ_0 hosting the atoms of the condensate was not allowed to vary as a function of N (in which case two-body interaction would naturally yield the scaling $E \propto N^2$).

Figure 4.2 clearly shows that the Thomas-Fermi approximation agrees very well with the exact numerical solution of the Gross-Pitaevskii equation (4.10) for large $Na_s/\bar{a} \gg 1$. Significant deviations in the condensate wavefunction, as can be seen in Fig. 4.2(b), occur only in the tails of the wavefunction, where the atom density is comparatively weak and the kinetic energy term in the Gross-Pitaevskii equation can thus no longer be neglected with respect to the interaction energy term. A more precise criterion for the validity of the Thomas-Fermi

approximation can be expressed in terms of the local healing length

$$\xi(\vec{r}) = \frac{\hbar}{\sqrt{2mgn(\vec{r})}}\,, \tag{4.26}$$

generalizing the concept of the healing length (4.15) for the case of inhomogeneous condensates. If the inequality $\xi(\vec{r}) \ll a_j$ with $a_j = \sqrt{\hbar/(m\omega_j)}$ holds for all $j = 1, 2, 3$, then Eq. (4.18) represents a valid local approxmation of Eq. (4.10). Identifying in a very approximate manner the mean atom density in the harmonic trap with $n \sim N/\bar{a}^3$, and using the relation (4.3), we infer the scaling

$$\frac{\xi}{\bar{a}} \sim \sqrt{\frac{\bar{a}}{8\pi N a_s}} \tag{4.27}$$

for the mean healing length ξ of the condensate, from which follows that $Na_s \gg \bar{a}$ is indeed a necessary and sufficient condition for the validity of the Thomas-Fermi approximation provided the trap is not particularly anisotropic.

In the regime of moderate or weak interaction effects, $Na_s \lesssim \bar{a}$, where the Thomas-Fermi approximation fails, the ground-state properties of the interactiong Bose-Einstein condensate in a harmonic trap can be approximately determined by a complementary approach that amounts to further pursuing the application of the variational principle beyond the level of the general Hartree ansatz. More precisely, we not only assume in this approach that all atoms share the same single-particle orbital but also specify the generic profile that this orbital is supposed to exhibit. Specifically, in view of the fact that in the absence of interaction the ground-state wavefunction acquires a Gaussian profile in parabolic confinement potentials, the condensate wavefunction will be chosen as

$$\psi_0(\vec{r}) = \sqrt{N}\prod_{j=1}^{3}\frac{1}{\sqrt{\sqrt{\pi}b_j}}\exp\left(-\frac{r_j^2}{2b_j^2}\right) \equiv \psi_0^{(b_1,b_2,b_3)}(\vec{r})\,, \tag{4.28}$$

with characteristic (positive) length-scale parameters b_1, b_2, b_3 that have to be adapted such that the energy expectation value associated with $\psi_0^{(b_1,b_2,b_3)}$ is minimized. Inserting the trial function (4.28) into Eq. (4.7) yields

$$E_{\rm GP}\left[\psi_0^{(b_1,b_2,b_3)}\right] = \frac{N}{4}\sum_{j=1}^{3}\hbar\omega_j\left(\frac{a_j^2}{b_j^2}+\frac{b_j^2}{a_j^2}\right) + \frac{N^2}{2}\frac{g}{\sqrt{2\pi}^3 b_1 b_2 b_3} \tag{4.29}$$

for the latter, with

$$a_j = \sqrt{\frac{\hbar}{m\omega_j}} \tag{4.30}$$

the oscillator length associated with the frequency ω_j. Clearly, the expression (4.29) diverges for both $b_j \to 0$ and $b_j \to \infty$ for all $j = 1, 2, 3$ and must thus, in

the case of a positive interaction parameter $g > 0$, exhibit a global minimum for a set of finite values for b_1, b_2, b_3. Setting

$$\frac{\partial}{\partial b_j} E_{\rm GP}\left[\psi_0^{(b_1,b_2,b_3)}\right] = 0 \tag{4.31}$$

for this minimum, this set of values has to satisfy the equations

$$\hbar\omega_j \left(\frac{b_j^2}{a_j^2} - \frac{a_j^2}{b_j^2}\right) = \frac{Ng}{\sqrt{2\pi}^3 b_1 b_2 b_3} \tag{4.32}$$

for $j = 1, 2, 3$.

In the regime of very weak interaction, the above equations are approximately solved via $b_j \simeq a_j$, with corrections to this approximation scaling linearly with Ng. Inserting this approximation into Eq. (4.29) yields

$$E_{\rm GP} \simeq \frac{N}{2}\sum_{j=1}^{3}\hbar\omega_j + \frac{N^2}{2}\frac{g}{(\sqrt{2\pi}\bar{a})^3} + O\left((Ng)^2\right) \tag{4.33}$$

for the total energy of the condensate, with $\bar{a} = (a_1 a_2 a_3)^{1/3}$. As expected, a quadratic scaling of the interaction energy with the particle number is obtained, given the fact that the ground-state wavefunction is not appreciably modified in this perturbative regime. The chemical potential of the condensate can then be derived according to

$$\mu = \frac{dE_{\rm GP}}{dN} \simeq \frac{1}{2}\sum_{j=1}^{3}\hbar\omega_j + \frac{Ng}{(\sqrt{2\pi}\bar{a})^3} + O\left((Ng)^2\right) . \tag{4.34}$$

Equations (4.32) can also be approximately solved in the opposite regime of very strong interaction, corresponding to the condition $Na_s \gg \bar{a}$, namely through

$$\begin{aligned} \hbar\omega_j \frac{b_j^2}{a_j^2} &= \frac{Ng}{\sqrt{2\pi}^3 b_1 b_2 b_3} + \hbar\omega_j \frac{a_j^2}{b_j^2} \\ &\simeq \frac{Ng}{\sqrt{2\pi}^3 b_1 b_2 b_3} + O\left((Ng)^{-1}\right) , \end{aligned} \tag{4.35}$$

where the ratio a_j^2/b_j^2 appearing on the right-hand side of Eq. (4.35) can be recursively determined from the inverse of that right-hand side. This yields

$$b_j = \left(\frac{2}{\pi}\right)^{1/10}\left(\frac{Na_s}{\bar{a}}\right)^{1/5}\frac{\bar{\omega}}{\omega_j}\bar{a} \tag{4.36}$$

with Eq. (4.3), from which we obtain the total energy

$$E_{\rm GP} = \frac{5}{4}\left(\frac{2}{\pi}\right)^{1/10}\left(\frac{Na_s}{\bar{a}}\right)^{2/5} N\hbar\bar{\omega} \simeq 1.142 N (Na_s/\bar{a})^{2/5}\hbar\bar{\omega} . \tag{4.37}$$

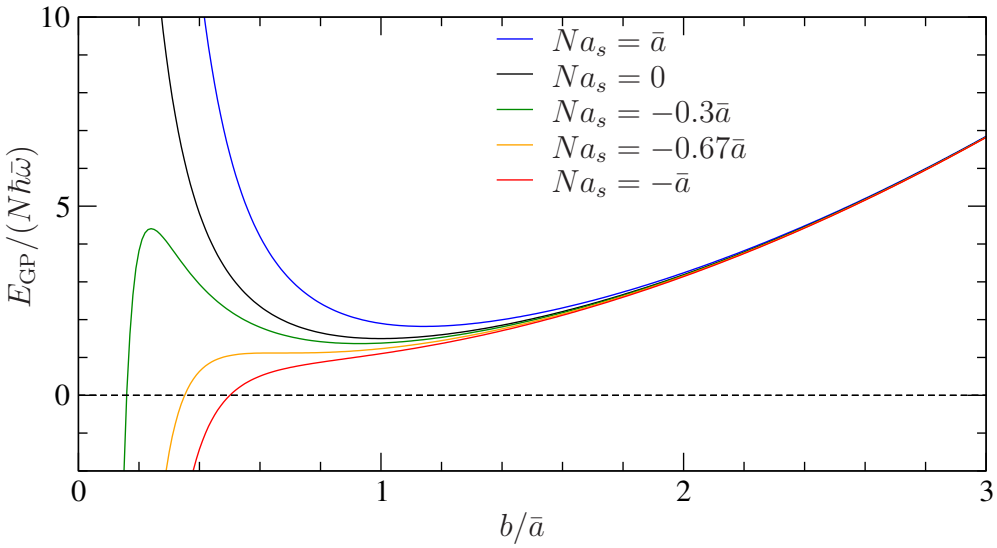

Figure 4.3: Variational energy (4.29) evaluated as a function of $b = b_1 = b_2 = b_3$ for a three-dimensional isotropic harmonic oscillator with the frequency $\bar{\omega}$ and the oscillator length $\bar{a} = \sqrt{\hbar/(m\omega)}$. A local minimum of the energy, which is also a global minimum for positive a_s, is encountered for $Na_s/\bar{a} > -0.67$. Below this critical value of the interaction strength, the variational approach does not yield an optimal Gaussian profile for the condensate, implying that the latter will inevitably be subject to collapse and subsequent disintegration.

Remarkably, the same scaling $\propto N^{7/5}$ with the particle number is thereby obtained as with the Thomas-Fermi approximation, and the comparison with the total energy expression (4.25) that the latter yielded reveals only a tiny difference in the numerical prefactor. This represents a complenetary confirmation of the validity of the Thomas-Fermi approximation in the strongly interacting regime. It also underlines the robustness of the variational approach which yields very good approximations even for parameter regimes that strongly deviate from the noninteracting case.

The variational approach can also be applied for negative interaction parameters $g < 0$, in which case the Gaussian trial wavefunction would undergo narrowing instead of widening. However, no local minimum exists beyond a certain critial attractive interaction strength, corresponding to $Na_s/\bar{a} \simeq -0.67$ for the case of an isotropic harmonic oscillator as can be seen in Fig. 4.3. Physically, this implies that for strong effective attraction cooling of the atomic gas does not lead to the formation of a stable condensate. Instead, the atomic cloud will auto-collapse due to self-attraction, giving rise to an enhanced density, and, in the course of this process, undergo disintegration via three-body collisions as was discussed at the end of Section 3.5.

Problems

4.1 Consider a Bose-Einstein condensate within a D-dimensional trapping potential $V(\mathbf{r})$ for $D = 1$ or 2, with $\mathbf{r} \equiv (r_1, \ldots, r_D)$, where the presence of a very tight isotropic harmonic confinement with frequency $\omega_\perp$ is assumed in the remaining $3 - D$ transverse dimensions. The Hartree ansatz for the ground state can then be performed for the condensate wavefunction

$$\psi_0(\vec{r}) = \sqrt{N}\psi_0(\mathbf{r}) \prod_{j=D+1}^{3} \chi_\perp(r_j) \tag{4.38}$$

with $\chi_\perp(r_j)$ the normalized noninteracting ground-mode eigenfunction along the r_j coordinate. Show that this Hartree ansatz yields a D-dimensional Gross-Pitaevskii equation

$$-\frac{\hbar^2}{2m}\frac{\partial^2}{\partial \mathbf{r}^2}\psi_0(\mathbf{r}) + V(\mathbf{r})\psi_0(\mathbf{r}) + g_D|\psi_0(\mathbf{r})|^2\psi_0(\mathbf{r}) = \mu\psi_0(\mathbf{r}) \tag{4.39}$$

with

$$g_1 = 2\hbar\omega_\perp a_s\,, \tag{4.40}$$

$$g_2 = \sqrt{8\pi}\hbar\omega_\perp a_\perp a_s \tag{4.41}$$

for $D = 1$ and 2, respectively, with $a_\perp = \sqrt{\hbar/(m\omega_\perp)}$.

4.2 Show that Eq. (4.14) with $gn = \mu - V_0$ represents the solution of the one-dimensional Gross-Pitaevskii equation (4.13) in the presence of the boundary conditions $\psi_0(0) = 0$ and $\psi_0(z) \to \sqrt{n}$ for $z \to \infty$.

4.3 Show that in the case of an attractive interaction, $g < 0$, the real-valued square-integrable solutions of the one-dimensional Gross-Pitaevskii equation (4.13) with $\mu < V_0$ are given by *solitonic* wavefunctions of the form

$$\psi_0(z) = \frac{\pm\sqrt{2n}}{\cosh\left[(z - z_0)/\tilde{\xi}\right]} \tag{4.42}$$

for arbitrary z_0, with $n = (\mu - V_0)/g > 0$ and $\tilde{\xi} = \hbar/\sqrt{-2mgn}$.

4.4 Consider the D-dimensional Gross-Pitaevskii equation

$$-\frac{\hbar^2}{2m}\frac{\partial^2}{\partial \mathbf{r}^2}\psi_0(\mathbf{r}) + V(\mathbf{r})\psi_0(\mathbf{r}) + g_D|\psi_0(\mathbf{r})|^2\psi_0(\mathbf{r}) = \mu\psi_0(\mathbf{r}) \tag{4.43}$$

for $D = 1$, 2, or 3, with $g_D > 0$ and $g_3 = g$. Show that in the presence of the anisotropic harmonic trapping potential

$$V(\mathbf{r}) = \sum_{j=1}^{D} \frac{1}{2}m\omega_j^2 r_j^2 \tag{4.44}$$

the Thomas-Fermi approximation yields the scalings

$$\mu = \left(\frac{3}{4}Ng_1\right)^{2/3}\left(\frac{1}{2}m\bar{\omega}^2\right)^{1/3}, \tag{4.45}$$

$$\mu = \sqrt{\frac{1}{\pi}Ng_2m\bar{\omega}^2}, \tag{4.46}$$

$$\mu = \left(\frac{15}{8\pi}Ng\right)^{2/5}\left(\frac{1}{2}m\bar{\omega}^2\right)^{3/5} \tag{4.47}$$

for $D = 1$, 2, and 3, respectively, with $\bar{\omega} = (\omega_1 \cdots \omega_D)^{1/D}$.

4.5 Consider a confinement potential that is defined in terms of a characteristic length scale a, such that it can be expressed as

$$V(\vec{r}) = \frac{\hbar^2}{2ma^2}\phi(\vec{r}/a) \tag{4.48}$$

with $\phi(\vec{\rho})$ a generic dimensionless trapping profile (*e.g.*, $\phi(\vec{\rho}) = \rho^2$). Show that the kinetic term in the Gross-Pitaevskii equation (4.10) is of minor importance with respect to the interaction term if the inequality $\xi(\vec{r}) \ll a$ holds for the local healing length (4.26).

4.6 Consider a Bose-Einstein condensate with N atoms, characterized by the s-wave scattering length a_s, which is confined in a three-dimensional isotropic harmonic oscillator potential characterized by the oscillator length a. Calculate the smallest negative value of Na_s/a for which the variational energy (4.29) exhibits a local minimum as a function of the parameter b ($= b_j$ for all $j = 1, 2, 3$).

4.7 Show that for harmonic confinement potentials in one spatial dimension the variational approach predicts the existence of stable Bose-Einstein condensates even in the presence of strongly attractive interaction.

Appendix A

Solutions to the problems

Problems of Chapter 1

1.1 In the case of a purely kinetic N-particle Hamiltonian, the classical phase space volume at the total energy E is given by

$$\Omega(E,N) = \int_V d^3r_1 \cdots \int_V d^3r_N \int d^3p_1 \cdots \int d^3p_N \delta\left(E - \sum_{i=1}^{N} \frac{p_i^2}{2m}\right) , \tag{A.1}$$

where V represents the volume in which the particles are confined. The integration over the position coordinates yields V^N. For the momentum integrals we introduce hyperspherical coordinates defined with respect to the supervector

$$\mathbf{P} \equiv (\mathbf{p}_1, \ldots, \mathbf{p}_N) = (p_{x1}, p_{y1}, p_{z1}, \ldots, p_{xN}, p_{yN}, p_{zN}) \in \mathbb{R}^{3N} . \tag{A.2}$$

This yields

$$\Omega(E,N) = V^N \Omega_{3N-1} \int_0^\infty P^{3N-1} \delta\left(E - \frac{P^2}{2m}\right) dP , \tag{A.3}$$

where Ω_{3N-1} denote the hypersurface of the unit sphere in $3N$ dimensions. The latter can be determined through the calculation of a $3N$ dimensional Gaussian integral, namely according to

$$\begin{aligned} \pi^{3N/2} &= \int e^{-P^2} d^{3N}P = \Omega_{3N-1} \int_0^\infty P^{3N-1} e^{-P^2} dP \\ &= \frac{\Omega_{3N-1}}{2} \int_0^\infty u^{3N/2-1} e^{-u} du = \frac{\Omega_{3N-1}}{2} \Gamma\left(\frac{3}{2}N\right) , \end{aligned} \tag{A.4}$$

where $\Gamma(x) = \int_0^\infty t^{x-1} e^{-t} dt$ is the Gamma function. The radial integral within Eq. (A.3) is obtained as

$$\int_0^\infty P^{3N-1} \delta\left(E - \frac{P^2}{2m}\right) dP = m(2mE)^{3N/2-1} . \tag{A.5}$$

This finally yields

$$\Omega(E,N) = \frac{V^N (2\pi m E)^{\frac{3}{2}N}}{\Gamma\left(\frac{3}{2}N\right) E}\,. \tag{A.6}$$

1.2 We start by noting that

$$\frac{1}{\pi}\mathrm{Re}\int_0^\infty e^{i(x+i\epsilon)t}dt = \frac{1}{\pi}\mathrm{Re}\left[\frac{1}{\epsilon - ix}\right] = \frac{\epsilon/\pi}{\epsilon^2 + x^2} \tag{A.7}$$

represents a regularization of Dirac's delta function in the limit $\epsilon \to 0_+$, which would work for a reasonably large class of test functions (namely those that do not diverge at infinity). The density of states (1.19) can therefore be expressed as

$$\begin{aligned} g(E,N) &= \sum_{n=0}^{\infty}\delta(E-E_n) = \mathrm{Tr}\left[\delta(E-\hat{H})\right] \\ &= \mathrm{Tr}\lim_{\epsilon\to 0_+}\frac{1}{\pi}\mathrm{Re}\int_0^\infty \exp\left[i(E-\hat{H}+i\epsilon)t\right]dt\,. \end{aligned} \tag{A.8}$$

The trace is now carried out in the configurational eigenbasis of the position space. Defining the eigenket $|\mathbf{R}\rangle$ of the supervector

$$\mathbf{R} \equiv (\mathbf{r}_1,\ldots,\mathbf{r}_N) = (x_1,y_1,z_1,\ldots,x_N,y_N,z_N) \in \mathbb{R}^{3N} \tag{A.9}$$

with the property $\langle\mathbf{R}|\mathbf{R}'\rangle = \delta(\mathbf{R}-\mathbf{R}')$ for all $\mathbf{R},\mathbf{R}' \in \mathbb{R}^{3N}$, we can express Eq. (A.8) as

$$g(E,N) = \lim_{\epsilon\to 0_+}\frac{1}{\pi}\mathrm{Re}\int d^{3N}R\int_0^\infty dt\,\langle\mathbf{R}|\exp[i(E-\hat{H}+i\epsilon)t]|\mathbf{R}\rangle\,. \tag{A.10}$$

We now use the fact that the Hamiltonian, as defined through Eq. (1.9), can be decomposed as $\hat{H} = \hat{T} + \hat{V}$ where $\hat{T}$ denotes its kinetic part and $\hat{V}$ comprises the external confinement potential as well as the internal interaction energy. The latter is diagonal in the above position eigenbasis and exhibits the matrix elements

$$\langle\mathbf{R}|\hat{V}|\mathbf{R}'\rangle = \left(\sum_{i=1}^N V(\mathbf{r}_i) + \frac{1}{2}\sum_{i\neq j=1}^N U(\mathbf{r}_i-\mathbf{r}_j)\right)\delta(\mathbf{R}-\mathbf{R}')\,. \tag{A.11}$$

The kinetic operator $\hat{T}$ would be diagonal in the complementary basis of momentum eigenstates $|\mathbf{P}\rangle$ whose normalized wavefunctions are given by

$$\langle\mathbf{R}|\mathbf{P}\rangle = \frac{1}{\sqrt{2\pi\hbar}^{3N}}\exp\left(\frac{i}{\hbar}\mathbf{P}\cdot\mathbf{R}\right)\,. \tag{A.12}$$

Its matrix elements within this momentum eigenbasis read

$$\langle \mathbf{P}|\hat{T}|\mathbf{P}'\rangle = \delta(\mathbf{P}-\mathbf{P}')\sum_{i=1}^{N}\frac{p_i^2}{2m}\,. \tag{A.13}$$

To make use of those two expressions (A.11) and (A.13), we employ the *Baker-Campbell-Hausdorff* relation

$$\exp[-i(\hat{T}+\hat{V})t] \simeq \exp(-i\hat{T}t)\exp(-i\hat{V}t)\exp\left(\frac{t^2}{2}[\hat{T},\hat{V}]\right)\,, \tag{A.14}$$

where leading corrections to the above approximation involve higher-order commutators, namely between $\hat{T}-\hat{V}$ and the commutator $[\hat{T},\hat{V}]$. The latter involves spatial derivatives of the confinement and the interaction potential, which are accompanied by a prefactor $-i\hbar$. Considering the formal limit $\hbar \to 0$, we consequently neglect the last exponential function on the right-hand side of Eq. (A.14) as well as further corrections to the above approximation. Using Eqs. (A.11)–(A.13) we then obtain

$$\begin{aligned}
\langle \mathbf{R}|\exp(-i\hat{H}t)|\mathbf{R}\rangle &\simeq \langle \mathbf{R}|\exp(-i\hat{T}t)\exp(-i\hat{V}t)|\mathbf{R}\rangle \\
&= \int d^{3N}P\,\langle \mathbf{R}|\mathbf{P}\rangle \int d^{3N}P'\,\langle \mathbf{P}|\exp(-i\hat{T}t)|\mathbf{P}'\rangle \\
&\quad \times \int d^{3N}R'\,\langle \mathbf{P}'|\mathbf{R}'\rangle\langle \mathbf{R}'|\exp(-i\hat{V}t)|\mathbf{R}\rangle \\
&= \int \frac{d^{3N}P}{(2\pi\hbar)^{3N}}\,\exp\left[-iH(\mathbf{r}_1,\mathbf{p}_1,\ldots,\mathbf{r}_N,\mathbf{p}_N)t/\hbar\right]
\end{aligned} \tag{A.15}$$

where H denotes here the classical equivalent (1.1) of the quantum many-body Hamiltonian $\hat{H}$. Inserting this expression into Eq. (A.10) and carrying out the resulting integral over t using again Eq. (A.7), we finally obtain

$$g(E,N) = \frac{1}{(2\pi\hbar)^{3N}}\int d^{3N}R\int d^{3N}P\,\delta\left[E-H(\mathbf{r}_1,\mathbf{p}_1,\ldots,\mathbf{r}_N,\mathbf{p}_N)\right]\,. \tag{A.16}$$

1.3 Using the expression

$$g(E) = \sum_n \delta(E-E_n) = C(N)E^{\frac{3}{2}N-1}\,, \tag{A.17}$$

for the density of states, we obtain according to Eq. (1.51) the partition function

$$Z = \mathrm{Tr}[e^{-\beta\hat{H}}] = \sum_n e^{-\beta E_n} = \int dE g(E)e^{-\beta E} = C(N)\beta^{-\frac{3}{2}N}\Gamma\left(\frac{3}{2}N\right) \tag{A.18}$$

where $\Gamma(x) = \int_0^\infty t^{x-1}e^{-t}dt$ denotes the Gamma function. The statistical averages of the expectation values of $\hat{H}$ and $\hat{H}^2$ are then evaluated within the canonical ensemble (1.50) as

$$\overline{\langle\hat{H}\rangle} = \mathrm{Tr}[\hat{H}\hat{\rho}] = \frac{1}{Z}\mathrm{Tr}[\hat{H}e^{-\beta\hat{H}}] = -\frac{1}{Z}\frac{\partial}{\partial\beta}Z = -\frac{\partial}{\partial\beta}\ln Z = \frac{3}{2}\frac{N}{\beta} \qquad \text{(A.19)}$$

and

$$\overline{\langle\hat{H}^2\rangle} = \mathrm{Tr}[\hat{H}^2\hat{\rho}] = \frac{1}{Z}\mathrm{Tr}[\hat{H}^2e^{-\beta\hat{H}}] = \frac{1}{Z}\frac{\partial^2}{\partial\beta^2}Z = \frac{\frac{3}{2}N\left(\frac{3}{2}N+1\right)}{\beta^2}\,, \qquad \text{(A.20)}$$

respectively. This straightforwardly yields

$$\overline{\langle\hat{H}^2\rangle} = \left(1+\frac{2}{3N}\right)\overline{\langle\hat{H}\rangle}^2\,, \qquad \text{(A.21)}$$

from which follows Eq. (1.53).

Problems of Chapter 2

2.1 The derivation carried out in Section 2.2 can be straightforwardly adapted to the case of noninteracting fermionic atoms. The key difference with respect to the bosonic case is that two or more fermions cannot occupy the same one-body state, which implies that the occupancies n_k of the single-particle basis states ϕ_k are restricted to the binary numbers 0 end 1. The partial partition function associated with this state is then evaluated as

$$Y_k = \sum_{n_k=0}^{1} e^{-\beta(E_k-\mu)n_k} = 1 + e^{-\beta(E_k-\mu)}\,, \qquad \text{(A.22)}$$

instead of the expression (2.24) referring to bosons. It is straightforward to show that all other calculation steps that are done in Section 2.2 are identical to the bosonic case, notably including Eq. (2.30) where summations over non-negative occupancies are to be replaced by summations over binary numbers. As in the bosonic case, we then end up with

$$\overline{\langle\hat{n}_k\rangle} = -\frac{1}{\beta}\frac{\partial}{\partial E_k}\ln Y_k\,, \qquad \text{(A.23)}$$

which straightforwardly yields Eq. (2.35).

2.2 Denoting by $\hat{n}_k = \hat{a}_k^\dagger\hat{a}_k$ the occupancy operator on the single-particle eigenstate ϕ_k, we evaluate in analogy with Eqs. (2.30) and (2.31)

$$\overline{\langle\hat{n}_k^2\rangle} = \mathrm{Tr}[\hat{\rho}\hat{n}_k^2] = \frac{1}{Y_k}\left(-\frac{1}{\beta}\frac{\partial}{\partial E_k}\right)^2 Y_k = \frac{e^{\beta(E_k-\mu)}+1}{\left(e^{\beta(E_k-\mu)}-1\right)^2}\,. \qquad \text{(A.24)}$$

Since we have $\overline{\langle \hat{n}_k \hat{n}_{k'} \rangle} = \overline{\langle \hat{n}_k \rangle}\,\overline{\langle \hat{n}_{k'} \rangle}$ for $k \neq k'$, with $\overline{\langle \hat{n}_k \rangle}$ given by Eq. (2.31), we can write

$$\overline{\langle \hat{n}_k \hat{n}_{k'} \rangle} = \overline{\langle \hat{n}_k \rangle}\,\overline{\langle \hat{n}_{k'} \rangle} + \delta_{kk'} \left(\overline{\langle \hat{n}_k \rangle}^2 + \overline{\langle \hat{n}_k \rangle} \right) \tag{A.25}$$

for all $k, k' \in \mathbb{N}_0$. We thereby obtain

$$\begin{aligned} (\Delta N)^2 &= \overline{\langle \hat{N}^2 \rangle} - \overline{\langle \hat{N} \rangle}^2 = \sum_{k,k'=0}^{\infty} \left(\overline{\langle \hat{n}_k \hat{n}_{k'} \rangle} - \overline{\langle \hat{n}_k \rangle}\,\overline{\langle \hat{n}_{k'} \rangle} \right) \\ &= \overline{\langle \hat{N} \rangle} + \sum_{k=0}^{\infty} \overline{\langle \hat{n}_k \rangle}^2 \end{aligned} \tag{A.26}$$

for the variance associated with the statistical mean value of the particle number operator.

The relative fluctuations of the particle number operator with respect to its mean value $N = \overline{\langle \hat{N} \rangle}$ can then be quantified in terms of the normalized standard deviation

$$\frac{\Delta N}{N} = \sqrt{\frac{1}{N} + \frac{1}{N^2} \sum_{k=0}^{\infty} \overline{\langle \hat{n}_k \rangle}^2}\,. \tag{A.27}$$

They are negligibly small in the thermodynamic limit $N \to \infty$ provided we have

$$\sum_{k=0}^{\infty} \overline{\langle \hat{n}_k \rangle}^2 \ll N^2 \tag{A.28}$$

in that case. This latter condition is generally satisfied at finite values for the temperature of the particle reservoir, where we can safely assume that approaching the thermodynamic limit via suitable tuning of the reservoir's chemical potential leads to the population of a rather large number of single-particle eigenstates of the system in a rather smooth manner, such that we have $\overline{\langle \hat{n}_k \rangle} \ll N$ for all k. It breaks down, however, below the Bose-Einstein condensation temperature, where the single-particle ground state of the system acquires a macroscopically large population $\overline{\langle \hat{n}_0 \rangle} \sim N$. In that latter case, the particle number fluctuations become become macroscopically large as well, *i.e.*, we have $\Delta N \sim N$ according to Eq. (A.27), and the equivalence between the canonical and the grand canonical ensemble can therefore no longer be taken for granted.

2.3 (a) Defining $\delta = -\ln z$ with the property $0 < \delta \ll 1$, we rewrite

$$g_p(z) = g_p(e^{-\delta}) = \sum_{l=1}^{\infty} \frac{e^{-l\delta}}{l^p} = \delta^{p-1} \sum_{l=1}^{\infty} \frac{e^{-l\delta}}{(l\delta)^p} \delta\,. \tag{A.29}$$

The last expression on the right-hand side of this equation represents a Riemann sum approximation of an integral, which yields

$$\sum_{l=1}^{\infty} \frac{e^{-l\delta}}{(l\delta)^p}\delta \simeq \int_0^{\infty} \frac{e^{-x}}{x^p}dx = \Gamma(1-p) \tag{A.30}$$

with

$$\Gamma(x) = \int_0^{\infty} t^{x-1}e^{-t}dt \tag{A.31}$$

the Gamma function. We therefore have

$$g_p(z) \simeq \Gamma(1-p)(-\ln z)^{p-1} \tag{A.32}$$

in leading order in $-\ln(z) \simeq 1-z$. Using $\Gamma(1/2) = \sqrt{\pi}$ we obtain Eq. (2.61) for $p = 1/2$.

Leading-order corrections to the approximate expression (A.32) can be evaluated by examining in more detail the Riemann sum approximation (A.30) near the lower integration bound $x \to 0$ where the integrand diverges. To this end, we define the function

$$\gamma_p(\delta) = \lim_{N\to\infty} \left(\sum_{l=1}^{N} \frac{e^{-l\delta}}{l^p} - \int_1^N \frac{e^{-l\delta}}{l^p}dl \right) . \tag{A.33}$$

Its limit for $\delta \to 0$ exists and is given by *Euler's generalized constant*

$$\gamma_p = \lim_{N\to\infty} \left(\sum_{l=1}^{N} \frac{1}{l^p} - \int_1^N \frac{1}{l^p}dl \right) , \tag{A.34}$$

which is evaluated as $\gamma_{1/2} \simeq 0.5396$ for $p = 1/2$. Noting that

$$\int_0^1 \frac{e^{-l\delta}}{l^p}dl = \frac{1}{1-p} + O(\delta) \tag{A.35}$$

for $0 < p < 1$, we obtain

$$g_p(e^{-\delta}) = \int_0^{\infty} \frac{e^{-l\delta}}{l^p}dl - \frac{1}{1-p} + \gamma_p + O(\delta) \tag{A.36}$$

and hence, using Eq. (A.30),

$$g_p(z) = \Gamma(1-p)(-\ln z)^{p-1} - \frac{1}{1-p} + \gamma_p + O(-\ln z)\,. \tag{A.37}$$

(b) From Eq. (2.46) we infer

$$\lambda_T \bar{n} = g_{1/2}(e^{\beta\mu}) \tag{A.38}$$

for $D = 1$. As the thermal de Broglie wavelength λ_T, defined according to Eq. (2.44), diverges for $T \to 0$, the solution of Eq. (A.38) in the limit of low temperatures implies a diverging Bose function $g_{1/2}(e^{\beta\mu}) \to \infty$ which is obtained for an argument $e^{\beta\mu}$ that approaches unity and thus corresponds to a vanishingly small exponent $\beta\mu \to 0_-$. We therefore can make use of the approximate evaluation (2.61) yielding

$$g_{1/2}(z) \simeq \sqrt{\frac{\pi}{1 - e^{\beta\mu}}} \simeq \sqrt{\frac{\pi}{-\beta\mu}}\,. \tag{A.39}$$

Solving Eq. (A.38) for μ in combination with this approximate expression (A.39) yields then

$$\mu \simeq -\frac{\pi k_B T}{\lambda_T^2 \bar{n}^2} \tag{A.40}$$

from which follows Eq. (2.62).

2.4 (a) For $0 < z < 1$ we have the convergent Taylor series expansion

$$\ln(1 - z) = -\sum_{l=1}^{\infty} \frac{z^l}{l} = -z - \frac{z^2}{2} - \frac{z^3}{3} - \ldots \tag{A.41}$$

which is identical with $-g_1(z)$ according to the definition (2.43) of the Bose function.

(b) From Eq. (2.46) we infer, for $D = 2$, the relation $g_1(e^{\beta\mu}) = \lambda_T^2 \bar{n}$. Inserting the explicit functional form (2.63) for $g_1(z)$ into this equation yields

$$\ln(1 - e^{\beta\mu}) = -\lambda_T^2 \bar{n}\,, \tag{A.42}$$

which is readily solved for μ according to

$$\mu = k_B T \ln\left(1 - e^{-\lambda_T^2 \bar{n}}\right)\,. \tag{A.43}$$

Inserting the expression (2.44) for the thermal de Broglie wavelength yields Eq. (2.64).

2.5 With Eq. (2.43) we calculate

$$g_p'(z) = \frac{d}{dz} \sum_{l=1}^{\infty} \frac{z^l}{l^p} = \sum_{l=1}^{\infty} \frac{l z^{l-1}}{l^p} = \frac{1}{z} \sum_{l=1}^{\infty} \frac{z^l}{l^{p-1}} = \frac{g_{p-1}(z)}{z}\,. \tag{A.44}$$

2.6 (a) For $T < T_c$ we have from Eq. (2.67) $E = \chi T^{p+1}$ with a prefactor χ that depends on N and V but is independent of T. Hence, the derivative with respect to T at fixed N and V yields

$$\frac{\partial E}{\partial T} = (p+1)\frac{E}{T} = (p+1)pk_B \left(\frac{k_B T}{E_0}\right)^p \zeta(p+1) \tag{A.45}$$

from which follows the low-temperature behaviour of the specific heat (2.69).

The evaluation of the high-temperature behaviour of c_V is slightly more complicated as it involves an implicit derivative. Deriving the expression (2.58) with respect to temperature for $T > T_c$ yields

$$\begin{aligned}\frac{\partial E}{\partial T} &= (p+1)pk_B \left(\frac{k_B T}{E_0}\right)^p g_{p+1}(e^{\beta\mu}) \\ &\quad + pk_B T \left(\frac{k_B T}{E_0}\right)^p g'_{p+1}(e^{\beta\mu}) \left.\frac{d}{dT} e^{\beta\mu}\right|_{N,V} ,\end{aligned} \tag{A.46}$$

where for the last term on the right-hand side of this equation we have to take into account the fact that μ implicitly depends on T and N, as displayed in Fig. 2.1(d) and expressed via Eq. (2.46). While we are unable to obtain from that latter equation an explicit expression for $\mu(T, N)$ in terms of known functions (except for the case $p = 1$, see Eq. (2.64)), the derivative expression required in Eq. (A.46) can nevertheless be yielded by deriving both sides of Eq. (2.66) with respect to T at fixed N and V:

$$0 = \frac{p}{T}\left(\frac{k_B T}{E_0}\right)^p g_p(e^{\beta\mu}) + \left(\frac{k_B T}{E_0}\right)^p g'_p(e^{\beta\mu}) \left.\frac{d}{dT} e^{\beta\mu}\right|_{N,V} . \tag{A.47}$$

We therefore determine

$$\left.\frac{d}{dT} e^{\beta\mu}\right|_{N,V} = -\frac{p}{T}\frac{g_p(e^{\beta\mu})}{g'_p(e^{\beta\mu})} . \tag{A.48}$$

Using $g'_{p+1}(z)/g'_p(z) = g_p(z)/g_{p-1}(z)$, which follows from the property (2.65), and $(k_B T/E_0)^p = N/g_p(e^{\beta\mu})$, which follows from Eq. (2.66) for $T > T_c$, we can rewrite Eq. (A.46) as

$$\frac{\partial E}{\partial T} = Npk_B \left((p+1)\frac{g_{p+1}(e^{\beta\mu})}{g_p(e^{\beta\mu})} - p\frac{g_p(e^{\beta\mu})}{g_{p-1}(e^{\beta\mu})}\right) . \tag{A.49}$$

This then yields the high-temperature behaviour of c_V.

(b) Let us first recall, as is also displayed in Fig. 2.1(d), that a monotonous increase of the temperature from T_c to ∞ at fixed particle number N implies a monotonous decrease of the chemical potential from 0 to $-\infty$ which is such that we have the limits $\beta\mu \to 0$ for $T \to T_c$ and $\beta\mu \to -\infty$ for $T \to \infty$. The argument $e^{\beta\mu}$ of the Bose function therefore approaches unity close to the critical temperature. For $p \leq 2$ this implies that the second term on the right-hand side of Eq. (A.49) vanishes there, owing to the diverging term $g_{p-1}(e^{\beta\mu})$ in the denominator. We then have

$$\lim_{T\to T_c} \frac{\partial E}{\partial T} = N k_B p(p+1) \frac{\zeta(p+1)}{\zeta(p)}\,, \tag{A.50}$$

independently of whether the critical temperature is approached from above, via Eq. (A.49), or from below, via Eq. (A.45). For $p > 2$, on the other hand, $g_{p-1}(z)$ approaches the finite value $\zeta(p-1)$ in the limit $z \to 1_-$. The specific heat therefore features a discontinuity at T_c in that case, and drops by an amount

$$\lim_{T\to T_c+} c_V - \lim_{T\to T_c-} c_V = -k_B \frac{p^2 \zeta(p)}{\zeta(p-1)} \tag{A.51}$$

when the temperature is increased across T_c.

(c) In the high-temperature limit $T \to \infty$, we have $z = e^{\beta\mu} \to 0$ and can therefore justify the approximation $g_p(z) \simeq z + z^2/2^p + O(z^3)$. A Taylor series expansion up to linear order in z yields

$$(p+1)\frac{g_{p+1}(z)}{g_p(z)} - p\frac{g_p(z)}{g_{p-1}(z)} \simeq 1 + \frac{p-1}{2^{p+1}} z + O(z^2)\,. \tag{A.52}$$

Solving Eq. (2.66) in leading order in z according to $z \simeq N[E_0/(k_B T)]^p$ allows us then to expand Eq. (A.49) in the high-temperature limit as

$$\frac{\partial E}{\partial T} \simeq N p k_B \left[1 + \frac{p-1}{2^{p+1}} N \left(\frac{E_0}{k_B T}\right)^p\right] \tag{A.53}$$

up to corrections that scale quadratically with z. Division by N yields Eq. (2.70).

2.7 We start by noting that $(e^{nx} - 1)^{-1}$ diverges as $1/(nx)$ for $x \to 0$ at finite n. Let us therefore first rewrite

$$\sum_{n=1}^{\infty} \frac{1}{e^{nx} - 1} = \lim_{N\to\infty} \left(\sum_{n=1}^{N} \frac{1}{nx} + \sum_{n=1}^{N} f(nx) \right) \tag{A.54}$$

where we define

$$f(\xi) = \frac{1}{e^{\xi} - 1} - \frac{1}{\xi} \,. \tag{A.55}$$

This latter function is regular at the origin, with the limit $f(\xi \to 0) = -1/2$. We can therefore approximate the sum over $f(nx)$ by an integration according to

$$\sum_{n=1}^{N} f(nx) \simeq \int_{1/2}^{N+1/2} f(nx) dn = \frac{1}{x} \int_{x/2}^{(N+1/2)x} f(\xi) d\xi \,. \tag{A.56}$$

This approximation is valid up to corrections that scale linearly in x, noting that we have here an implementation of the so-called midpoint rule for the evaluation of the integral on the right-hand side of Eq. (A.56) via a Riemann sum. Using $\int \xi^{-1} d\xi = \ln \xi$ and $\int (e^{\xi} - 1)^{-1} d\xi = \ln(1 - e^{-\xi})$ (see also Eq. (2.63) for this latter identity), we calculate

$$\int_{x/2}^{(N+1/2)x} f(\xi) d\xi = \ln \left(\frac{1 - e^{-(N+1/2)x}}{1 - e^{-x/2}} \right) - \ln(2N + 1) \,. \tag{A.57}$$

Insertion into Eq. (A.54) yields, after performing the limit $N \to \infty$,

$$\sum_{n=1}^{\infty} \frac{1}{e^{nx} - 1} = \frac{\gamma}{x} - \frac{1}{x} \ln \left[2(1 - e^{-x/2}) \right] + O(x) \tag{A.58}$$

with the Euler-Mascheroni constant (2.91). Using the Taylor expansions of the exponential function and the logarithm, we obtain

$$\ln \left[2(1 - e^{-x/2}) \right] = \ln x - x/4 + O(x^2) \,, \tag{A.59}$$

from which follows Eq. (2.90).

2.8 Let us first consider the case $T > T_c$. We infer from Eqs. (2.100) and (2.101)

$$n(\boldsymbol{\rho}) = \frac{1}{(2\pi\hbar)^3} \int d^3p \frac{e^{i\mathbf{p}\cdot\boldsymbol{\rho}/\hbar}}{e^{\beta[p^2/(2m) - \mu]} - 1} \,. \tag{A.60}$$

With the help of the geometric series (2.41) we calculate

$$n(\boldsymbol{\rho}) = \frac{1}{\lambda_T^3} \sum_{l=1}^{\infty} \frac{e^{l\beta\mu}}{l^{3/2}} e^{-\pi\rho^2/(l\lambda_T^2)} \,. \tag{A.61}$$

For large $\rho/\lambda_T \to \infty$ we are entitled to approximate the sum by an integral, yielding

$$n(\boldsymbol{\rho}) \simeq \frac{1}{\lambda_T^3} \int_0^{\infty} \frac{e^{f(l)}}{l^{3/2}} dl \tag{A.62}$$

with

$$f(l) = l\beta\mu - \frac{\pi\rho^2}{l\lambda_T^2}\,. \tag{A.63}$$

Indeed, this function f exhibits a global maximum at

$$l_0 = \sqrt{\frac{\pi}{-\beta\mu}}\frac{\rho}{\lambda_T} \tag{A.64}$$

where it is evaluated as

$$f(l_0) = -2\sqrt{-\pi\beta\mu}\frac{\rho}{\lambda_T} \tag{A.65}$$

and exhibits the curvature

$$f''(l_0) = \frac{2\beta\mu}{\rho/\lambda_T}\sqrt{\frac{-\beta\mu}{\pi}}\,. \tag{A.66}$$

We thus have $l_0 \to \infty$ and $f''(l_0) \to 0$ in the limit $\rho/\lambda_T \to \infty$, which implies that near this global maximum of f the approximation of the sum by an integration is very well justified in this limit.

We now perform the change of integration variable

$$l \mapsto u = \frac{\rho}{\lambda_T}\sqrt{\frac{\pi}{l}} - \sqrt{-\beta\mu l}\,, \tag{A.67}$$

which is inverted through

$$l = \frac{4\pi r^2/\lambda_T^2}{\left(\sqrt{u^2 + 4\sqrt{-\pi\beta\mu}\frac{\rho}{\lambda_T}} + u\right)^2} \tag{A.68}$$

With this expression for l we straightforwardly calculate

$$f(l) = l\beta\mu - \frac{\pi\rho^2}{l\lambda_T^2} = -2\sqrt{-\pi\beta\mu}\frac{\rho}{\lambda_T} - u^2 \tag{A.69}$$

as well as

$$l^{-3/2}dl = -\frac{\lambda_T}{\sqrt{\pi}r}\left(1 + \frac{u}{\sqrt{u^2 + \sqrt{-\pi\beta\mu}\frac{\rho}{\lambda_T}}}\right)du\,. \tag{A.70}$$

Using $\int_{-\infty}^{\infty} u(u^2 + \sqrt{-\pi\beta\mu}\rho/\lambda_T)^{-1/2}e^{-u^2}du = 0$, we then evaluate

$$\int_0^\infty l^{-3/2}e^{f(l)}dl = \frac{\lambda_T}{r}\exp\left(-2\sqrt{-\pi\beta\mu}\frac{\rho}{\lambda_T}\right)\,, \tag{A.71}$$

from which, with Eq. (A.62), follows Eq. (2.103).

The key approximation (A.62), consisting in the replacement of the sum (A.61) by an integral, can be justified also in the limit $\beta\mu \to 0$, corresponding to the case $T < T_c$, even though in that case f does no longer exhibit a global maximum. We therefore have $\lambda_T^{-3} \sum_{l=1}^{\infty} l^{-3/2} e^{-\pi\rho^2/(l\lambda_T^2)} \simeq \lambda_T^{-2}\rho^{-1}$ for $\rho \gg \lambda_T$. The validity of Eq. (2.103) can thus be shown also for temperatures below the critical temperature.

Problems of Chapter 3

3.1 The starting point of this calculation is the general nonrelativistic expression

$$\begin{aligned}\vec{j}(\vec{r},t) &= \frac{q\hbar}{2mi}\left[\phi^\dagger(\vec{r},t)\vec{\nabla}\phi(\vec{r},t) - \left(\vec{\nabla}\phi^\dagger(\vec{r},t)\right)\phi(\vec{r},t)\right] \\ &\quad + \frac{q\hbar}{2m}\vec{\nabla}\times\phi^\dagger(\vec{r},t)\vec{\sigma}\phi(\vec{r},t) \end{aligned} \tag{A.72}$$

for the electric current of a particle with the the mass m and the charge q that is exposed to an electrostatic environment. Here, $\phi(\vec{r},t)$ denotes the Pauli spinor describing the two-component wavefunction of the particle evaluated at position $\vec{r}$ and time t, and $\vec{\sigma} \equiv (\sigma_x, \sigma_y, \sigma_z)$ is the vector of the Pauli matrices. This expression (A.72) is derived from the more general definition

$$\vec{j}(\vec{r},t) = qc\psi^\dagger(\vec{r},t)\vec{\alpha}\psi(\vec{r},t) \tag{A.73}$$

of the electric current density in the framework of the relativistic Dirac equation

$$i\hbar\frac{\partial}{\partial t}\psi(\vec{r},t) = -i\hbar c\vec{\alpha}\cdot\vec{\nabla}\psi(\vec{r},t) + mc^2\beta\psi(\vec{r},t) + V(\vec{r})\psi(\vec{r},t) \tag{A.74}$$

describing the time evolution of the four-component Dirac spinor ψ in the presence of the electrostatic potential energy $V(\vec{r})$, with the 4×4 matrices

$$\alpha_l = \begin{pmatrix} 0 & \sigma_l \\ \sigma_l & 0 \end{pmatrix} \tag{A.75}$$

for $l = 1, 2, 3$ and

$$\beta = \begin{pmatrix} \mathbb{I} & 0 \\ 0 & -\mathbb{I} \end{pmatrix}, \tag{A.76}$$

where $\mathbb{I}$ is the unit matrix in two dimensions. Defining

$$\psi(\vec{r},t) \equiv e^{-imc^2t/\hbar}\begin{pmatrix} \phi(\vec{r},t) \\ \tilde{\phi}(\vec{r},t) \end{pmatrix} \tag{A.77}$$

and solving the resulting equation for the antiparticle component $\tilde{\phi}$ as

$$\tilde{\phi}(\vec{r},t) \simeq \frac{\hbar}{2imc}\vec{\sigma}\cdot\vec{\nabla}\phi(\vec{r},t) + O(1/c^2) \tag{A.78}$$

in leading order in $1/c$ transforms the expression (A.73) into

$$\vec{j}(\vec{r},t) = \frac{\hbar q}{2imc}\left[\phi^\dagger(\vec{r},t)\vec{\sigma}\left(\vec{\sigma}\cdot\vec{\nabla}\phi(\vec{r},t)\right) + \left(\vec{\nabla}\phi^\dagger(\vec{r},t)\cdot\vec{\sigma}\right)\vec{\sigma}\phi(\vec{r},t)\right]. \tag{A.79}$$

Equation (A.72) is then obtained using $\sigma_k\sigma_l = \delta_{kl} + i\epsilon_{klm}\sigma_m$ with δ_{kl} and ϵ_{klm} the Kronecker and Levi-Civita symbols, respectively.

In the case of an electron with the charge $q = -e$ that is contained within an isotropic s-orbital of a hydrogen-like atom, we can write the Pauli spinor as

$$\phi(\vec{r},t) = \psi_s(|\vec{r}|)e^{-iE_st/\hbar}\vec{e}_s\,, \tag{A.80}$$

where $\psi_s : \mathbb{R}_+ \to \mathbb{R}, r \mapsto \psi_s(r)$ represents the s orbital, E_s is its eigenenergy, and $\vec{e}_s$ denotes the unit vector along the orientation of the electron spin. Introducing the spatial probability density of the electron as $\rho_s(r) = |\psi_s(r)|^2$ as well as the Bohr magneton $\mu_B = e\hbar/(2m)$, we obtain the expression

$$\vec{j}(\vec{r},t) = \mu_B\vec{e}_s\times\vec{\nabla}\rho_s(|\vec{r}|) \equiv \vec{j}(\vec{r}) \tag{A.81}$$

for the electric current density that is associated with this state.

According to the Biot-Savart law, this electric current density generates the magnetic field

$$\vec{B}(\vec{r}\,') = \frac{\mu_0}{4\pi}\vec{\nabla}'\times\int d^3r\frac{1}{|\vec{r}\,'-\vec{r}|}\vec{j}(\vec{r})\,, \tag{A.82}$$

where μ_0 is the vacuum permeability. This magnetic field is evaluated at the position $\vec{r}\,' = 0$ of the nucleus as

$$\vec{B}(0) = \frac{\mu_0}{4\pi}\int d^3r\,\vec{j}(\vec{r})\times\vec{\nabla}\frac{1}{|\vec{r}|} = \frac{\mu_0\mu_B}{4\pi}\int d^3r\left(\vec{e}_s\times\vec{\nabla}\rho_s(|\vec{r}|)\right)\times\vec{\nabla}\frac{1}{|\vec{r}|}\,, \tag{A.83}$$

where the integration domain must leave out the origin. Using

$$\vec{\nabla}\frac{1}{|\vec{r}|} = -\frac{1}{|\vec{r}|^3}\vec{r}, \tag{A.84}$$

$$\vec{\nabla}\rho_s(|\vec{r}|) = \frac{\rho_s'(|\vec{r}|)}{|\vec{r}|}\vec{r} \tag{A.85}$$

for all $\vec{r}\in\mathbb{R}^3\backslash\{0\}$, as well as

$$(\vec{e}_s\times\vec{r})\times\vec{r} = (\vec{e}_s\cdot\vec{r})\vec{r} - |\vec{r}|^2\vec{e}_s\,, \tag{A.86}$$

we can therefore evaluate the expression (A.83) in spherical coordinates as

$$\begin{aligned}\vec{B}(0) &= \frac{\mu_0\mu_B}{4\pi}2\pi\lim_{r_0\to 0}\int_{r_0}^{\infty}dr\rho_s'(r)\int_0^{\pi}d\theta\,\sin\theta(1-\cos^2\theta)\vec{e}_s \\ &= -\frac{2}{3}\mu_0\mu_B\rho_s(0)\vec{e}_s\,. \end{aligned} \tag{A.87}$$

3.2 The Hamiltonian (3.10)

$$H = A\vec{I}\cdot\vec{S} + CS_z \tag{A.88}$$

is diagonalized within the basis constituted by the simultaneous eigenstates $|m_I, m_s\rangle$ of the operators $\vec{I}^2$, I_z, $\vec{S}^2$, S_z, satisfying

$$\vec{I}^2|m_F, m_s\rangle = I(I+1)|m_I, m_s\rangle\,, \tag{A.89}$$
$$I_z|m_I, m_s\rangle = m_I|m_I, m_s\rangle\,, \tag{A.90}$$
$$\vec{S}^2|m_I, m_s\rangle = \frac{3}{4}|m_I, m_s\rangle\,, \tag{A.91}$$
$$S_z|m_I, m_s\rangle = m_s|m_I, m_s\rangle \tag{A.92}$$

for all $m_I \in \{-I, -I+1, \ldots, I\}$ and all $m_s \in \{-1/2, 1/2\}$. To this end, we express

$$\vec{I}\cdot\vec{S} = I_xS_x + I_yS_y + I_zS_z = \frac{1}{2}(I_+S_- + I_-S_+) + I_zS_z \tag{A.93}$$

with $I_\pm = I_x \pm iI_y$ and $S_\pm = S_x + iS_y$ the ladder operators associated with the angular momenta $\vec{I}$ and $\vec{S}$, satisfying

$$I_\pm|m_I, m_s\rangle = \sqrt{I(I+1) - m_I(m_I \pm 1)}|m_I \pm 1, m_s\rangle\,, \tag{A.94}$$
$$S_\pm|m_I, m_s\rangle = \sqrt{3/4 - m_s(m_s \pm 1)}|m_I, m_s \pm 1\rangle \tag{A.95}$$

for all $m_I \in \{-I, -I+1, \ldots, I\}$ and all $m_s \in \{-1/2, 1/2\}$. We therefore obtain

$$\begin{aligned}\vec{I}\cdot\vec{S}|m_I, 1/2\rangle &= \frac{1}{2}\sqrt{I(I+1) - m_I(m_I+1)}|m_I+1, -1/2\rangle \\ &\quad + \frac{m_I}{2}|m_I, 1/2\rangle\,, \end{aligned} \tag{A.96}$$

$$\begin{aligned}\vec{I}\cdot\vec{S}|m_I+1, -1/2\rangle &= +\frac{1}{2}\sqrt{I(I+1) - m_I(m_I+1)}|m_I, 1/2\rangle \\ &\quad - \frac{m_I+1}{2}|m_I+1, -1/2\rangle \end{aligned} \tag{A.97}$$

for all $m_I \in \{-I, -I+1, \ldots, I-1\}$ and

$$\vec{I}\cdot\vec{S}|\pm I, \pm 1/2\rangle = \frac{I}{2}|\pm I, \pm 1/2\rangle\,. \tag{A.98}$$

Consequently, the Hamiltonien (A.88) separates into the 2×2 blocks

$$H_{m_I} = \frac{1}{2} \begin{pmatrix} m_I A + C & A\sqrt{I(I+1) - m_I(m_I+1)} \\ A\sqrt{I(I+1) - m_I(m_I+1)} & -(m_I+1)A - C \end{pmatrix} \tag{A.99}$$

within the subspaces spanned by the states $|m_I, 1/2\rangle$ and $|m_I+1, -1/2\rangle$ for all $m_I \in \{-I, -I+1, \ldots, I-1\}$, whose diagonalization straightforwardly yield the eigenvalues

$$E^{\pm}_{m_I} = -\frac{A}{4} \pm \frac{1}{2}\sqrt{A^2(I+1/2)^2 + C^2 + AC(2m_I+1)}\,. \tag{A.100}$$

The remaining two eigenstates of H are given by $|\pm I, \pm 1/2\rangle$ with the associated eigenvalues $E^{\pm}_I = IA/2 \pm C/2$.

3.3 The starting point for this calculation is the Schrödinger equation

$$i\hbar\frac{\partial}{\partial t}\Psi(\vec{r}, \vec{r}_e, t) = \mathcal{H}\Psi(\vec{r}, \vec{r}_e, t) \tag{A.101}$$

for the wavefunction describing the two-body system that is constituted by the valence electron and the atomic core, where the associated two-body Hamiltonian is given by Eq. (3.20). This two-body wavefunction is subjected to the gauge transformation $\Psi \mapsto \psi$ defined by

$$\Psi(\vec{r}, \vec{r}_e, t) = \psi(\vec{r}, \vec{r}_e, t)e^{-ie\chi(\vec{r}, \vec{r}_e, t)/\hbar} \tag{A.102}$$

with

$$\chi(\vec{r}, \vec{r}_e, t) = \int_{\vec{r}}^{\vec{r}_e} \vec{A}(\vec{r}\,', t) \cdot d\vec{r}\,' \tag{A.103}$$

for all times t and all positions $\vec{r}$, $\vec{r}_e$ of the atomic nucleus and the valence electron, respectively, where the integral on the right-hand side of Eq. (A.103) is supposed to be carried out along a straight line from $\vec{r}$ to $\vec{r}_e$., *i.e.*, we define

$$\int_{\vec{r}}^{\vec{r}_e} \vec{A}(\vec{r}\,', t) \cdot d\vec{r}\,' \equiv \int_0^1 \vec{A}\,(\vec{r} + s(\vec{r}_e - \vec{r}), t) \cdot (\vec{r}_e - \vec{r})ds \tag{A.104}$$

for all $\vec{r}$, $\vec{r}_e$ and all t. Inserting this gauge transformation (A.102) into the Schrödinger equation (A.101) yields

$$i\hbar\frac{\partial}{\partial t}\Psi(\vec{r}, \vec{r}_e, t) = \left(i\hbar\frac{\partial}{\partial t}\psi(\vec{r}, \vec{r}_e, t) + e\frac{\partial}{\partial t}\chi(\vec{r}, \vec{r}_e, t)\right) e^{-ie\chi(\vec{r}, \vec{r}_e, t)/\hbar} \tag{A.105}$$

on its left-hand side, where we approximately evaluate

$$\frac{\partial}{\partial t}\chi(\vec{r}, \vec{r}_e, t) = -e\int_{\vec{r}}^{\vec{r}_e} \vec{E}(\vec{r}\,', t) \cdot d\vec{r}\,' \simeq e(\vec{r} - \vec{r}_e) \cdot \vec{E}(\vec{r}, t) \tag{A.106}$$

using the expression (3.21) for the electric field $\vec{E}$ and the fact that the latter varies very weakly on a spatial scale that is comparable to Bohr's radius.

For the evaluation of the kinetic terms on the right-hand side of the Schrödinger equation, we calculate

$$\begin{aligned}\left(\vec{p}-e\vec{A}(\vec{r},t)\right)\Psi(\vec{r},\vec{r}_e,t) &= \left[\left(\vec{p}-e\vec{A}(\vec{r},t)-e\frac{\partial\chi}{\partial\vec{r}}(\vec{r},\vec{r}_e,t)\right)\psi(\vec{r},\vec{r}_e,t)\right] \\ &\quad\times e^{-ie\chi(\vec{r},\vec{r}_e,t)/\hbar}, \qquad \text{(A.107)}\\ \left(\vec{p}_e+e\vec{A}(\vec{r}_e,t)\right)\Psi(\vec{r},\vec{r}_e,t) &= \left[\left(\vec{p}_e+e\vec{A}(\vec{r}_e,t)-e\frac{\partial\chi}{\partial\vec{r}_e}(\vec{r},\vec{r}_e,t)\right)\psi(\vec{r},\vec{r}_e,t)\right] \\ &\quad\times e^{-ie\chi(\vec{r},\vec{r}_e,t)/\hbar}. \qquad \text{(A.108)}\end{aligned}$$

To evaluate the spatial gradient of the scalar gauge field χ with respect to $\vec{r}_e$, we form the difference

$$\begin{aligned}\chi(\vec{r},\vec{r}_e+\delta\vec{r},t)-\chi(\vec{r},\vec{r}_e,t) &= \int_{\vec{r}}^{\vec{r}_e+\delta\vec{r}}\vec{A}(\vec{r}\,',t)\cdot d\vec{r}\,' - \int_{\vec{r}}^{\vec{r}_e}\vec{A}(\vec{r}\,',t)\cdot d\vec{r}\,' \\ &= \int_{\vec{r}_e}^{\vec{r}_e+\delta\vec{r}}\vec{A}(\vec{r}\,',t)\cdot d\vec{r}\,' - \oint_\Gamma \vec{A}(\vec{r}\,',t)\cdot d\vec{r}\,' \\ &\simeq \vec{A}(\vec{r}_e,t)\cdot\delta\vec{r} - \oint_\Gamma \vec{A}(\vec{r}\,',t)\cdot d\vec{r}\,' \qquad \text{(A.109)}\end{aligned}$$

where the loop integral $\oint_\Gamma$ is perfomed along the triangle path Γ going along straight lines from $\vec{r}$ to $\vec{r}_e$, from $\vec{r}_e$ to $\vec{r}_e+\delta\vec{r}$, and finally from $\vec{r}_e+\delta\vec{r}$ back to $\vec{r}$. Using Stokes' theorem, the expression (3.22) for the magnetic field, as well as the fact that the latter does not significantly vary on a length scale corresponding to Bohr's radius, this loop integral can be approximately evaluated as

$$\begin{aligned}\oint_\Gamma \vec{A}(\vec{r}\,',t)\cdot d\vec{r}\,' &= \iint \vec{\nabla}\times\vec{A}(\vec{r}\,',t)\cdot d\vec{S} = \iint \vec{B}(\vec{r}\,',t)\cdot d\vec{S} \\ &\simeq \vec{B}(\vec{r},t)\cdot\left(\frac{1}{2}(\vec{r}_e-\vec{r})\times\delta\vec{r}\right) \\ &= \frac{1}{2}\left(\vec{B}(\vec{r},t)\times(\vec{r}_e-\vec{r})\right)\cdot\delta\vec{r}, \qquad \text{(A.110)}\end{aligned}$$

where we have introduced by $\iint d\vec{S}$ the surface integral over the area of the triangle, with $d\vec{S}$ being the properly oriented unit vector perpendicular to the surface. This finally yields

$$\frac{\partial\chi}{\partial\vec{r}_e}(\vec{r},\vec{r}_e,t) \simeq \vec{A}(\vec{r}_e,t) - \frac{1}{2}\vec{B}(\vec{r},t)\times(\vec{r}_e-\vec{r}). \qquad \text{(A.111)}$$

Performing a similar calculation for the spatial gradient of χ with respect to $\vec{r}$, we obtain

$$\frac{\partial\chi}{\partial\vec{r}}(\vec{r},\vec{r}_e,t) \simeq -\vec{A}(\vec{r},t) - \frac{1}{2}\vec{B}(\vec{r},t)\times(\vec{r}_e-\vec{r})\,. \tag{A.112}$$

We finally assume that the magnetic component $\vec{B}$ of the electromagnetic field described by the vector potential $\vec{A}$ is very small compared to the electric field $\vec{E}$ and can be neglected in the following. This latter approximation transforms Eqs. (A.107) and (A.108) into

$$\left(\vec{p}-e\vec{A}(\vec{r},t)\right)\Psi(\vec{r},\vec{r}_e,t) \simeq e^{-ie\chi(\vec{r},\vec{r}_e,t)/\hbar}\vec{p}\psi(\vec{r},\vec{r}_e,t)\,, \tag{A.113}$$

$$\left(\vec{p}_e+e\vec{A}(\vec{r}_e,t)\right)\Psi(\vec{r},\vec{r}_e,t) \simeq e^{-ie\chi(\vec{r},\vec{r}_e,t)/\hbar}\vec{p}_e\psi(\vec{r},\vec{r}_e,t)\,. \tag{A.114}$$

From this and Eq. (A.106) follow the gauge-transformed Schrödinger equation

$$i\hbar\frac{\partial}{\partial t}\psi(\vec{r},\vec{r}_e,t) = \frac{p^2}{2m}\psi(\vec{r},\vec{r}_e,t) + H\Psi(\vec{r},\vec{r}_e,t) \tag{A.115}$$

where H is the one-body Hamiltonian defined by Eq. (3.23).

3.4 For the application of time-dependent perturbation theory, we employ the *interaction representation*, which amounts to decomposing the wavefunction describing the valence electron of the atom according to

$$|\psi\rangle_t = \sum_\nu C_\nu(t)e^{-iE_\nu t/\hbar}|\nu\rangle \tag{A.116}$$

within the eigenbasis $(|\nu\rangle)_{\nu\in\mathbb{N}_0}$ of the unperturbed intra-atomic Hamiltonian

$$H_0 = -\frac{\hbar^2}{2m}\frac{\partial^2}{\partial\vec{\rho}^2} + \mathcal{V}(\vec{\rho}) = \sum_\nu E_\nu|\nu\rangle\langle\nu|\,. \tag{A.117}$$

Furthermore, we formally assume that the strength of the perturbation is adiabatically ramped from zero to a given finite value in the course of time evolution, namely such that we perform the replacement $\vec{\mathcal{E}}_0(\vec{r}) \mapsto \vec{\mathcal{E}}_0(\vec{r})e^{\epsilon t}$ within the expression (3.24) for the external electric field, where we shall take the limit $\epsilon \to 0_+$ in the end. The Schrödinger equation describing the time evolution of the intra-atomic wavefunction in the presence of the laser field can then be written as

$$i\hbar\frac{\partial}{\partial t}|\psi\rangle_t = \left(H_0 + H_1(t)\right)|\psi\rangle_t \tag{A.118}$$

with the perturbation Hamiltonian

$$H_1(t) = e\vec{\rho}\cdot\vec{\mathcal{E}}_0(\vec{r})\cos\left(\omega t - \varphi(\vec{r})\right)e^{\epsilon t}\,. \tag{A.119}$$

Projecting this Schrödinger equation (A.118) onto the eigenstates $|\nu\rangle$ of the unperturbed intra-atomic Hamiltonian (A.117) yields the system of equations

$$i\hbar\frac{\partial}{\partial t}C_\nu(t) = \sum_{\nu'}\langle\nu|H_1(t)|\nu'\rangle C_{\nu'}(t)e^{it(E_\nu - E_{\nu'})/\hbar} \tag{A.120}$$

for the amplitudes C_ν.

We now assume that the system is initially, *i.e.*, in the asymptotic past, prepared in the ground state $|0\rangle$, such that we can set $C_\nu(t_0) = \delta_{\nu 0}$ for all ν at the initial time $t_0 \to -\infty$. Defining $\omega_\nu = (E_\nu - E_0)/\hbar$ for all ν, the equation (A.120) is then approximately solved as

$$C_\nu(t) \simeq \frac{1}{i\hbar}\int_{-\infty}^{t}\langle\nu|H_1(t')|0\rangle C_0(t')e^{i\omega_\nu t'}dt' \tag{A.121}$$

in linear order in H_1. Using furthermore the fact that we have $\langle\nu|\vec{\rho}|\nu\rangle = 0$ for all eigenstates $|\nu\rangle$, due to the fact that the latter exhibit a well-defined (even or odd) parity in the presence of the spherically isotropic potential $\mathcal{V}(\vec{\rho}) \equiv \mathcal{V}(|\vec{\rho}|)$, we obtain in lowest nonvanishing order

$$i\hbar\frac{\partial}{\partial t}C_0(t) \simeq \frac{1}{i\hbar}\sum_{\nu\neq 0}\int_{-\infty}^{t}\langle 0|H_1(t)|\nu\rangle\langle\nu|H_1(t')|0\rangle C_0(t')e^{i\omega_\nu(t'-t)}dt' \tag{A.122}$$

for the time evolution of the ground state amplitude C_0, where corrections to the approximate expression (A.122) scale quartically with H_1.

Making now the ansatz $C_0(t) = \exp(-i\delta_0(t))$, we obtain from Eq. (A.122) the equation

$$\begin{aligned}
\hbar\frac{d}{dt}\delta_0(t) &= \frac{1}{i\hbar}\sum_{\nu\neq 0}\left|\langle\nu|e\vec{\rho}\cdot\vec{\mathcal{E}}_0(\vec{r})|0\rangle\right|^2 e^{\epsilon t}\cos(\omega t - \varphi(\vec{r})) \\
&\quad\times\int_{-\infty}^{t}e^{\epsilon t'}\cos(\omega t' - \varphi(\vec{r}))e^{i\omega_\nu(t'-t)}e^{i(\delta_0(t')-\delta_0(t))} \qquad \text{(A.123)} \\
&= \frac{e^{2\epsilon t}}{4i\hbar}\sum_{\nu\neq 0}\left|\langle\nu|e\vec{\rho}\cdot\vec{\mathcal{E}}_0(\vec{r})|0\rangle\right|^2 \\
&\quad\times\left(\frac{1+e^{2i(\omega t-\varphi_0(\vec{r}))}}{\epsilon + i(\omega_\nu+\omega)} + \frac{1+e^{2i(\omega t-\varphi_0(\vec{r}))}}{\epsilon + i(\omega_\nu-\omega)}\right) \qquad \text{(A.124)}
\end{aligned}$$

describing the time evolution of the phase δ_0, where we use the fact that owing to Eq. (A.123) we have $\delta_0(t') - \delta_0(t) \sim O(\mathcal{E}_0^2)$ for all t, t', such that we can set $\exp[i(\delta_0(t') - \delta_0(t))] \simeq 1$ within this equation (A.123). Performing the limit $\epsilon \to 0_+$ within Eq. (A.124) and neglecting contributions that are

highly oscillatory in time (and will therefore vanish if a temporal average over a finite time interval is performed), we finally obtain

$$C_0(t) = e^{-i\Delta E_0 (t-t_0)/\hbar} \tag{A.125}$$

with the ground state energy shift

$$\Delta E_0 = \frac{1}{4} \sum_{\nu \neq 0} \left| \langle \nu | e \vec{\rho} \cdot \vec{\mathcal{E}}_0(\vec{r}) | 0 \rangle \right|^2 \left(\frac{1}{E_0 - E_\nu - \hbar\omega} + \frac{1}{E_0 - E_\nu + \hbar\omega} \right) . \tag{A.126}$$

The expression (3.25) is recovered from Eq. (A.126) in the case that we have $\omega_\nu \gg \omega_1$ for all $\nu > 1$, which allows us to appproximate the sum within Eq. (A.126) by a single term corresponding to the denominator $E_0 - E_1 + \hbar\omega$.

3.5 In accordance with the assumption that the inner core-shell electrons are not appreciably affected by the atom-atom interaction, we consider the two interacting atoms as being very similar to hydrogen. We therefore permit ourselves to describe each one of those atoms by a two-body system composed of a valence electron, located within an s shell, and an atomic core featuring the screened nuclear charge number $Z = 1$. From the expression (3.33) in combination with Eqs. (3.29)–(3.31), we infer the perturbation operator

$$\begin{aligned} V &= V_{eN}(X_1, \xi_2) + V_{eN}(X_2, \xi_1) + V_{ee}(\xi_1, \xi_2) + V_{NN}(X_1, X_2) \\ &\simeq \frac{e^2}{4\pi\epsilon_0} \left(\frac{1}{|\vec{r}_1 - \vec{r}_2|} + \frac{1}{|\vec{r}_{e,1} - \vec{r}_{e,2}|} - \frac{1}{|\vec{r}_1 - \vec{r}_{e,2}|} - \frac{1}{|\vec{r}_{e,1} - \vec{r}_2|} \right) \end{aligned} \tag{A.127}$$

with respect to the unperturbed situation of two independent neutral atoms, where we assume that electron i is associated with the nucleus i for $i = 1$ and 2.

Performing a Taylor series expansion of the expression (A.127) in the local atomic coordinates $\vec{\rho}_i = \vec{r}_{e,i} - \vec{r}_i \equiv (x_i, y_i, z_i)$ of the electron i yields in lowest nonvanishing order

$$V \simeq \frac{e^2}{4\pi\epsilon_0 r^3} \left(\vec{\rho}_1 \cdot \vec{\rho}_2 - 3 z_1 z_2 \right) \tag{A.128}$$

with $r = |\vec{r}_1 - \vec{r}_2|$, where we set the z axis of our coordinate system parallel to the distance vector $\vec{r}_1 - \vec{r}_2$ of the atoms. This perturbation operator features a vanishing expectation value within the spherically isotropic s state in which the valence electron is located. Furthermore, owing to the quantum defect that is induced by the presence of the core, the energy level of this s state is, for alkali atoms, decreased with respect to the levels

of other states with higher angular momentum $l > 0$ in the same valence shell. Consequently, the impact of the operator V onto the lowest energy level of the two-atom system under consideration has to be evaluated using nondegenerate perturbation theory in second order. This gives rise to an asymptotic scaling $U(r) \simeq -C/r^6$ of the atom-atom interaction energy at large inter-atomic distance r.

3.6 From Eqs. (3.42) and (3.43) we infer

$$d\vec{R} = \frac{1}{2}d\vec{r}_1 + \frac{1}{2}d\vec{r}_2\,, \tag{A.129}$$

$$d\vec{r} = d\vec{r}_1 - d\vec{r}_2\,, \tag{A.130}$$

from which result the two equations

$$\frac{\partial}{\partial\vec{r}_1} = \sum_{j=x,y,z}\left(\frac{\partial R_j}{\partial r_{1,i}}\frac{\partial}{\partial R_j} + \frac{\partial r_j}{\partial r_{1,i}}\frac{\partial}{\partial r_j}\right)\vec{e}_i = \frac{1}{2}\frac{\partial}{\partial\vec{R}} + \frac{\partial}{\partial\vec{r}}\,, \tag{A.131}$$

$$\frac{\partial}{\partial\vec{r}_2} = \sum_{j=x,y,z}\left(\frac{\partial R_j}{\partial r_{2,i}}\frac{\partial}{\partial R_j} + \frac{\partial r_j}{\partial r_{2,i}}\frac{\partial}{\partial r_j}\right)\vec{e}_i = \frac{1}{2}\frac{\partial}{\partial\vec{R}} - \frac{\partial}{\partial\vec{r}}\,. \tag{A.132}$$

We therefore obtain

$$\frac{\partial^2}{\partial\vec{r}_1^{\,2}} = \frac{1}{4}\frac{\partial^2}{\partial\vec{R}^2} + \frac{\partial^2}{\partial\vec{r}^{\,2}} + \frac{1}{2}\frac{\partial^2}{\partial\vec{R}\partial\vec{r}} + \frac{1}{2}\frac{\partial^2}{\partial\vec{r}\partial\vec{R}}\,, \tag{A.133}$$

$$\frac{\partial^2}{\partial\vec{r}_2^{\,2}} = \frac{1}{4}\frac{\partial^2}{\partial\vec{R}^2} + \frac{\partial^2}{\partial\vec{r}^{\,2}} - \frac{1}{2}\frac{\partial^2}{\partial\vec{R}\partial\vec{r}} - \frac{1}{2}\frac{\partial^2}{\partial\vec{r}\partial\vec{R}} \tag{A.134}$$

from which results Eq. (3.45).

3.7 We start from the diagonalization of the Hamiltonian

$$H_0 = -\frac{\hbar^2}{2m_r}\frac{\partial^2}{\partial\vec{r}^{\,2}} = \int d^3k\frac{\hbar^2k^2}{2m_r}|k\rangle\langle k| \tag{A.135}$$

within the eigenbasis of the plane-wave states $\langle\vec{r}|\vec{k}\rangle = (2\pi)^{-3/2}\exp(i\vec{k}\cdot\vec{r})$. The associated retarded Green function is then expressed as

$$G_0(E) = (E - H_0 + i\epsilon)^{-1} = \int d^3k\frac{1}{E - \frac{\hbar^2k^2}{2m_r} + i\epsilon}|k\rangle\langle k| \tag{A.136}$$

in the limit $\epsilon \to 0_+$. Its position representation is therefore obtained as

$$\begin{aligned}\langle\vec{r}|G_0(E)|\vec{r}\,'\rangle &= \frac{1}{(2\pi)^3}\int d^3k\frac{e^{i\vec{k}\cdot(\vec{r}\,'-\vec{r})}}{E - \frac{\hbar^2k^2}{2m_r} + i\epsilon} \\ &= -\frac{m_r}{4\pi^3\hbar^2}\int d^3k\frac{e^{i\vec{k}\cdot(\vec{r}\,'-\vec{r})}}{k^2 - k_E^2 - i\delta}\end{aligned} \tag{A.137}$$

with $k_E = \sqrt{2m_r E}/\hbar$ and $\delta = 2m_r\epsilon/\hbar^2$.

Using spherical coordinates with the polar angle defined with respect to the $\vec{r}' - \vec{r}$ axis and defining $\rho = |\vec{r} - \vec{r}'|$, we evaluate the integral on the right-hand side of Eq. (A.137) as

$$\begin{aligned}
\langle\vec{r}|G_0(E)|\vec{r}'\rangle &= -\frac{m_r}{4\pi^3\hbar^2}2\pi\int_0^\infty k^2dk\int_0^\pi \sin\theta d\theta\frac{e^{ik|\vec{r}-\vec{r}'|\cos\theta}}{k^2-k_E^2-i\delta} \\
&= -\frac{m_r}{2i\pi^2\hbar^2|\vec{r}-\vec{r}'|}\int_0^\infty \frac{e^{ik|\vec{r}-\vec{r}'|}-e^{-ik|\vec{r}-\vec{r}'|}}{k^2-k_E^2-i\delta}kdk \\
&= -\frac{m_r}{2i\pi^2\hbar^2|\vec{r}-\vec{r}'|}\int_{-\infty}^\infty \frac{ke^{ik|\vec{r}-\vec{r}'|}}{k^2-k_E^2-i\delta}dk \\
&= -\frac{m_r}{2\pi\hbar^2|\vec{r}-\vec{r}'|}\exp\left(i\sqrt{k_E^2+i\delta}|\vec{r}-\vec{r}'|\right) \qquad \text{(A.138)}
\end{aligned}$$

using, in the last step, the residue theorem. In the limit $\delta \to 0_+$ we obtain

$$\langle\vec{r}|G_0(E)|\vec{r}'\rangle = -\frac{m_r}{2\pi\hbar^2}\frac{e^{ik_E|\vec{r}-\vec{r}'|}}{|\vec{r}-\vec{r}'|}\,. \qquad \text{(A.139)}$$

3.8 As the wave packet is prepared far away from the origin, we can safely assume that it first evolves freely, without being affected by the presence of the scattering potential. It is therefore possible to identify a time t_0 in the asymptotic past until which the wavefunction is given by the general expression (3.50). We are then concerned with the problem of calculating the solution of the Schrödinger equation (3.49) in the presence of the initial condition (3.50) at $t = t_0$.

This problem can be solved by means of a Laplace transformation. To this end, which we formally rewrite Eq. (3.49) as

$$i\hbar\frac{\partial}{\partial t}|\psi_t\rangle = (H_0 + U)|\psi_t\rangle \qquad \text{(A.140)}$$

with $\langle\vec{r}|\psi_t\rangle = \psi(\vec{r}, t)$ for all $\vec{r}, t$ and the hermitian kinetic an potential energy operators

$$\begin{aligned}
H_0 &= -\frac{\hbar^2}{2m_r}\,, \qquad \text{(A.141)} \\
U &= U(\vec{r})\,. \qquad \text{(A.142)}
\end{aligned}$$

The Laplace transform of the wave vector $|\psi_t\rangle$ is defined as

$$|\tilde{\psi}_E\rangle = \frac{1}{i\hbar}\int_{t_0}^\infty |\psi_t\rangle e^{i(E+i\epsilon)(t-t_0)/\hbar}dt \qquad \text{(A.143)}$$

in terms of a real energy parameter $E \in \mathbb{R}$, where the positive imaginary part $\epsilon > 0$ is needed to enforce the convergence of the integral appearing on the right-hand side of Eq. (A.143). Its associated inverse transform is given by

$$|\psi_t\rangle = \frac{i}{2\pi} \int_{-\infty}^{\infty} |\tilde{\psi}_E\rangle e^{-i(E+i\epsilon)(t-t_0)/\hbar} dE \tag{A.144}$$

for all $t > t_0$. Evaluating

$$\frac{1}{i\hbar} \int_{t_0}^{\infty} \left(i\hbar \frac{\partial}{\partial t} |\psi_t\rangle \right) e^{i(E+i\epsilon)(t-t_0)/\hbar} dt = (E + i\epsilon)|\tilde{\psi}_E\rangle - |\psi_{t_0}\rangle \tag{A.145}$$

through integration by parts, we obtain the Laplace transform of the Schrödinger equation (A.140) as

$$(E - H_0 - U + i\epsilon)\, |\tilde{\psi}_E\rangle = |\psi_{t_0}\rangle\,. \tag{A.146}$$

This equation is formally solved as

$$|\tilde{\psi}_E\rangle = G(E)|\psi_{t_0}\rangle \tag{A.147}$$

where we introduce by

$$G(E) = (E - H_0 - U + i\epsilon)^{-1} \tag{A.148}$$

the retarded Green function associated with the Hamiltonian H_0+U. Defining by

$$G_0(E) = (E - H_0 + i\epsilon)^{-1} \tag{A.149}$$

the Green function of the unperturbed free motion, we have the identity

$$G_0^{-1}(E) = G^{-1}(E) + U \tag{A.150}$$

from which we straightforwardly obtain, by applying the operator $G_0(E)$ onto Eq. (A.150) and by applying the latter onto $G(E)$, the self-consistent *Dyson equation*

$$G(E) = G_0(E) + G_0(E)UG(E) \tag{A.151}$$

that the Green function $G(E)$ has to fulfill.

Considering the initial profile (3.50) of the wavefunction at the time t_0 and making use of the linearity of the Green operator $G(E)$, we can write the sought-after solution of the time evolution problem under consideration as

$$|\psi_t\rangle = \int d^3k\, \alpha(\vec{k}) |\psi_{\vec{k},t}\rangle e^{-iE_k t_0/\hbar} \tag{A.152}$$

with $\langle \vec{r} | \psi_{\vec{k},t_0} \rangle = \exp(i\vec{k} \cdot \vec{r})$ for all $\vec{r}$ and

$$|\psi_{\vec{k},t}\rangle = \frac{i}{2\pi} \int_{-\infty}^{\infty} |\tilde{\psi}_{\vec{k},E}\rangle e^{-i(E+i\epsilon)(t-t_0)/\hbar} dE \tag{A.153}$$

for all $t > t_0$ where the Laplace transformed wave vector $|\tilde{\psi}_{\vec{k},E}\rangle$ satisfies the self-consistent equation

$$|\tilde{\psi}_{\vec{k},E}\rangle = G_0(E)|\psi_{\vec{k},t_0}\rangle + G_0(E)U|\tilde{\psi}_{\vec{k},E}\rangle\,. \tag{A.154}$$

Using the fact that the plane wave $|\psi_{\vec{k},t_0}\rangle$ is an eigenstate of H_0, we evaluate

$$\langle\vec{r}|G_0(E)|\psi_{\vec{k},t_0}\rangle = \frac{e^{i\vec{k}\cdot\vec{r}}}{E - E_k + i\epsilon} \tag{A.155}$$

with $E_k = \hbar^2k^2/(2m_r)$ for all $\vec{r}$. Using furthermore the position representation (A.139) of the unperturbed Green function which was derived in the previous problem, we obtain the position representation of the wave vector $|\tilde{\psi}_{\vec{k},E}\rangle$ as

$$\langle\vec{r}|\tilde{\psi}_{\vec{k},E}\rangle = \frac{1}{E - E_k + i\epsilon}\psi_{\vec{k}}(\vec{r}) \tag{A.156}$$

with the scattering wavefunction $\psi_{\vec{k}}$ satisfying the self-consistent Lippmann-Schwinger equation

$$\psi_{\vec{k}}(\vec{r}) = e^{i\vec{k}\cdot\vec{r}} - \frac{m_r}{2\pi\hbar^2}\int d^3r'\frac{e^{ik|\vec{r}-\vec{r}'|}}{|\vec{r}-\vec{r}'|}U(\vec{r}')\psi_{\vec{k}}(\vec{r}')\,. \tag{A.157}$$

By evaluating the integral on the right-hand side of Eq. (A.153) with the residue theorem, where we take into account the pole at $E = E_k - i\epsilon$ that is introduced through the expression (A.156), we obtain

$$\langle\vec{r}|\psi_{\vec{k},t}\rangle = \psi_{\vec{k}}(\vec{r})e^{-iE_k(t-t_0)/\hbar}\,, \tag{A.158}$$

from which follows

$$\psi(\vec{r},t) = \langle\vec{r}|\psi_t\rangle = \int d^3k\,\alpha(\vec{k})\psi_{\vec{k}}(\vec{r})e^{-iE_kt/\hbar} \tag{A.159}$$

for all $\vec{r}$ and all $t > t_0$.

3.9 To show the validity of Eq. (3.54) for the scattering wavefunction satisfying the Lippmann-Schwinger equation (3.53), we first note that we can write

$$\frac{\partial^2}{\partial\vec{r}^2}\frac{e^{ik|\vec{r}-\vec{r}'|}}{|\vec{r}-\vec{r}'|} = \frac{\partial^2}{\partial\vec{\rho}^2}\frac{e^{ik\rho}}{\rho}\bigg|_{\vec{\rho}=\vec{r}-\vec{r}'} \tag{A.160}$$

for all $\vec{r},\vec{r}'$. By the application of the product rule, we calculate

$$\frac{\partial}{\partial\vec{\rho}}\frac{e^{ik\rho}}{\rho} = \frac{1}{\rho}\frac{\partial}{\partial\vec{\rho}}e^{ik\rho} + e^{ik\rho}\frac{\partial}{\partial\vec{\rho}}\frac{1}{\rho} = \frac{ik\rho - 1}{\rho^3}e^{ik\rho}\vec{\rho} \tag{A.161}$$

and hence

$$\frac{\partial}{\partial\vec{\rho}}\cdot\frac{\partial}{\partial\vec{\rho}}\frac{e^{ik\rho}}{\rho}=\left(\frac{3-2ik\rho}{\rho^3}+\frac{ik\rho-1}{\rho^3}(3+ik\rho)\right)e^{ik\rho}=-k^2\frac{e^{ik\rho}}{\rho} \quad \text{(A.162)}$$

for all $\vec{\rho}\neq 0$. To figure out what happens at the origin, we integrate the Laplacian of $e^{ik\rho}/\rho$ over a sphere S of infinitesimal radius $R\to 0$ centred about the origin. This yields with Gauss's law

$$\iiint_S\frac{\partial^2}{\partial\vec{\rho}^2}\frac{e^{ik\rho}}{\rho}d^3\rho=\oiint_{\partial S}\frac{\partial}{\partial\vec{\rho}}\frac{e^{ik\rho}}{\rho}\cdot d\vec{S}=4\pi(ikR-1)e^{ikR}\overset{R\to 0}{\longrightarrow}-4\pi \quad \text{(A.163)}$$

with $d\vec{S}$ the normal unit vector oriented outside the sphere, from which we infer

$$\frac{\partial^2}{\partial\vec{\rho}^2}\frac{e^{ik\rho}}{\rho}=-k^2\frac{e^{ik\rho}}{\rho}-4\pi\delta(\vec{\rho}) \quad \text{(A.164)}$$

for all $\vec{\rho}$. With this relation, we evaluate

$$-\frac{\hbar^2}{2m_r}\frac{\partial^2}{\partial\vec{r}^2}\psi_{\vec{k}}(\vec{r})=\frac{\hbar^2k^2}{2m_r}\psi_{\vec{k}}(\vec{r})-U(\vec{r})\psi_{\vec{k}}(\vec{r}) \quad \text{(A.165)}$$

for $\psi_{\vec{k}}$ satisfying Eq. (3.53), which proves Eq. (3.54).

3.10 Inserting the expressions (3.57), (3.60), (3.61), and (3.62) into Eq. (3.55) yields

$$\begin{aligned}0 &= \psi_{\vec{k}}(\vec{r})-e^{i\vec{k}\cdot\vec{r}}+\frac{a(\theta)}{r}e^{ikr}\\ &= \sum_{l=0}^{\infty}P_l(\cos\theta)\frac{A_l}{r}\sin(kr-l\pi/2+\delta_l)\\ &\quad -\sum_{l=0}^{\infty}i^l(2l+1)P_l(\cos\theta)\frac{1}{kr}\sin(kr-l\pi/2)+\frac{a(\theta)}{r}e^{ikr}\\ &= \frac{1}{r}\left(\mathcal{A}e^{ikr}+\mathcal{B}e^{-ikr}\right) \quad \text{(A.166)}\end{aligned}$$

with

$$\mathcal{A} = \frac{1}{2i}\sum_{l=0}^{\infty}P_l(\cos\theta)\left(A_le^{i\delta_l}-\frac{i^l}{k}(2l+1)\right)e^{-il\pi/2}+a(\theta)\,, \quad \text{(A.167)}$$

$$\mathcal{B} = -\frac{1}{2i}\sum_{l=0}^{\infty}P_l(\cos\theta)\left(A_le^{-i\delta_l}-\frac{i^l}{k}(2l+1)\right)e^{il\pi/2}\,. \quad \text{(A.168)}$$

As Eq. (A.166) has to be valid for all r, we must have $\mathcal{A}=\mathcal{B}=0$. We infer from the expression (A.168)

$$A_l=\frac{i^l}{k}(2l+1)e^{i\delta_l} \quad \text{(A.169)}$$

for all $l \in \mathbb{N}_0$. Inserting this result into the expression (A.167) then yields

$$a(\theta) = -\frac{1}{k}\sum_{l=0}^{\infty}(2l+1)\sin\delta_l e^{i\delta_l}P_l(\cos\theta)\,. \tag{A.170}$$

3.11 We start from the radial Schrödinger equation (3.58) which is rewritten as

$$-\chi_l''(r) + \frac{l(l+1)}{r^2}\chi_l(r) + \frac{2m_r}{\hbar^2}u(r)\chi_l(r) = k^2\chi_l(r)\,. \tag{A.171}$$

As we have the scaling $u(r) \sim -r^{-n}$ with $n > 3$ for large $r \to \infty$, we can define a characteristic length scale

$$r_1 = \lim_{r\to\infty}\left(-\frac{2m_r}{\hbar^2}u(r)r^n\right)^{1/(n-2)} \tag{A.172}$$

such that we can approximate

$$\frac{2m_r u(r)}{\hbar^2} \simeq -\frac{r_1^{n-2}}{r^n} \tag{A.173}$$

for large r. The limit $k \to 0$ allows us to introduce another length scale r_2 satisfying $r_1 \ll r_2 \ll k^{-1}$, which is such that we can justify to perform the approximation (A.173) within Eq. (A.171) for $r > r_2$, while for $r < r_2$ the right-hand side of Eq. (A.171) can safely be set to zero.

We therefore can approximate the radial Schrödinger equation (A.171) as

$$-\chi_l''(r) + \frac{l(l+1)}{r^2}\chi_l(r) + \frac{2m_r}{\hbar^2}u(r)\chi_l(r) = 0 \tag{A.174}$$

for $0 < r \leq r_2$. Its solution is, in the presence of the boundary condition $\chi_l(0) = 0$, uniquely defined up to a global prefactor. As the wave number k does not appear within Eq. (A.174), any nontrivial dependence of χ_l on k must be contained within this prefactor, *i.e.*, such that we have the factorization $\chi_l(r) = C_l(k)\tilde{\chi}_l(r)$ with a k-dependent constant $C_l(k)$ and a function $\tilde{\chi}_l$ that is independent of k. Treating the right-hand side of Eq. (A.171) in a perturbative manner gives rise to first-order correction terms to this function $\tilde{\chi}_l$ which logically scale quadratically with k.

For $r \geq r_2$, on the other hand, we can approximate the radial Schrödinger equation (A.171) as

$$-\chi_l''(r) + \frac{l(l+1)}{r^2}\chi_l(r) - \frac{r_1^{n-2}}{r^n}\chi_l(r) = k^2\chi_l(r)\,. \tag{A.175}$$

Noting that we have $r_1 \ll r$ for all values of r for which this equation is defined, we can employ a perturbative approach to solve Eq. (A.175),

where we treat the asymptotic tail of the scattering potential as a weak perturbation to the free radial equation

$$-\chi_l''(r) + \frac{l(l+1)}{r^2}\chi_l(x) = k^2\chi_l(r)\,. \tag{A.176}$$

The general solution of this free radial equation is straightforwardly written as the linear combination

$$\chi_l(r) = \mathcal{C}_l\phi_{l+}(kr) + \mathcal{S}_l\phi_{l-}(kr) \tag{A.177}$$

of the two functions

$$\phi_{l+}(x) = xj_l(x)\,, \tag{A.178}$$
$$\phi_{l-}(x) = xy_l(x) \tag{A.179}$$

that are defined in terms of the spherical Bessel functions j_l and y_l. Owing to the well-known properties of those Bessel functions, we infer the asymptotic behaviour

$$\phi_{l+}(x) \simeq \sin(x - l\pi/2)\,, \tag{A.180}$$
$$\phi_{l-}(x) \simeq -\cos(x - l\pi/2) \tag{A.181}$$

for $x \to \infty$ as well as

$$\phi_{l+}(x) \simeq \frac{x^{l+1}}{(2l+1)!!}\left(1 - \frac{x^2}{4l+6} + O(x^4)\right)\,, \tag{A.182}$$
$$\phi_{l-}(x) \simeq -\frac{(2l-1)!!}{x^l}\left(1 + \frac{x^2}{4l-2} + O(x^4)\right) \tag{A.183}$$

for $x \to 0$ where we define $(2n+1)!! = (2n+1)(2n-1)\cdots 3\cdot 1$ for all $n \in \mathbb{N}_0$. Since we aim to asymptotically match the expression (3.60) of the radial wavefunction, such that we have $\chi_l(r) = A_l \sin(kr - l\pi/2 + \delta_l)$ for large r, we set $\mathcal{C}_l = A_l\cos\delta_l$ and $\mathcal{S}_l = -A_l\sin\delta_l$ within Eq. (A.177).

Our aim is now to refine the expressions (A.182) and (A.183) such that those two solutions account for the presence of the asymptotic tail of the scattering potential in a perturbative manner. This task can be achieved via the self-consistent equation

$$\chi_l(r) = \phi_{l\pm}(kr)\left(1 - (kr_1)^{n-2}\int_{kr}^1 \frac{dx}{\phi_{l\pm}^2(x)}\int_x^1 \frac{\phi_{l\pm}(x')}{x'^n}\chi_l(x')dx'\right) \tag{A.184}$$

that the solution of Eq. (A.175) has to satisfy if we require that it should match $\phi_{l\pm}(kr)$ for $kr = 1$. We here assume that the presence of the perturbative term $\propto r^{-n}$ within Eq. (A.175) can be strictly neglected for $kr \geq 1$

(which is certainly valid in the limit $k \to 0$) and use the fact that the spherical Bessel functions $j_l(x)$ and $y_l(x)$ do not exhibit a zero within $0 < x \leq 1$. The integral equation (A.184) can be iteratively solved by successively inserting more and more refined approximations for χ_l on its right-hand side. In linear order in the perturbation, we thereby obtain the refinements

$$\tilde{\phi}_{l\pm}(x) = \phi_{l\pm}(x) \left(1 - (kr_1)^{n-2} \int_x^1 \frac{dx'}{\phi_{l\pm}^2(x')} \int_{x'}^1 \frac{\phi_{l\pm}^2(x'')}{x''^n} dx'' \right) \tag{A.185}$$

for the two approximate solutions ϕ_{l+} and ϕ_{l-}.

It is worthwhile to investigate the scaling of those two refined approximations in the limit of small x. We first note, by virtue of Eqs. (A.182) and (A.183), that the unperturbed solutions scale for small x as $\phi_{l\pm}(x) \propto \pm x^{\nu_{l\pm}}$ with the exponents $\nu_{l+} = l+1$ and $\nu_{l-} = -l$. The integrand of the inner integral on the right-hand side of Eq. (A.185) therefore scales as $\propto (x'')^{2\nu_{l\pm}-n}$ for small x''. This implies that this inner integral diverges as $\propto (x')^{2\nu_{l\pm}-n+1}$ for small x' if $2\nu_{l\pm} < n-1$, while it gives rise to a finite expression for $x' \to 0$ if $2\nu_{l\pm} \geq n$ and to a logarithmic scaling $\propto \ln(x')$ if $2\nu_{l\pm} = n-1$. As the denominator in the integrand of the outer integral contributes an additional factor $\propto (x')^{-2\nu_{l\pm}}$ for small x', we obtain for this outer integral the scaling $\propto x^{-n+2}$ if $2\nu_{l\pm} < n-1$, $\propto x^{-2\nu_{l\pm}+1}$ if $2\nu_{l\pm} \geq n$, as well as $\propto -x^{-n+2} \ln x$ for the special case $2\nu_{l\pm} = n-1$.

Hence, since we have $2\nu_{l-} = -2l < n-1$, we can approximately rewrite the expression (A.185) for $\tilde{\phi}_{l-}$ as

$$\tilde{\phi}_{l-}(kr) \simeq \phi_{l-}(kr) \left[1 - C(r_1/r)^{n-2} \right] \tag{A.186}$$

for small $kr \ll 1$, with a constant $C > 0$ that is independent of k. Since we have $r_1 \ll r_2 \leq r$, the perturbative correction to the unperturbed expression (A.183) can safely be neglected. We can therefore rely on the approximation $\tilde{\phi}_{l-}(kr) \simeq \phi_{l-}(kr)$ for all $r \geq r_2$. Analogous conclusions are drawn for $\tilde{\phi}_{l+}$ if we have $2\nu_{l+} = 2l+2 < n-1$. As for $\tilde{\phi}_{l-}$, we obtain for small $kr \ll 1$

$$\tilde{\phi}_{l+}(kr) \simeq \phi_{l+}(kr) \left[1 - C(r_1/r)^{n-2} \right] , \tag{A.187}$$

with a constant $C > 0$ that is independent of k. Since we have $r_1 \ll r_2 \leq r$, we are therefore entitled to approximate $\tilde{\phi}_{l+}(kr) \simeq \phi_{l+}(kr)$ for all $r \geq r_2$.

Consequently, provided we have $2l+3 < n$, the solution (A.177) can be approximated as

$$\chi_l(r) \simeq A_l \left(\frac{\cos\delta_l}{(2l+1)!!} (kr)^{l+1} + (2l-1)!! \frac{\sin\delta_l}{(kr)^l} \right) \tag{A.188}$$

for $r_2 \leq r \ll k^{-1}$. This behaviour has to be matched at $r = r_2$ with the solution of the Schrödinger equation (A.174). As was pointed out above,

the latter solution can feature a dependence on k only within its global prefactor. Hence, we need to have $\tan\delta_l \propto (kr_2)^{2l+1}$ in order for the expression (A.188) to match the solution of Eq. (A.174), from which follows $\delta_l \propto k^{2l+1}$ in the limit $kr_2 \to 0$.

The situation is fundamentally different, however, if $2l+3 > n$. Going one level beyond the leading-order evaluation of Eq. (A.185), we obtain, in that case, from the above considerations the approximate expression

$$\begin{aligned}\tilde{\phi}_{l+}(kr) &\simeq \phi_{l+}(kr)\left[1 - C\frac{(kr_1)^{n-2}}{(kr)^{2l+1}}\left(1 + c_l(kr)^2\right)\right] \\ &\simeq \frac{\mathcal{C}_l}{(2l+1)!!}\left[(kr)^{l+1} - C\frac{(kr_1)^{n-2}}{(kr)^l}\left(1 + c_l(kr)^2\right)\right] \qquad \text{(A.189)}\end{aligned}$$

for small $kr \ll 1$, with a constant $C > 0$ that is independent of k and with $c_l = (2l+1)/[(2l+3)(2l-1)]$. As we have $2l+3 > n$, the second term on the right-hand side of Eq. (A.189) becomes more important than the first term in the formal limit $k \to 0$. We therefore evaluate Eq. (A.177) as

$$\begin{aligned}\chi_l(r) &\simeq \frac{A_l}{(kr)^l}(2l-1)!!\sin\delta_l\left(1 + \frac{(kr)^2}{4l-2}\right) \\ &\quad - \frac{A_l}{(kr)^l}\frac{C\cos\delta_l}{(2l+1)!!}(kr_1)^{n-2}\left(1 + c_l(kr)^2\right) \qquad \text{(A.190)}\end{aligned}$$

for $r_2 \leq r \ll k^{-1}$, where we account for the leading corrections in $(kr)^2$. Noting that first-order corrections to the zeroth order expression of the scattering wavefunction must scale as k^2 while any other nontrivial dependence on k must be contained within a global prefactor, we find that we must have the scaling $\delta_l \simeq \tan\delta_l \propto k^{n-2}$ in the limit $k \to 0$.

The above reasoning can effectively be maintained for $2l+3 = n$. In that case, the constant C appearing within Eq. (A.187) has to be amended by a logarithmic prefactor, namely such that we have

$$\tilde{\phi}_{l+}(kr) \simeq \phi_{l+}(kr)\left[1 + C(r_1/r)^{n-2}\ln(kr)\right], \qquad \text{(A.191)}$$

with $C > 0$ being independent of k. Hence, in the formal limit $k \to 0$ while keeping r_2/r_1 constant, the second term on the right-hand side of Eq. (A.191) becomes therefore more important than the first one, and we obtain for Eq. (A.177) the approximation

$$\chi_l(r) \simeq \frac{A_l}{(kr)^l}\left((2l-1)!!\sin\delta_l + \frac{C\cos\delta_l}{(2l+1)!!}(kr_1)^{n-2}\ln(kr)\right) \qquad \text{(A.192)}$$

for $r_2 \leq r \ll k^{-1}$. Since the logarithmic prefactor $\ln(kr)$ is of minor importance as compared to the power law $\propto k^{n-2}$, we obtain again the scaling $\delta_l \propto k^{2l+1} = k^{n-2}$ for this particular case.

It remains to be verified to which extent the above findings remain valid when going to higher iteration orders in the perturbative solution of the self-consistent equation (A.184). This consideration specifically concerns $\tilde{\phi}_{l+}$ in the case $2l+3 \geq n$, for which it was found that the "perturbative" correction term, scaling as $\propto k^{n-l-2}$ in Eq. (A.189), becomes more important than the "unperturbed" term, scaling as $\propto k^{l+1}$ for small k. To this end, we insert the refined expression (A.189) for $\tilde{\phi}_{l+}$ into the right-hand side of Eq. (A.184) in order to thereby obtain an even better approximation for this particular solution of the differential equation (A.175). As we have $\tilde{\phi}_{l+}(x) \propto x^{-l}$ for small x in the case $2l+3 \geq n$, amended by the logarithmic prefactor $\ln(x)$ in the special case $2l+3 = n$, it can be straightforwardly shown that the resulting second-order corrections to the expression (A.189) are of negligible importance and do not alter the scaling law $\delta_l \propto k^{n-2}$ in that case.

3.12 The radial Schrödinger equation (3.58) for $l = 0$ in the presence of the piecewise constant potential is solved through the general ansatz

$$\chi_0(r) = \begin{cases} B_0 \sin(\kappa_k r) & : r < r_0 \\ A_0 \sin(kr - \delta_0) & : r > r_0 \end{cases} \tag{A.193}$$

with

$$\kappa_k = \sqrt{k^2 + 2m_r U_0/\hbar^2}\,, \tag{A.194}$$

where we already account for the boundary condition $\chi_0(0) = 0$ as well as for the definition of the s-wave scattering phase δ_0. At $r = r_0$ both χ_0 and its first derivative χ_0' have to be continuous. This yields the two equations

$$B_0 \sin(\kappa_k r_0) = A_0 \sin(kr_0 - \delta_0)\,, \tag{A.195}$$

$$\kappa_k B_0 \cos(\kappa_k r_0) = k A_0 \cos(kr_0 - \delta_0)\,. \tag{A.196}$$

From Eq. (A.195) we obtain $B_0 = \alpha_k A_0$ with α_k being defined by Eq. (3.75). Dividing Eq. (A.195) through Eq. (A.196) yields the relation

$$\frac{1}{\kappa_k} \tan(\kappa_k r_0) = \frac{1}{k} \tan(kr_0 - \delta_0) \tag{A.197}$$

which is solved for δ_0 as

$$\delta_0 = kr_0 - \arctan\left[\frac{k}{\kappa_k} \tan(\kappa_k r_0)\right] \tag{A.198}$$

in accordance with Eq. (3.77).

3.13 (a) We calculate for this purpose the partial Fourier transform of the

Lippmann-Schwinger equation (3.94), yielding

$$\begin{aligned}\int d^3r' T_k(\vec{r},\vec{r}\,')e^{i\vec{k}\cdot\vec{r}\,'} &= U(\vec{r})e^{i\vec{k}\cdot\vec{r}} - \frac{m_r U(\vec{r})}{2\pi\hbar^2}\int d^3r'' \frac{e^{ik|\vec{r}-\vec{r}\,''|}}{|\vec{r}-\vec{r}\,''|} \\ &\quad \times \int d^3r' T_k(\vec{r}\,'',\vec{r}\,')e^{i\vec{k}\cdot\vec{r}\,'} \\ &= U(\vec{r})\psi_{\vec{k}}(\vec{r}) \qquad \text{(A.199)}\end{aligned}$$

according to the definition (3.95). Hence, Eq. (3.95) can be rewritten as

$$\psi_{\vec{k}}(\vec{r}) = e^{i\vec{k}\cdot\vec{r}} - \frac{m_r}{2\pi\hbar^2}\int d^3r'' \frac{e^{ik|\vec{r}-\vec{r}\,''|}}{|\vec{r}-\vec{r}\,''|} U(\vec{r}\,'')\psi_{\vec{k}}(\vec{r}\,'')\,, \qquad \text{(A.200)}$$

which is identical to the Lippmann-Schwinger equation (3.53) for the scattering wavefunction.

(b) We approach this problem via the Born series for the T matrix, yielding

$$T_k(\vec{r},\vec{r}\,') = \lim_{n\to\infty} T_k^{(n)}(\vec{r},\vec{r}\,') \qquad \text{(A.201)}$$

where we iteratively define

$$\begin{aligned}T_k^{(0)}(\vec{r},\vec{r}\,') &= u(r)\delta(\vec{r}-\vec{r}\,')\,, \qquad \text{(A.202)} \\ T_k^{(n)}(\vec{r},\vec{r}\,') &= -\frac{m_r u(r)}{2\pi\hbar^2}\int d^3r'' \frac{e^{ik|\vec{r}-\vec{r}\,''|}}{|\vec{r}-\vec{r}\,''|} T_k^{(n-1)}(\vec{r}\,'',\vec{r}\,') \qquad \text{(A.203)}\end{aligned}$$

for all $n > 0$. We straightforwardly verify $\int u(r)\vec{r}\,d^3r = 0$ for the spherically symmetric scattering potential and hence have

$$\int d^3r \int d^3r' T_k^{(0)}(\vec{r},\vec{r}\,')\vec{r} = \int d^3r \int d^3r' T_k^{(0)}(\vec{r},\vec{r}\,')\vec{r}\,' = 0\,. \qquad \text{(A.204)}$$

Suppose now that $T_k^{(n-1)}$ satisfies the property (3.97). for some $n > 0$. Via Eq. (A.203) we can then directly infer

$$\int d^3r \int d^3r' T_k^{(n)}(\vec{r},\vec{r}\,')\vec{r}\,' = 0 \qquad \text{(A.205)}$$

and hence prove the identity (3.97) for the T matrix. The analogous identity (3.96) will be proven by showing that the functions

$$U_k^{(n)}(\vec{r}) = \int d^3r' T_k^{(n)}(\vec{r},\vec{r}\,') \qquad \text{(A.206)}$$

are spherically symmetric, *i.e.*, depend only on the radius $r = |\vec{r}|$. This is trivially the case for $n = 0$ where we have $U_k^{(0)}(\vec{r}) = u(r)$. Assuming

spherical symmetry for $U_k^{(n-1)}$, *i.e.* $U_k^{(n-1)}(\vec{r}) \equiv u_k^{(n-1)}(r)$, we calculate, using Eq. (A.203) and employing spherical coordinates,

$$\begin{aligned} U_k^{(n)}(\vec{r}) &= -\frac{m_r u(r)}{2\pi\hbar^2} \int d^3r' \frac{e^{ikr'}}{r'} u_k^{(n-1)}(|\vec{r}-\vec{r}\,'|) \\ &= -\frac{m_r u(r)}{\hbar^2} \int_{-1}^{1} d\eta \int_0^\infty r' dr' u_k^{(n-1)} \left(\sqrt{r^2 + r'^2 - 2rr'\eta} \right) e^{ikr'} \\ &\equiv u_k^{(n)}(r)\,, \end{aligned} \tag{A.207}$$

i.e., we obtain spherical symmetry for $U_k^{(n)}$. This then proves the identity (3.96).

(c) In leading order in $1/r$, using

$$\frac{e^{ik|\vec{r}-\vec{r}\,'|}}{|\vec{r}-\vec{r}\,'|} = \frac{e^{ikr}}{r} e^{-ik\vec{e}_r\cdot\vec{r}\,'} \left(1 + O(r'/r)\right)\,, \tag{A.208}$$

the scattering wavefunction (3.95) is asymptotically evaluated as

$$\psi_{\vec{k}}(\vec{r}) = e^{i\vec{k}\cdot\vec{r}} - \frac{m_r}{2\pi\hbar^2} \frac{e^{ikr}}{r} \int d^3r' \int d^3r'' T_k(\vec{r}\,', \vec{r}\,'') e^{-ik\vec{e}_r\cdot\vec{r}\,'} e^{i\vec{k}\cdot\vec{r}\,''}\,. \tag{A.209}$$

A comparison with Eq. (3.55) yields the expression

$$a(\theta) = \frac{m_r}{2\pi\hbar^2} \int d^3r \int d^3r' T_k(\vec{r}, \vec{r}\,') e^{-ik\vec{e}_r\cdot\vec{r}\,'} e^{i\vec{k}\cdot\vec{r}\,''} \tag{A.210}$$

for the scattering amplitude as a function of the T matrix, which is in principle valid for any k. Using the Taylor series expansion

$$e^{-ik\vec{e}_r\cdot\vec{r}\,'} e^{i\vec{k}\cdot\vec{r}\,''} = 1 - ik\vec{e}_r\cdot\vec{r}\,' + i\vec{k}\cdot\vec{r}\,'' + O(k^2) \tag{A.211}$$

as well as the properties (3.96) and (3.97) shown in the previous exercise, we obtain the statement of Eq. (3.98).

(d) Equation (3.100) is straightforwardly shown by evaluating Eq. (3.98) in the limit $k \to 0$. To prove the scaling of linear corrections in k, we formally solve the Lippmann-Schwinger equation (3.94) in terms of the Born series via the introduction of the operators $\hat{T}_k$, $\hat{U}$, and $\hat{G}_k$ whose matrix elements in position space are given by

$$\langle\vec{r}|\hat{T}_k|\vec{r}\,'\rangle = T_k(\vec{r}, \vec{r}\,')\,, \tag{A.212}$$

$$\langle\vec{r}|\hat{U}|\vec{r}\,'\rangle = U(\vec{r})\delta(\vec{r}-\vec{r}\,')\,, \tag{A.213}$$

$$\langle\vec{r}|\hat{G}_k|\vec{r}\,'\rangle = -\frac{m_r}{2\pi\hbar^2} \frac{e^{ik|\vec{r}-\vec{r}\,'|}}{|\vec{r}-\vec{r}\,'|}\,. \tag{A.214}$$

Equation (3.94) is then rewritten and formally solved as

$$\hat{T}_k = \hat{U} + \hat{U}\hat{G}_k\hat{T}_k = \hat{U}\sum_{n=0}^{\infty}\left(\hat{G}_k\hat{U}\right)^n . \tag{A.215}$$

We now perform a Taylor series expansion $\hat{G}_k = \hat{G}_0 + k\hat{G}_0' + O(k^2)$ of the Green operator, with

$$\langle\vec{r}|\hat{G}_0|\vec{r}\,'\rangle = -\frac{m_r}{2\pi\hbar^2|\vec{r}-\vec{r}\,'|}\,, \tag{A.216}$$

$$\langle\vec{r}|\hat{G}_0'|\vec{r}\,'\rangle = -\frac{im_r}{2\pi\hbar^2}\,. \tag{A.217}$$

The corresponding Taylor series expansion of the T matrix is then written as $\hat{T}_k = \hat{T}_0 + k\hat{T}_0' + O(k^2)$, where we obtain from Eq. (A.215)

$$\hat{T}_0 = \hat{U}\sum_{n=0}^{\infty}\left(\hat{G}_0\hat{U}\right)^n , \tag{A.218}$$

$$\begin{aligned}\hat{T}_0' &= \hat{U}\sum_{n=1}^{\infty}\sum_{l=0}^{n-1}\left(\hat{G}_0\hat{U}\right)^l\hat{G}_0'\hat{U}\left(\hat{G}_0\hat{U}\right)^{n-l-1}\\ &= \hat{T}_0\hat{G}_0'\hat{T}_0\,.\end{aligned} \tag{A.219}$$

Using Eq. (A.217), this yields the relation

$$\begin{aligned}\int d^3r\int d^3r'T_0'(\vec{r},\vec{r}\,') &= -\frac{im_r}{2\pi\hbar^2}\left(\int d^3r\int d^3r'T_0(\vec{r},\vec{r}\,')\right)^2\\ &= -\frac{2\pi i\hbar^2a_s^2}{m_r}\end{aligned} \tag{A.220}$$

with the expression (3.100) for the s-wave scattering length. Hence, we obtain from Eq. (3.98)

$$\begin{aligned}a(\theta) &= \frac{m_r}{2\pi\hbar^2}\int d^3r\int d^3r'\left[T_0(\vec{r},\vec{r}\,') + kT_0'(\vec{r},\vec{r}\,')\right] + O(k^2)\\ &= a_s - ika_s^2 + O(k^2)\,.\end{aligned} \tag{A.221}$$

3.14 Let us first calculate the Fourier transform of the function $f(\vec{k}) = k^{-2}$. Using spherical coordinates, this integration yields

$$\begin{aligned}\int d^3k\frac{e^{i\vec{k}\cdot\vec{r}}}{k^2} &= 2\pi\int_0^{\infty}dk\int_0^{\pi}\sin\theta d\theta e^{ikr\cos\theta} = 4\pi\int_0^{\infty}\frac{\sin kr}{kr}dk\\ &= \frac{2\pi^2}{r}\,.\end{aligned} \tag{A.222}$$

Using $g_k = \int u(r) e^{i\vec{k}\cdot\vec{r}} d^3r = \int u(r') e^{-i\vec{k}\cdot\vec{r}'} d^3r'$, we can now calculate

$$\begin{aligned} \int \frac{g_k^2}{k^2} d^3k &= \int d^3r u(r) \int d^3r' u(r') \int d^3k \frac{e^{i\vec{k}\cdot(\vec{r}-\vec{r}')}}{k^2} \\ &= 2\pi^2 \int d^3r \int d^3r' \frac{u(r)u(r')}{|\vec{r}-\vec{r}'|} = \frac{2\pi^2 g^2}{\rho}\,, \end{aligned} \tag{A.223}$$

from which follows Eq. (3.101).

Problems of Chapter 4

4.1 Inserting the D-dimensional ansatz (4.38) into Eq. (4.7) yields

$$E_{\rm GP}[\psi_0] = E_\perp + \int d^D r \left[\psi_0^*(\mathbf{r}) \left(-\frac{\hbar^2}{2m} \frac{\partial^2}{\partial \mathbf{r}^2} + V(\mathbf{r}) \right) \psi_0(\mathbf{r}) + \frac{g_D}{2} |\psi_0(\mathbf{r})|^4 \right] \tag{A.224}$$

with $E_\perp = (3-D)\hbar\omega_\perp/2$ the ground-state energy of a $(3-D)$ dimensional isotropic harmonic oscillator with the frequency $\omega_\perp$ and

$$g_D = g \prod_{j=D+1}^{3} \int dr_j |\chi_\perp(r_j)|^4 \,. \tag{A.225}$$

Using the well-known expression

$$\chi_\perp(r) = \pi^{-1/4} a_\perp^{-1/2} e^{-r^2/(2a_\perp^2)} \tag{A.226}$$

for the ground-state wavefunction of a one-dimensional harmonic oscillator with the oscillator length $a_\perp = \sqrt{\hbar/(m\omega_\perp)}$, we evaluate

$$\int dr |\chi_\perp(r)|^4 = \frac{1}{\sqrt{2\pi} a_\perp} \tag{A.227}$$

and thus obtain

$$g_D = \frac{g}{(\sqrt{2\pi} a_\perp)^{(3-D)}} \,. \tag{A.228}$$

Equations (4.40) and (4.41) result then from inserting $g = 4\pi\hbar^2 a_s/m$ into the above expression.

4.2 While it can be straightforwardly shown, through derivations of the tanh function, that the expression (4.14) satisfies the one-dimensional Gross-Pitaevskii equation (4.13), we proceed here via an explicit integration of Eq. (4.13), also in order to show that Eq. (4.14) is the unique solution if the boundary conditions $\psi_0(0) = 0$ and $\lim_{z\to\infty} \psi_0(z) = \sqrt{n} = \sqrt{(\mu - V_0)/g}$

are imposed. To this end, let us introduce a dimensionless condensate wavefunction χ_0 through

$$\psi_0(z) \equiv \sqrt{n}\chi_0(z/\xi) \tag{A.229}$$

for all z. Equation (4.13) is then equivalent to

$$-\chi_0''(\zeta) + \chi_0^3(\zeta) = \chi_0(\zeta)\,. \tag{A.230}$$

Multiplying this equation with $2\chi'(\zeta)$ and integrating it over ζ yields

$$-[\chi_0'(\zeta)]^2 + \chi_0^4(\zeta)/2 = \chi_0^2(\zeta) - C\,, \tag{A.231}$$

where the constant resulting from this first integral has to be set to $C = 1/2$ in order to fulfill the asymptotic boundary condition $\chi_0(\zeta) \stackrel{\zeta\to\infty}{=} 1$. We then have

$$[\chi_0'(\zeta)]^2 = \frac{1}{2}\left[1 - \chi_0^2(\zeta)\right]^2 \tag{A.232}$$

from which follows

$$\chi_0'(\zeta) = \pm\frac{1}{\sqrt{2}}\left[1 - \chi_0^2(\zeta)\right]\,. \tag{A.233}$$

Using the other boundary condition $\chi_0(0) = 0$ and taking into account only the upper sign (without loss of generality since the opposite choice would only yield a sign change in the condensate wavefunction), this latter first-order differential equation is readily integrated yielding

$$\zeta = \int_0^{\chi_0(\zeta)} \frac{\sqrt{2}}{1-x^2}dx = \frac{1}{\sqrt{2}}\ln\left(\frac{1+\chi_0(\zeta)}{1-\chi_0(\zeta)}\right)\,. \tag{A.234}$$

Solving this equation for $\chi_0(\zeta)$ yields

$$\chi_0(\zeta) = \tanh(\zeta/\sqrt{2})\,, \tag{A.235}$$

from which Eq. (4.14) can be inferred.

4.3 As in the case of the previous problem, we introduce a dimensionless condensate wavefunction χ_0 through

$$\psi_0(z) \equiv \sqrt{n}\chi_0(z/\tilde{\xi}) \tag{A.236}$$

for all z. Equation (4.13) is then equivalent to

$$-\chi_0''(\zeta) - \chi_0^3(\zeta) + \chi_0(\zeta) = 0\,. \tag{A.237}$$

A first integral of this second-order differential equation, after multiplication with $2\chi_0'(\zeta)$, yields

$$-[\chi_0'(\zeta)]^2 - \chi_0^4(\zeta)/2 + \chi_0^2(\zeta) = C \tag{A.238}$$

with an integration constant C that has to vanish if χ_0 is square-integrable and thus fulfills $\lim_{\zeta\to\pm\infty}\chi_0(\zeta)=0$. Setting $C=0$, we obtain

$$\chi_0'(\zeta)=\pm\chi_0(\zeta)\sqrt{1-\chi_0^2(\zeta)/2}\,. \tag{A.239}$$

We infer that $|\chi_0(\zeta)|$ attains a local and global maximum with the value $\sqrt{2}$ and that only the lower (minus) sign allows for a real-valued solution of the above equation. Assuming, without loss of generality, χ_0 to be strictly positive, Eq. (A.239) is solved via

$$\zeta-\zeta_0=\int_{1/\chi_0(\zeta_0)}^{1/\chi_0(\zeta)}\frac{dx}{x\sqrt{1-x^2/2}}=\operatorname{arcosh}\frac{\sqrt{2}}{\chi_0(\zeta)}-\operatorname{arcosh}\frac{\sqrt{2}}{\chi_0(\zeta_0)}\,. \tag{A.240}$$

Identifying ζ_0 with the global maximum of χ_0, *i.e.*, $\chi_0(\zeta_0)=\sqrt{2}$, we finally obtain

$$\chi_0(\zeta)=\frac{\sqrt{2}}{\cosh(\zeta-\zeta_0)}\,, \tag{A.241}$$

from which follows Eq. (4.42).

4.4 The scaling of the chemical potential μ with the population N of the condensate is determined from the normalization condition $\int d^Dr\, n(\mathbf{r})=N$, where the Thomas-Fermi approximation for the density is given by

$$n(\mathbf{r})=\begin{cases}\dfrac{1}{g_D}\left(\mu-\displaystyle\sum_{j=1}^{D}\frac{1}{2}m\omega_j^2r_j^2\right) & : \quad \mu>\sum_{j=1}^{D}\frac{1}{2}m\omega_j^2r_j^2\\ 0 & : \quad \text{otherwise}\end{cases}\,. \tag{A.242}$$

Performing the change of integration variables $r_j\mapsto\rho_j=\sqrt{m/\mu}\omega_jr_j$, the normalization condition is evaluated as

$$N=\frac{\mu}{g_D}\sqrt{\frac{\mu}{m}}^D\bar{\omega}^D\mathcal{I} \tag{A.243}$$

with

$$\begin{aligned}\mathcal{I} &= \int d^D\rho\left(1-\frac{1}{2}\sum_{j=1}^{D}\rho_j^2\right)\theta\left(1-\frac{1}{2}\sum_{j=1}^{D}\rho_j^2\right)\\ &= \Omega(D-1)\int_0^{\sqrt{2}}(1-\rho^2/2)\rho^{D-1}d\rho=\frac{2^{D/2+1}\Omega(D-1)}{D(D+2)}\end{aligned} \tag{A.244}$$

where

$$\Omega(D-1)=\frac{2\pi^{D/2}}{\Gamma(D/2)} \tag{A.245}$$

is the area of the unit sphere in the D-dimensional space. This yields

$$N = \frac{4\sqrt{2\pi}^D}{D(D+2)\Gamma(D/2)} \frac{\mu^{1+D/2}}{g_D(m\bar{\omega}^2)^{D/2}}\,, \tag{A.246}$$

from which follows

$$\mu = \left(\frac{1}{4}D(D+2)\Gamma(D/2)Ng_D\right)^{2/(2+D)} \left(\frac{m\bar{\omega}^2}{2\pi}\right)^{D/(2+D)}\,. \tag{A.247}$$

Particularizing for $D = 1$, 2, and 3 respectively yields

$$N = \frac{4}{3}\frac{\mu^{3/2}}{g_1\sqrt{m\bar{\omega}^2/2}}\,, \tag{A.248}$$

$$N = \frac{\pi\mu^2}{g_2 m\bar{\omega}^2}\,, \tag{A.249}$$

$$N = \frac{8\pi}{15}\frac{\mu^{5/2}}{g_3(m\bar{\omega}^2/2)^{3/2}}\,, \tag{A.250}$$

from which follow Eqs. (4.45)–(4.47).

4.5 We start by defining dimensionless coordinates $\vec{\rho} = \vec{r}/a$, a dimensionless chemical potential $\tilde{\mu} = 2ma^2\mu/\hbar^2$, and a dimensionless condensate wavefunction

$$\chi(\vec{\rho}) = \sqrt{\frac{2mga^2}{\hbar^2}}\psi(a\vec{\rho})\,. \tag{A.251}$$

Using

$$\Delta\psi(\vec{r}) = \frac{1}{a^2}\sqrt{\frac{\hbar^2}{2mga^2}}\Delta\chi(\vec{\rho})\,, \tag{A.252}$$

the Gross-Pitaevskii equation (4.10) can be rewritten as

$$-\Delta\chi(\vec{\rho}) + \phi(\vec{\rho})\chi(\vec{\rho}) + |\chi(\vec{\rho})|^2\chi(\vec{\rho}) = \tilde{\mu}\chi(\vec{\rho})\,. \tag{A.253}$$

At fixed and finite $\vec{\rho}$, for which $\phi(\vec{\rho})$ would attain finite values as well, the importance of the kinetic term can be neglected with respect to the interaction term if

$$|\chi(\vec{\rho})|^2 \gg 1\,. \tag{A.254}$$

In that case, one would have $\chi(\vec{\rho}) \simeq \sqrt{\tilde{\mu} - \phi(\vec{\rho})}$ via the Thomas-Fermi approximation, with $\tilde{\mu} \gg \phi(\vec{\rho})$, and the application of the Laplacian would yield $\Delta\chi(\vec{\rho}) \simeq -\Delta\phi(\vec{\rho})/[2\sqrt{\tilde{\mu} - \phi(\vec{\rho})}] \simeq -\Delta\phi(\vec{\rho})/[2\sqrt{\tilde{\mu}}]$ in leading order, giving rise to the importance hierarchy $|\Delta\chi(\vec{\rho})| \ll |\phi(\vec{\rho})|\chi(\vec{\rho}) \ll |\chi(\vec{\rho})|^2\chi(\vec{\rho})$. Using the definition (4.26) of the local healing length $\xi(\vec{r})$, with $n(\vec{r}) = |\psi(\vec{r})|^2$, we can rewrite Eq. (A.251) as $\chi(\vec{\rho}) = a/\xi(a\vec{\rho})$. The inequality (A.254) is then equivalent to

$$\xi^2(\vec{r}) \ll a^2\,. \tag{A.255}$$

4.6 Let us start by defining a dimensionless interaction strength

$$\eta = \frac{Ng}{\sqrt{2\pi}^3 \hbar\omega a^3} = \sqrt{\frac{2}{\pi}}\frac{Na_s}{a} \tag{A.256}$$

and by introducing a dimensionless variational parameter $x = b/a$. Equation (4.29) is then rewritten as

$$E_{\rm GP} = N\hbar\omega\left(\frac{3}{4}(x^2 + x^{-2}) + \frac{\eta}{2}x^{-3}\right) \equiv E_{\rm GP}(x)\,. \tag{A.257}$$

Its first and second derivative with respect to x are evaluated as

$$E'_{\rm GP}(x) = N\hbar\omega\left(\frac{3}{2}(x - x^{-3}) - \frac{3\eta}{2}x^{-4}\right), \tag{A.258}$$

$$E''_{\rm GP}(x) = N\hbar\omega\left(\frac{3}{2}(1 + 3x^{-4}) + 6\eta x^{-5}\right). \tag{A.259}$$

At the critical value of Na_s/a that is to be calculated, the local minimum of $E_{\rm GP}$ as a function of x turns into an inflection point. We thus have $E'_{\rm GP}(x) = 0$ and $E''_{\rm GP}(x) = 0$ at that particular point, and hence also $x^5 E''_{\rm GP}(x) - x^4 E'_{\rm GP}(x) = 0$. From that latter equation straightforwardly follows $x = -5\eta/4$. The equation $E'_{\rm GP}(-5\eta/4) = 0$ can be rewritten as $5^5\eta^4 = 4^4$ and is solved by $\eta = -4/5^{5/4}$, taking into account that the critical interaction strength has to be negative. This yields

$$\frac{Na_s}{a} = -\frac{4}{5^{5/4}}\sqrt{\frac{\pi}{2}} \simeq -0.6705 \tag{A.260}$$

as smallest value of the dimensionless interaction strength parameter for which $E_{\rm GP}$ exhibits a local minimum.

4.7 In one spatial dimension (assuming tight confinement in the other two perpendicular directions) the trial function to be used for applying the variational approach is given by

$$\psi_0^{(b)}(x) = \sqrt{\frac{N}{\sqrt{\pi}b}}\exp\left(-\frac{x^2}{2b^2}\right). \tag{A.261}$$

Using

$$\int_{-\infty}^{\infty}\left|\frac{d}{dx}\psi_0^{(b)}(x)\right|^2 dx = \frac{1}{2b^2}\,, \tag{A.262}$$

$$\int_{-\infty}^{\infty} x^2\left|\psi_0^{(b)}(x)\right|^2 dx = \frac{b^2}{2}\,, \tag{A.263}$$

$$\int_{-\infty}^{\infty}\left|\psi_0^{(b)}(x)\right|^4 dx = \frac{N^2}{\sqrt{2\pi}b}\,, \tag{A.264}$$

the Gross-Pitaevskii energy functional for a one-dimensional condensate in the presence of the (longtitudinal) confinement potential $V(x) = \frac{1}{2}m\omega^2 x^2$ is evaluated as

$$\begin{aligned} E_{\mathrm{GP}}\left[\psi_0^{(b)}\right] &= \int_{-\infty}^{\infty}\left[\psi_0^{(b)*}(x)\left(-\frac{\hbar^2}{2m}\frac{d^2}{dx^2}+V(x)\right)\psi_0^{(b)}(x)+\frac{g}{2}|\psi_0^{(b)}(x)|^4\right]dx \\ &= \frac{N\hbar\omega}{4}\left(\frac{a^2}{b^2}+\frac{b^2}{a^2}\right)+\frac{N^2}{2}\frac{g}{\sqrt{2\pi}^3 b} \end{aligned} \tag{A.265}$$

with $a = \sqrt{\hbar/(m\omega)}$. Independently of the sign and the strength of g, this expression diverges to $E_{\mathrm{GP}} \to +\infty$ for $b \to \infty$ as well as for $b \to 0$. The existence of a local and global minimum at a finite value of b is thus granted for all g, contrary to the situation in three spatial dimensions.